

**Water Resources Research Center
Annual Technical Report
FY 2007**

Introduction

The major water science issue in Maryland is the recovery of the Chesapeake Bay. It is the largest economic asset in the State and is estimated to contribute millions of dollars annually to Maryland's fiscal resources. Four of the five projects funded by the Maryland Water Resources Research Center deal with the Bay. These projects are directed locally at streams, rivers, and wetlands. Last summer's drought had an adverse effect on one of our projects along the Anacostia River.

One issue that is receiving a great amount of research attention is the impact of road salts in streams and wetlands. Nitrogen cycles in streams are being disrupted as the salt concentrations increase. The impacts on denitrification could increase the amounts of nutrients that reach the Bay, exacerbating current water quality challenges.

Major problems in monitoring nitrogen balance have been time and expense. Maryland scientists have developed a system whereby they can estimate nitrogen levels in wetlands using hyperspectral radiometry to measure reflection from leaf surfaces. These measurements could tell us if salts are causing increased nitrogen levels in wetlands. The impact of sea level rise on coastal wetlands in the Chesapeake bay is also under investigation. Sea level rise is likely to result in increases in salinity and soil waterlogging in low-salinity marshes, causing stress and mortality of salt intolerant species and altering vegetation diversity and species composition. Another project funded by the Center deals with finding out how different types of vegetation affect the health of wetlands.

The Center tries to keep abreast with the other Federal and State agencies involved in problems in the Bay. A good example of this cooperation revolves around the annual fall conference cosponsored by the Center. In 2007, it focused on the Water Issues that the state of Maryland could face by the year 2030. This event is well-attended and acts as an effective information transfer mechanism for the Center.

Research Program Introduction

Salinity effects on using hyperspectral radiometry to determine leaf nitrogen of emergent wetland macrophytes

Basic Information

Title:	Salinity effects on using hyperspectral radiometry to determine leaf nitrogen of emergent wetland macrophytes
Project Number:	2006MD124B
Start Date:	3/1/2006
End Date:	2/29/2008
Funding Source:	104B
Congressional District:	5th &8th District of Maryland
Research Category:	Biological Sciences
Focus Category:	Ecology, Wetlands, Water Quality
Descriptors:	
Principal Investigators:	David R Tilley, Andrew Baldwin

Publication

Progress Report to
Maryland Water Resources Research Center
**Salinity effects on using hyperspectral radiometry to determine leaf nitrogen
of emergent wetland macrophytes**

David Tilley* and Andrew Baldwin

Department of Environmental Science & Technology, University of Maryland,
College Park

*dtilley@umd.edu 301-405-8027

Table of Contents

1. SUMMARY OF PURPOSE AND PROGRESS	2
1.1 PURPOSE.....	2
1.2 PROGRESS.....	2
1.3 STUDENT SUPPORT.....	2
2. STATEMENT OF CRITICAL REGIONAL OR STATE WATER PROBLEM.....	2
3. EXPECTED RESULTS OR BENEFITS	3
4. NATURE, SCOPE AND OBJECTIVES OF THE PROJECT	4
5. METHODS, PROCEDURES, AND FACILITIES.....	5
5.1 PROCEDURES.....	5
5.1.1 <i>Experimental Design</i>	5
5.1.2 <i>Data Collection</i>	7
5.1.3 <i>Data Analysis</i>	7
5.2 FACILITIES.....	8
6. RELATED RESEARCH.....	8
6.1 HYPERSPECTRAL RADIOMETRY FOR ECOSYSTEM ASSESSMENT	8
7. RESULTS TO DATE	13
8. LITERATURE CITED.....	14

1. Summary of Purpose and Progress

1.1 Purpose

This is a research project using leaf-based hyperspectral radiometry to measure the solar radiation reflectance of common emergent marsh macrophytes exposed to combinations of nitrogen-ammonia and salinity in a greenhouse to replicate field conditions. We are attempting to determine the significance of the effects of nitrogen and salinity on leaf reflectance. We will also develop hyperspectral reflectance models predictive of leaf tissue nitrogen, availability of nitrogen and salinity stress. The work will lead to a fundamental understanding of wetland plant response to nutrients and salinity and practical applications as a tool for assessing the health of wetland, which the US EPA has identified as a national priority for meeting Clean Water Act legislation.

1.2 Progress

The experiment is underway with data collection in progress. We have collected plants and have them growing at the UM Research Greenhouse Complex. We have taken initial radiometric readings of plant leaves using an ASD integrating sphere attached to an ASD hand-held spectroradiometer. Data collection will be finalized by the end of August 2008. Since we only have a partial set of initial measurements, we were not able to conduct any data analysis as of the writing of this progress report. However, we have included an example of reflectance measurements made to date. Our work is on schedule to be completed by February 2009.

1.3 Student Support

One M.S. student (Aaron Lewis) from the MEES program at UM has been supported on the grant.

2. Statement of critical regional or State water problem

The Clean Water Act (CWA) stipulates that States report the health and quality of all water bodies, including wetlands, in a National Water Quality Inventory Report, but only 4% of wetlands were included in the most recent edition (USEPA 2002a). By 2012 the USEPA's leniency will end and States will be required to report wetland water quality and ecological health (USEPA 2001). The lack of reporting stems from technical difficulties associated with sampling wetlands and unresolved issues in defining wetland health. In Maryland, water quality monitoring and reporting is conducted by the Maryland Department of the Environment (MDE) and the Maryland Department of Natural Resources (DNR). Recently, MDE received an EPA grant to develop guidelines for programs to monitor wetland water quality (Denise Clearwater, MDE, pers. comm.).

The low monitoring rate of wetlands is due largely to the time and expense of intensive direct sampling in areas that are difficult to access. Presently, the U.S. EPA National Health and Environmental Research Lab is working directly with seven states to test less intensive sampling methods, such as rapid biological assessment and GIS analysis of land use (e.g., Landscape Development Intensity Index), in an effort to fully develop wetland assessment tools (Richard Sumner, USEPA, pers. comm.). However, it is clear that more tools need to be developed and tested to increase the nation's capability for assessing wetland water quality and ecological health and to meet statutory requirements of the CWA.

Nitrogen is a ubiquitous pollutant that shifts wetland plant composition, lowers diversity and increases productivity (DiTommaso and Aarssen 1989; Morris 1991; Baldwin

unpublished data). Agricultural and urban runoff and atmospheric deposition are sources of excess nitrogen to wetlands and open-water systems, such as Chesapeake Bay. In general anthropogenic inputs of nutrients to the biosphere are increasingly viewed as a global threat to ecosystem integrity (Vitousek et al. 1997; Fenn et al. 1998). Although Maryland's load of total nitrogen to Chesapeake Bay decreased by 28% from 1986 to 2001, nitrogen loading remains a priority concern for achieving the 2000 Chesapeake Bay Agreement (MDNCWG 2001). Statewide, point source nitrogen loads have decreased from 14,300 MT to 7710 MT (46%) and agricultural loads have dropped from 14,600 MT to 9590 MT (34%). Urban loads, on the other hand, have grown 19%, from 5370 MT to 6390 MT.

3. Expected Results or Benefits

Our research efforts are focused on developing wetland hyperspectral radiometry as an assessment tool complimentary to existing techniques, which will quantify nitrogen (Tilley et al. 2004) and possibly metals (Tilley and Baldwin 2005) in marsh plant tissue, and distinguish which marshes have high nitrogen availability (Tilley et al. 2004), whether they are freshwater or brackish systems. Development of these fundamental capabilities would eventually lead to the ability to remotely sense which wetlands were under stress from high nutrient or metal loading in coastal environments. Thus, our work will assist the States and US EPA in meeting the statutory requirements, which will lead to improved management of the nation's wetlands.

Our proposed research project supports the program objectives of the MWRRRC by exploring new ideas in wetland remote sensing for water quality monitoring, fostering the research of a junior faculty (Tilley has completed 4 y at UMCP, receiving his Ph.D. in 1999), and training students in a new technology. In general, our research develops information necessary to protect and enhance water quality and habitats supporting natural ecosystem function and to translate new research knowledge and technologies to decision makers and citizens of the Chesapeake Bay, Mid-Atlantic region and the nation.

In addition to meeting a statutory need for monitoring wetlands, wetland hyperspectral radiometry would help environmental managers screen large expanses of wetlands to identify which ones are nitrogen "hot-spots"; that is potential sites receiving excessive amounts of non-point source runoff. Identifying these major sources of NPS runoff, which has traditionally been very difficult, would allow for directed application of environmental management techniques to reduce nitrogen in runoff and groundwater. This capability will benefit society by improving science-based management of agricultural operations and urban stormwater management to reduce impacts on coastal resources. Locally, this is important since agriculture and urban runoff are two of the predominant causes of eutrophication in the Chesapeake Bay (Jaworski et al. 1992; Chesapeake Bay Program 1995).

By 2012 States will be required by the U.S. EPA to report on the water quality conditions and ecological health of wetlands. Thus, development of wetland hyperspectral radiometry is timely and will have a significant impact on state monitoring strategies and capabilities.

The emerging field of precision agriculture, whereby satellite, airborne, and handheld spectroradiometers are employed to measure nitrogen status of crops, demonstrates the potential of employing remote sensing technologies to understand the nutrient status of wetland ecosystems. Advancing the capability of wetland remote sensing

to quantify the nitrogen status of wetlands can (1) provide a tool for the large scale monitoring of water quality in difficult-to-access wetlands, (2) offer a rapid screening method for identifying nitrogen “hot-spots” in a watershed, (3) enable near real-time monitoring in areas suspected of producing significant quantities of non-point source (NPS) pollution, and (4) be used to monitor wetlands used as treatment filters.

4. Nature, scope and objectives of the project

Having developed proof-of-concept that elevated availability of nitrogen changed the visible and near-infrared reflectance of common wetland macrophytes (Tilley et al. 2003; Tilley et al. 2005a), that low level changes in salinity in the brackish range altered visible and near-infrared reflectance of marsh macrophytes (Tilley et al. in review), and that partial least squares (PLS) regression modeling (explained below) predicted nitrogen effects on leaf reflectance of common marsh macrophytes and the availability of sub-surface nitrogen in tidal freshwater marshes (Tilley et al. 2004), an important next step for coastal applications is to investigate the effects of salinity and its interactive effects with nitrogen on the reflectance of emergent marsh macrophytes. This can lead to the development of PLS/hyperspectral models that are predictive of marsh nitrogen and salinity across the fresh/brackish coastal gradient. This ability will be especially useful where coastal marshes are periodically inundated with brackish water during drought years (Baldwin, personal observation) or are gradually shifting to brackish conditions due to relative sea level rise. Also, our previous experiments never evaluated salt marsh species like *Spartina alterniflora* or *Spartina patens* so the proposed research will include these species.

Specific objectives are:

1. Determine whether salinity decreases near-infrared and increases visible reflectance of freshwater and salt/brackish marsh macrophytes;
2. Determine whether there is an interaction effect between nitrogen and salinity on near-infrared and visible reflectance of freshwater and salt/brackish marsh macrophytes;
3. Determine whether species has a significant effect on leaf hyperspectral reflectance across a nitrogen and salinity gradient.
4. Determine whether PLS models that use hyperspectral reflectance can distinguish the nitrogen levels of leaf tissue across a gradient of salinity expected at the tidal freshwater/ brackish interface.
5. Determine whether PLS models that use hyperspectral reflectance can distinguish the salinity of the water column across a gradient of salinity expected at the tidal freshwater/ brackish interface.

Timeline. Due to unforeseen difficulties in hiring a graduate research assistant, collecting and culturing plants the project was delayed by more than one year. Our original schedule stipulated that the project could be completed by February 2007. The revised schedule assumes that we will have the final report for the project completed by May of 2009. The remaining schedule has us completing data collection by the end of August and completing data analysis by the end of November, and finalizing our report by May 2009.

5. Methods, Procedures, and Facilities

5.1 Procedures

5.1.1 Experimental Design

Greenhouse marsh microcosms containing one each of four common marsh species (*Acorus calamus*, *Phragmites australis*, *Typha latifolia*, and *Spartina alterniflora*) will be treated with four levels of salinity and four levels of N in a 4x4x4 factorial treatment arrangement in a completely randomized design with four replicates of each treatment, resulting in 64 combinations and 256 individual plants.

Plants were grown in Hydroton expanded clay pellets and supplemented with fifty percent Hoagland's nutrient solution with modified nutrient levels for controlling nitrogen (Hoagland and Arnon 1950). Each plant was placed in its own basin and received 1.5 liters of Hoagland's solution a week. Deionized water was used to refill the basins through out the week. All solutions were created using lab grade components and deionized water. The macronutrient solution concentrations were 0.00125 M K₂SO₄, .0025 M CaCl₂, .00025 M KH₂PO₄, and .0005 M MgSO₄. The micronutrient solution was composed of H₃BO₃, MnCl₂*4H₂O, ZnSO₄*7H₂O, CuSO₄*5H₂O, and H₂Mo*H₂O. Plants were also supplemented with five milliliters 0.00005 M Fe-EDDHA solution per week. Nitrogen was added to the solutions as NH₃Cl. The solutions were changed weekly, and the solution basins were rinsed with deionized water to limit build up of salts. Target salinity levels will be 0, 1, 3, and 7 ppt while N levels will be background, 3.3, 6.7, 10 mg-N l⁻¹ (Table 2).

Some seedlings were collected from local marshes near College Park, while others were purchased from a local nursery (Environmental Concern, Inc.). Previously we have successfully collected plants for use in greenhouse studies using similar methods (Baldwin et al. 2001; Tilley et al. in press) and Louisiana delta plain coastal marshes (Baldwin and Mendelsohn 1998). Because ammonium is the dominant form of available N in wetlands, ammonium chloride has been used by us (Clarke and Baldwin 2002) and others (e.g., Wang 1991) in ammonia toxicity studies. Resulting chloride concentrations will be far below levels toxic to aquatic plants (230 mg L⁻¹, USEPA 2002b).

Table 2. Nitrogen and salinity treatments for marsh microcosms will be replicated four times with each microcosm containing one potted individual of each of four plant species.

		Salinity (parts per thousand, ppt)			
		0 (S0)	1 (S1)	3 (S2)	7 (S3)
Nitrogen (mg-N L ⁻¹)	Nominal (N0)	N0×S0	N0×S1	N0×S2	N0×S3
	3.3 (N1)	N1×S0	N1×S1	N1×S2	N1×S3
	6.7 (N2)	N2×S0	N2×S1	N2×S2	N2×S3
	10 (N3)	N3×S0	N3×S1	N3×S2	N3×S3

The levels of salinity chosen were based on ranges that we have observed at tidal freshwater marshes on the Nanticoke River (Baldwin, unpublished data). Normally, salinity levels are <0.5 ppt, but during the late summer months or drought years salinity can increase to several ppt due to decreased freshwater flow. Nitrogen levels were selected to bracket levels measured in Nanticoke tidal freshwater wetlands (1-2 mg/L, Tilley et al. 2004) to an upper bound level (20 mg-N/L) that could reasonably be expected to occur in

wetlands receiving agricultural non-point source runoff or wastewater treatment discharge (some forms of agriculture such as confined animal operations can generate even higher ammonium concentrations that are toxic to wetland plants; Clarke and Baldwin 2002).



Fig. 1. Emergent wetland macrophytes growing hydroponically in individual containers with modified Hoagland's solution in UM research greenhouse.

5.1.2 Data Collection

Measurements of leaf photosynthesis, transpiration and hyperspectral reflectance will be made prior to application of treatments, near the mid-point of the experiment, and at the end of the 4 week period. Photosynthesis and transpiration (net CO₂ and H₂O exchange, respectively) will be measured with a portable infrared gas analyzer (Analytical Development Company, Herts, England: model LCA-2). Leaves will be clamped with the LCA-2, ambient air pulled through at constant flow rate, and CO₂ and H₂O inlet and outlet concentrations measured.

Reflectance was measured using a hyperspectral radiometer with an attached integrating sphere (Analytical Spectral Devices, Boulder, CO: model ASD Handheld 325-1075 nm). Leaf samples were clipped from experimental units one at a time and readings were performed immediately. Samples were taken from plants located in the greenhouse over the course of 48 hours. Leaves located at or below the second node from the top of the plant were selected for the species *Spartina alterniflora* and *Phragmites australis*, while center leaves were selected for *Typha latifolia* and *Acorus calamus*. The intention was to sample young leaves that were newly matured. Leaf reflectance was to be taken at the beginning, three week, and six week marks of the treatment. Initial readings were made before treatments were applied.

Not all leaf samples were not wide enough to fill the viewing aperture on the Integrating Sphere. Thus, it was necessary to modify the aperture using a split press. The split press was composed of two pieces of black plastic with a three millimeter slit centered on one of the pieces. Black plastic was used because the material must be uniformly and highly absorptive throughout the radiometer's spectral range. Leaf samples were pressed between the pieces of plastic and placed within the integrating sphere's bracket for readings. This ensured that a uniform area was measured for all samples and allowed for the reading of relative reflectance.

Percent reflectance will be found by dividing leaf reflectance by the reflectance of a calibrated white panel (LabSphere, North Sutton, NH: Spectralon). Leaf samples will be harvested from each plant at the end of the treatment period to analyze for N concentration at an independent lab.

5.1.3 Data Analysis.

A full factorial mixed effects analysis of variance (ANOVA) will be conducted to examine the effects of N, salinity, and species on leaf photosynthesis, transpiration, spectral band reflectance, reflectance indices, and leaf N concentration using SPSS for Windows 12.0 (SPSS Inc., Chicago, IL). Differences among means will be distinguished with Tukey's honestly significant difference procedure. Significant differences will be defined at the 0.05 probability level. Partial Least Squares (described below) regression will be used to develop predictive models of N and salinity treatment levels and leaf N concentrations. We will use Unscrambler 9.0 (Camo Process, Oslo, Norway) to conduct PLS. Sample data will be split into training and test sets to perform calibration and validation, respectively. The number of PLS components to include in the final model will be chosen for the model with the minimum root mean square error of prediction (RMSEP) based on the independent test set. The coefficient of determination of the final model will also indicate model efficacy. Various pre-processing transformations will be tested including normalization, first and

second derivatives, and multiplicative scatter correction which can reduce scatter and non-linear effects.

5.2 Facilities

Our proposed research will be carried out using the Ecosystem Engineering Design Laboratory, Wetland Ecology and Engineering Laboratory, and University of Maryland Research Greenhouse Complex. Both laboratories are housed within the Department of Environmental Science & Technology at the University of Maryland, and are well-stocked with standard and advanced equipment and materials for ecological and environmental research including spectrophotometers, light meters, a portable photosynthesis system, a digital canopy LAI meter, hip and chest waders, soil augers, drying ovens, a muffle furnace, refrigerators, a grinding mill, balances, glassware, and safety equipment. Specific equipment used in the proposed research includes an ASD Handheld Hyperspectral Radiometer with Integrating Sphere, a Spectralon Calibrated White Panel, Unscrambler 9.0 multivariate data analysis software and SPSS for Windows 12.0 for ANOVA. Additionally, we have a 24-ft pontoon boat, a 17-ft single hull craft and a jon boat, all with trailers, that can be used to visit marsh sites for collecting donor plant material. The Biological Resources Engineering department also has several trucks and vans for towing the boats to collect plants.

6. Related Research

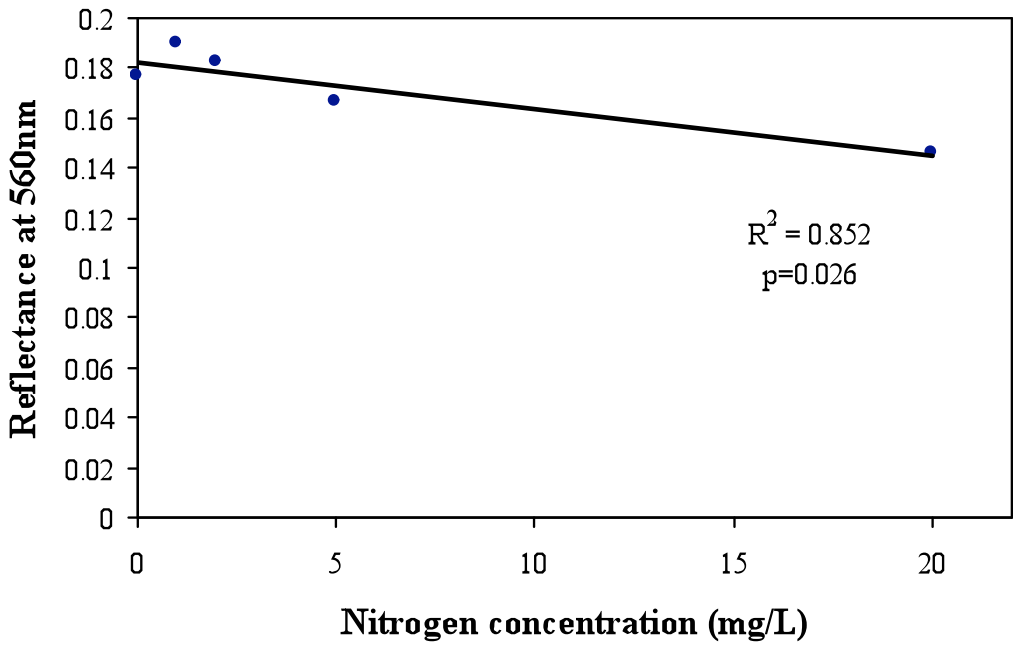
6.1 Hyperspectral Radiometry for Ecosystem Assessment

Hyperspectral radiometry measures the electro-magnetic energy reflected from a surface in hundreds of narrow (1–10 nm) spectral bands in the ultraviolet (UV), visible (VIS), near-infrared (NIR) and shortwave-infrared (SWIR) portions of the spectrum. Hyperspectral radiometric imaging can be conducted on the ground with commercially available equipment or from above with airborne (e.g., AVIRIS) and satellite (e.g., Hyperion) systems. In ecosystem radiometry, hyperspectral reflectance is affected by the vegetation's photopigments (e.g., chlorophylls and carotenoids; Hader and Tevini 1987), other leaf biochemicals (e.g., cellulose, lignin; Curran and Kupiec, 1995), inorganic elements (e.g., water, nitrogen, metals), plant morphology, ground cover, soil properties, incident irradiance quality and other environmental factors. When using hyperspectral radiometry to assess the nitrogen levels of leaves or whole ecosystem canopies, much of the effect is due to the strong relationship between reflectance, chlorophyll and nitrogen, although other indirectly associated nitrogen effects (e.g., higher leaf water content) may be partially responsible for the response.

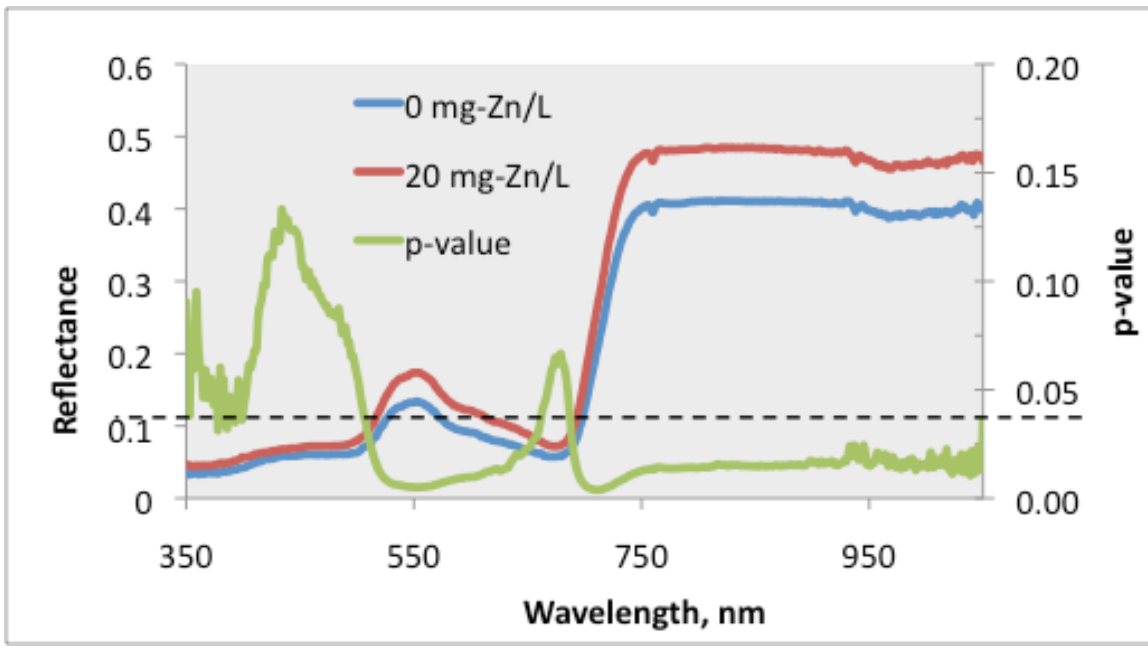
Historically, radiometric remote sensing techniques have been employed to delineate wetland types and track their quantity and location, but recently the techniques have been employed to assess wetland quality and stress levels based on nutrients, metals, salinity, and invasive species (Anderson and Perry 1996; Penuelas et al. 1997; Tilley et al. 2003; Tilley et al. 2004; Wilson and Ustin 2004; Xue et al. 2004; Poynter-Jenkins et al. 2005; Tilley et al. in press). Of course, hyperspectral radiometry has been widely used to assess the condition of open-water aquatic ecosystems--classifying the trophic status of lakes (Koponen et al. 2002, Thiemann and Kaufmann 2000) and estuaries (Froidefond et al. 2002), characterizing algal and red tide blooms (Stumpf 2001, Kahru and Mitchell 1998), and identifying and classifying submerged aquatic vegetation (Williams et al. 2003). Research on applying the techniques to assess the health of emergent wetlands needs acceleration.

Our most recent wetland radiometric studies (Tilley et al. 2005b; Tilley et al. 2005c) have, for example, used partial least squares (PLS) regression (described below) to predict sub-surface water total nitrogen levels in the absence of salinity ($R^2=70\%$). These findings supported our earlier efforts that found leaf reflectance indices [e.g., Photochemical Reflectance Index: $(R_{531}-R_{570})/(R_{531}+R_{570})$; red-edge (wavelength of maximum slope at red—near-infrared transition); and simple ratios (e.g., R_{493}/R_{678}) responsive to water column ammonia in a brackish treatment marsh (Ahmed 2001; Tilley et al. 2003). The PRI was found by others (Gamon et al. 1997) to be positively related to nitrogen, phosphorus, and potassium fertilization rates for annual, deciduous and evergreen upland species. The red-edge is responsive to leaf chlorophyll concentration, which is strongly influenced by nitrogen availability (Carter and Miller 1994). Strachan et al. (2002) included PRI along with the red-edge as necessary members of a multi-index reflectance model developed for classifying nitrogen application rates in corn (*Zea mays*). Read et al. (2002) found a simple blue to red reflectance ratio (R_{415}/R_{710}) as a strong indicator ($R^2 = 0.70$) of leaf nitrogen in cotton (*Gossypium hirsutum*). We have also found that the normalized difference vegetation index (NDVI) and floating water-band index (fWBI) were responsive to small (1 part per thousand) changes in salinity in a brackish treatment marsh over a range of 2 to 5 ppt (Tilley et al., in review).

Figure 2 provides an example of the findings we made during the first MWRRC funded project. High nitrogen availability decreased reflectance in the green waveband (Figure 2a) and blue and red wavebands (data not shown), which indicated that more photosynthetically active radiation was absorbed when more nitrogen was available. Preliminary results from our newest, on-going experiment (Tilley and Baldwin 2005) revealed that heavy metal (Zn) stress in common marsh macrophytes significantly increased reflectance in the green, red and near-infrared wavebands (Figure 2b), which supports our notion that wetland hyperspectral radiometry can be used to assess heavy metal stress in wetlands.



A



B

Fig. 2. (A) Effect of elevated nitrogen on greenband reflectance (560 nm) and (B) effect of elevated Zinc on visible (400-700 nm) and near-infrared (700 -1050 nm) reflectance of *Spartina* and *Typha*.

The large amount of spectral data gathered with hyperspectral radiometry presents a strong case for employing multivariate data analysis techniques that can handle multicollinearity (e.g., the correlation among spectral bands). Partial least squares (PLS) regression is a type of eigenvector analysis that can reduce full-spectrum data to a small set of independent latent factors (i.e., PLS-components) that explain the most about dependent variable response (Esbensen 2002). PLS regression is related to principal components analysis (PCA), which decomposes the independent spectral data (matrix **X**) to its principal components (latent factors) to ascertain which spectral bands are related and possibly important in explaining dependent variable response. Whereas PCA decomposes the **X** matrix while completely ignoring the **Y** matrix, PLS regression exploits information contained in the response matrix (**Y**) to decompose the spectral data (**X**) to latent factors that are used to build a regression model that explains the most about **Y**. Thus, PLS overcomes the multicollinearity problem, which is a concern with a method such as stepwise multiple linear regression (MLR) (Grossman et al. 1996) that has been used extensively in analyzing hyperspectral images.

PLS has a proven history in chemometrics and is becoming a preferred method for relating hyperspectral reflectance to ecosystem properties as shown by Smith et al. (2003) and Townsend et al. (2003) who used it to develop highly predictive reflectance models of temperate forest canopy nitrogen concentration from airborne and satellite hyperspectral images, respectively. More recently Wilson and Ustin (2004) used PLS discriminant analysis (PLS-DA) of leaf hyperspectral reflectance to classify the Cu and Cd exposure levels of three salt marsh species (*Frankenia* spp., *Salicornia* spp., and *Scirpus* spp.), finding relatively low prediction errors (4.4 to 8.8%). Kooistra et al. (2003) used PLS to relate the reflectance of a facultative upland grass species (*Lolium perenne*) growing in a restored Dutch floodplain to the Zn concentration of the soil. Preliminary results from our wetland imaging (Poynter-Jenkins et al. 2005b) suggested that PLS-DA could detect the presence of invasive species like *Phragmites australis* (88% accuracy) and classify the cover of dominant species like *Polygonum arifolium* (62% accuracy). We have also found success using PLS to build hyperspectral models predictive of nitrogen availability based on (1) individual leaf reflectance in pot-studies (Fig. 3) and (2) field-based canopy reflectance of two tidal freshwater marshes with distinctly different species compositions (Poynter-Jenkins et al. 2005a). As mentioned above, we have a funded project to assess whether we can build a PLS/hyperspectral model predictive of leaf Zn concentration in three common coastal marsh macrophytes (*Phragmites*, *Typha*, and *Spartina*; Tilley and Baldwin 2005).

Therefore, there is mounting evidence that the combination of PLS and hyperspectral imaging can create an effective tool for assessing many features of wetlands including N availability, species composition and heavy metal-induced stress. One major question about applying the technique to assess nitrogen levels in coastal wetlands located at the freshwater/brackish fringe is whether salinity produces a strong counteractive effect on the nitrogen signal because salinity has been found to increase visible reflectance and reduce near-infrared (Wang et al. 2002), which is opposite of nitrogen. This is the major question we propose to address in the Md. Water Resources funded project. Clarification of this question will continue to advance wetland hyperspectral radiometry as a practical tool for assessing wetland water quality and ecological health.

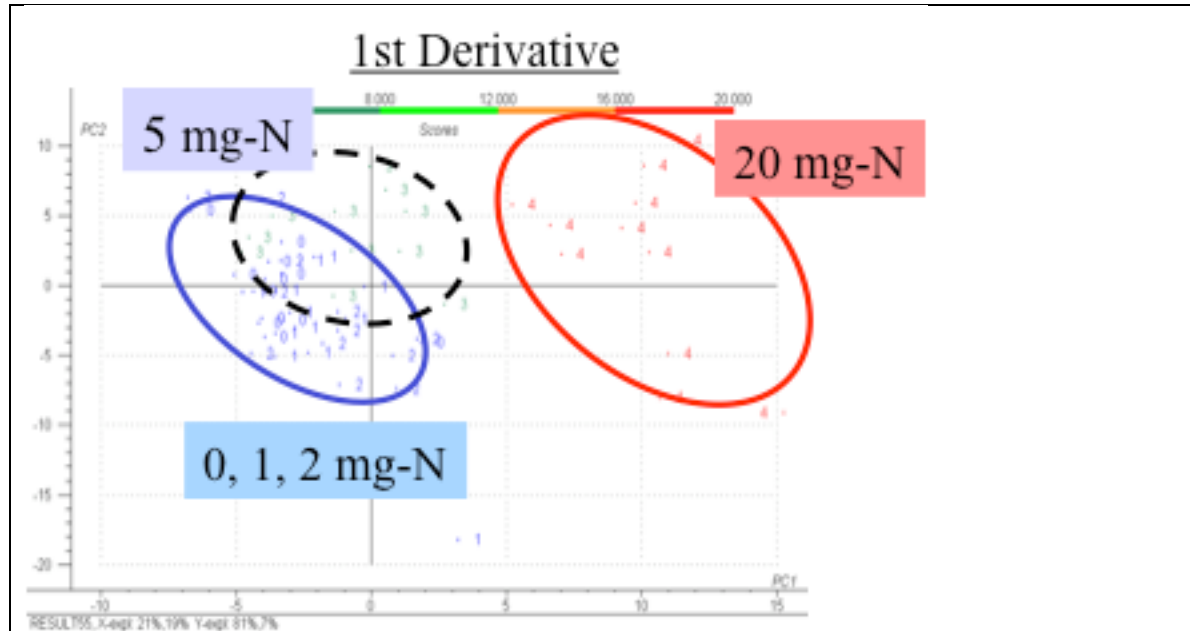


Fig. 3. Partial Least Squares (PLS) regression modeling of 1st Wavelength Derivative of Reflectance classified nitrogen treatment. The 20 mg-N/L treatment was clearly distinguished by the first PLS-component (abscissa) while the second PLS-component (ordinate) indicated some separation of the 5 mg-N treatment. The first PLS-component used 21% of spectral variation to explain 81% of nitrogen treatment. In contrast, the first PLS-component of the model that used the untransformed reflectance used 98% of the spectral variation to explain only 3% of the nitrogen treatment, while the second PLS-component used an additional 1% to explain 37% of nitrogen treatment. Thus, spectral derivative transforms improve predictive efficacy of nitrogen.

7. Results to date

Preliminary results shown in Fig. 4 revealed that the solar reflectance differed among the species. However, *Spartina alterniflora* and *Phragmites australis* appeared to have similar reflectance curves. As expected for vegetation, each species absorbed solar radiation strongly in the blue and red wavebands but reflected more in the green and NIR.

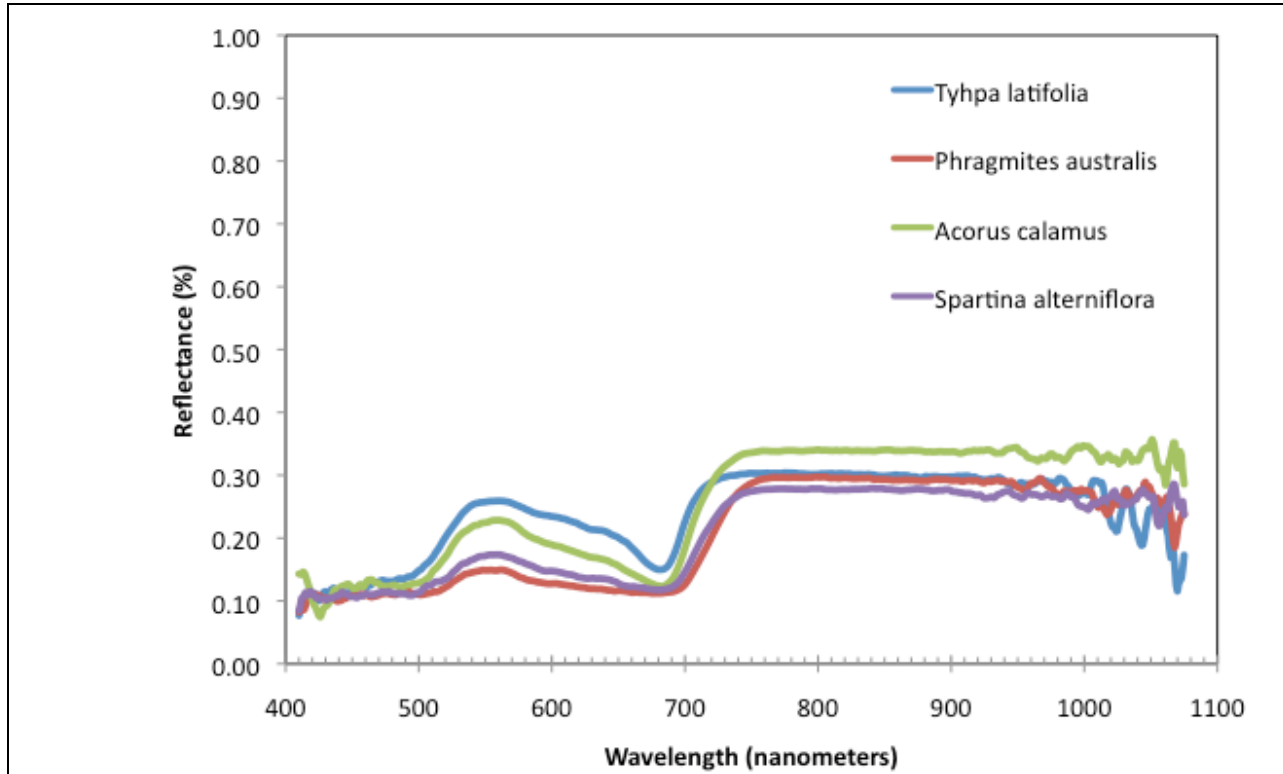


Fig. 4. Preliminary data: Example of solar reflectance of four emergent wetland macrophytes (n=1) growing in modified Hoagland's solution before treatments.

8. Literature Cited

- Ahmed, M., 2001. Spectral reflectance patterns of wetland vegetation along a water quality gradient in a self-organizing mesohaline constructed wetland in south Texas. M.S. thesis, Texas A&M University—Kingsville. 80 pp.
- Anderson, J.E. and J.E. Perry, 1996. Characterization of wetland plant stress using leaf spectral reflectance: Implications for wetland remote sensing. *Wetlands* 16(4):477-487.
- Baldwin, A.H., M.S. Egnotovitch, and E. Clarke, 2001. Hydrologic change and vegetation of tidal freshwater marshes: Field, greenhouse, and seed bank experiments. *Wetlands* 21: 519-31.
- Baldwin, A.H., and F.N. Pendleton, 2003. Interactive effects of animal disturbance and elevation on vegetation of a tidal freshwater marsh. *Estuaries* 26: 905-915.
- Baldwin, A.H., and I.A. Mendelssohn, 1998. Effects of salinity and water level on coastal marshes: an experimental test of disturbance as a catalyst for vegetation change. *Aquatic Botany* 1250: 1-14.
- Carter, G.A., R.L. Miller, 1994. Early detection of plant stress by digital imaging within narrow stress-sensitive wavebands. *Remote Sensing of Environment* 50(3):295-302
- Chesapeake Bay Program. The state of the Chesapeake Bay. CBP/TRS 260/02, EPA 903-R-02-002. 2002. Annapolis, Maryland, Environmental Protection Agency.
- Clarke, E., and A.H. Baldwin, 2002. Responses of wetland plant species to ammonia and water level. *Ecological Engineering* 18: 257-264.
- Curran, P.J., J.A. Kupiec, 1995. Imaging spectrometry: a new tool for ecology. pp. 71-88, in: *Advances in Environmental Remote Sensing* (F.M. Danson and S.E. Plummer, eds.) Wiley & Sons, New York.
- DiTommaso, A., and L. W. Aarssen. 1989. Resource manipulations in natural vegetation - a review. *Vegetatio* 84: 9-29.
- Esbensen, K.H., 2002. *Multivariate Data Analysis in Practice: An introduction to multivariate data analysis and experimental design* (5th Ed.). CAMO Technologies, Woodbridge. 598 pp.
- Grossman, Y.L., S.L. Ustin, S. Jacquemond, E.W. Sanderson, G. Schmuck, J. Verdebout, 1996. Critique of stepwise multiple linear regression for the extraction of leaf biochemistry information from leaf reflectance data. *Remote Sensing of Environment* 56:182-193.
- Fenn, M. E., M. A. Poth, J. D. Aber, J. S. Baron, B. T. Bormann, D. W. Johnson, A. D. Lemly, S. G. McNulty, D. E. Ryan, and R. Stottleymer. 1998. Nitrogen excess in North American ecosystems: Predisposing factors, ecosystem responses, and management strategies. *Ecological Applications* 8: 706-733.
- Froidefond, J., L. Gardel, D. Guiral, M. Parra, J. TERNON, 2002. Spectral remote sensing reflectances of coastal waters in French Guiana under the Amazon influence. *Remote Sensing of Environment* 80:225-232
- Gamon, J.A., L. Serrano, J.S. Surfus, 1997. The photochemical reflectance index: an optical indicator of photosynthetic radiation use efficiency across species, functional types and nutrient levels. *Oecologia* 112:492-501
- Hader, D.P., M. Tevini, 1987. *General Photobiology*. Pergamon Press, Oxford. 323 pp.
- Hoagland, D.R. and D.I. Arnon. 1950 The water-culture method for growing plants without soil. *California Agricultural Experiment Station Circular* 347:1-32.
- Jaworski, N. A., P. M. Groffman, A. A. Keller, and J. C. Prager. 1992. A watershed nitrogen and phosphorus balance: The Upper Potomac River Basin. *Estuaries* 15: 83-95.

- Kahru, M., B.G. Mitchell, 1998. Spectral reflectance and absorption of a massive red tide off southern California. *J. Geophysical Research-Oceans* 103(C10):21601-21609
- Kooistra, L, R.S. Leuven, R. Wehrens, P.H. Nienhuis, L.M.C. Buydens, 2003. A comparison of methods to relate grass reflectance to soil metal contamination. *Intl J Rem Sens* 24(24): 4995-5010
- Koponen, S., J. Pulliainen, K. Kallio, M. Hallikainen, 2002. Lake water quality classification with airborne hyperspectral spectrometer and simulated MERIS data. *Remote Sensing of Environment* 79:51-59
- MDNCWG, 2001. Maryland's Interim Nutrient Cap Strategy. Maryland Nutrient Cap Workgroup. http://www.dnr.state.md.us/bay/tribstrat/nutrient_cap.html visited: June 18, 2003.
- Mendelssohn, I.A., K.L. McKee, T. Kong, 2001. A comparison of physiological indicators of sublethal stress in wetland plants. *Environmental and Experimental Botany* 46: 263-275
- Morris, J. T. 1991. Effects of nitrogen loading on wetland ecosystems with particular reference to atmospheric deposition. *Annual Review of Ecology and Systematics* 22: 257-279.
- Penuelas, J., I. Filella, J.A. Gamon, C. Field, 1997. Assessing photosynthetic radiation-use efficiency of emergent aquatic vegetation from spectral reflectance. *Aquatic Botany* 58:307-315
- Peterson, J.E., and A.H. Baldwin, 2004. Variations in seed and spore banks across a tidal freshwater landscape. *American Journal of Botany* 91: 1251-1259.
- Poynter-Jenkins, E.E., D.R. Tilley, A.H. Baldwin, 2005a. Quantification of sub-surface water nitrogen levels in tidal freshwater marshes using hyperspectral reflectance. (Paper No. 051044) ASAE International Meeting, July 17-20, 2005, Tampa, Florida.
- Poynter-Jenkins, E.E., A.H. Baldwin, D.R. Tilley, 2005b. Modeling vegetation characteristics using hyperspectral reflectance and partial least squares regression in tidal freshwater marshes. AEEES 5th Annual Meeting, May 18-20, Columbus, OH
- Read, J.J., L. Tarpley, J.M. McKinion, K.R. Reddy, 2002. Narrow-waveband reflectance ratios for remote estimation of nitrogen status in cotton. *J. Environ. Qual.* 31:1442-1452.
- Smith, M.L., M.E. Martin, L. Plourde, S.V. Ollinger, 2003. Analysis of hyperspectral data for estimation of temperate forest canopy nitrogen concentration: comparison between an airborne (AVIRIS) and a spaceborne (Hyperion) sensor. *IEEE Transactions on Geoscience and Remote Sensing* 41(6):1332-1337
- Strachan, I.B., E. Pattey, J.B. Boisvert, 2002. Impact of nitrogen and environmental conditions on corn as detected by hyperspectral reflectance. *Remote Sensing of Environment* 80:213-224.
- Stumpf, R.P., 2001. Applications of satellite ocean color sensors for monitoring and predicting harmful algal blooms. *Human and Ecological Risk Assessment.* 7(5):1363-1368
- Thiemann, S., H. Kaufmann, 2000. Determination of chlorophyll content and trophic state of lakes using field spectrometer and IRS-1C satellite data in the Mecklenburg Lake District, Germany. *Remote Sensing of Environment* 73:227-235
- Tilley, D.R., M.T. Brown, 1998. Wetland networks for stormwater management in subtropical urban watersheds. *Ecological Engineering* 10(2):131-158.
- Tilley, D.R., A.H. Baldwin, 2005. Detection of heavy metals in emergent wetland macrophytes using hyperspectral radiometry. Grant from Maryland Agricultural Experiment Station, College Park.

- Tilley, D.R., M. Ahmed, J. Son, H. Badrinarayanan, (in review). Hyperspectral reflectance response of freshwater macrophytes to salinity in a brackish treatment marsh. Submitted to *Journal of Environmental Quality* (submitted August 2005).
- Tilley, D.R., M. Ahmed, J. Son, H. Badrinarayanan, 2003. Hyperspectral reflectance of emergent macrophytes as an indicator of water column ammonia in an oligohaline, subtropical marsh. *Ecological Engineering* 21(2-3): 153-163.
- Tilley, D.R., Badrinarayanan, H., R. Rosati and J. Son, 2002. Constructed wetlands as recirculation filters in large-scale shrimp aquaculture. *Aquacultural Engineering* 26(2):81-109.
- Tilley, D.R., A.H. Baldwin, and E. Poynter, 2004. A Progress Report to Maryland Sea Grant College on the Project Hyperspectral Reflectance of Freshwater Tidal Emergent Macrophytes as a Remote Sensing Tool for Assessing Wetland Nitrogen Status (R/CT-03). Maryland Sea Grant College, University of Maryland.
- Tilley, D.R., A.H. Baldwin, E.E. Poynter-Jenkins (in press). Hyperspectral reflectance response of four freshwater emergent macrophytes to nitrogen fertilization. *Remote Sensing of Environment*
- Tilley, D.R., A.H. Baldwin, E.P. Jenkins, 2005a. Leaf-scale hyperspectral reflectance models for determining the nitrogen status of freshwater wetlands. Final report to Maryland Water Resources Research Center, College Park.
- Tilley, D.R., A.H. Baldwin, E.P. Jenkins, 2005b. Modeling emergent macrophyte response to nitrogen fertilization based on partial least squares regression of hyperspectral leaf reflectance. 26th Annual Meeting of Society of Wetland Scientists, June 6-9, 2005, Charleston, S.C.,
- Tilley, D.R., E.P. Jenkins, A.H. Baldwin, 2005c. Partial least squares regression modeling of wetland hyperspectral reflectance to detect response to nitrogen fertilization. Fifth Annual meeting of the American Ecological Engineering Society, May 18-20, Columbus, OH.
- Townsend, P.A., J.R. Folster, R.A. Chastain, Jr., W.S. Currie, 2003. Application of imaging spectroscopy to mapping canopy nitrogen in the forests of the central Appalachian Mountains using Hyperion and AVIRIS. *IEEE Transactions on Geoscience and Remote Sensing* 41(6):1347-1354
- UMCP 2003. University of Maryland state-of-the-art research greenhouse complex. <http://www.agnr.umd.edu/MAES/profiles%2Epdf> Last visited 11/9/05
- USEPA, 2001. 2002 integrated water quality monitoring and assessment report guidance. Memorandum from R.H. Wayland III, Director of Office of Wetlands, Oceans, and Watershed to EPA Regional Water Management Directors, EPA Regional Science and Technology Directors, and State, Territory, and Authorized Tribe Water Quality Program Directors. November 19, 2001.
- USEPA, 2002a. National Water Quality Inventory 2000 Report. U.S. Environmental Protection Agency, Office of Water, EPA-841-R-02-001. Washington, D.C.
- USEPA, 2002b. National recommended water quality criteria: 2002. EPA 822-R-02-047. U.S. Environmental Protection Agency, Office of Water, Office of Science and Technology, Washington, DC
- Vitousek, P. M., J. D. Aber, R. W. Howarth, G. E. Likens, P. A. Matson, D. W. Schindler, W. H. Schlesinger, and D. G. Tilman. 1997. Human alteration of the global nitrogen cycle: sources and consequences. *Ecological Applications* 7: 737-750.

- Wang, D., C. Wilson, M.C. Shannon, 2002. Interpretation of salinity and irrigation effects on soybean canopy reflectance in visible and near-infrared spectrum domain. *Int. J. Remote Sens.* 23(5):811-824
- Williams, D.J., N.B. Rybick, A.V. Lombana, T.M. O'Brien, R.B. Gomez, 2003. Preliminary investigation of submerged aquatic vegetation mapping using hyperspectral remote sensing. *Environmental Monitoring and Assessment* 81:383-392
- Wilson, M.D, S.L. Ustin, 2004. Classification of contamination in salt marsh plants using hyperspectral reflectance. *IEEE Transactions on Geoscience and remote Sensing* 42(5): 1088-1095
- Xue, L., W. Cao, W. Luo, T. Dai, Y. Zhu, 2004. Monitoring leaf nitrogen status in rice with canopy spectral reflectance. *Agron. J.* 96:135-142.

Grant No. 07HQGR0067 Development of IWR NETS–NaSS – Phase 3

Basic Information

Title:	Grant No. 07HQGR0067 Development of IWR NETS–NaSS – Phase 3
Project Number:	2006MD162S
Start Date:	12/1/2006
End Date:	7/31/2007
Funding Source:	Supplemental
Congressional District:	MD–5
Research Category:	Not Applicable
Focus Category:	None, None, None
Descriptors:	
Principal Investigators:	

Publication

1. Wang, S.L., and Schonfeld, P. "Demand Elasticity and Benefit Measurement in a Waterway Simulation Model," forthcoming in the Transp. Res. Record, 2007.

**Genetic Algorithms for Selecting and Scheduling
Waterway Projects**

(Phase 3 Draft Report)

By Shiaaulir Wang, Ning Yang and Paul Schonfeld

*Department of Civil and Environmental Engineering
University of Maryland, College Park*

June 15, 2007

Table of Contents

Abstract.....	5
Introduction.....	6
Enhanced Features in Project Scheduling Problems.....	6
Multiple Projects with Different Implementation Times at the Same Lock.....	6
Construction Time and Capacity Reduction.....	8
Tradeoffs between Construction Times and Costs.....	10
Demand Elasticity and Benefit Measurement in Simulation Model.....	13
Demand Function.....	14
Measurement of User Benefit.....	16
Objective Function.....	18
Improvements to Genetic Algorithms.....	18
Generation of “Weighted” Sequences.....	18
Development of “Smart” and Problem-Specific Genetic Operator.....	19
Parallel Computing with GAs.....	20
Model Test (Enhanced SIMOPT).....	22
Incorporating Dynamic Demand into Simulation Model.....	22
Test Network.....	26
Model Inputs.....	27
Test Results.....	28
Adding Constraints (Multiple Projects with Different Implementation Time).....	28
Measuring Net Present Worth with Dynamic Demand.....	32
Including Construction Time and Capacity Reduction.....	34
Tradeoffs between Construction Times and Costs.....	36
Other GA Applications for Waterway Operations.....	38
Network Level Maintenance Planning and Scheduling.....	39
Lock Component Level Maintenance Planning and Scheduling.....	46
Conclusions.....	48
References.....	50
Appendix GA Phase 3 Scope of Work.....	51

List of Tables

Table 1 Project Information	27
Table 2 Optimized Results (Minimization Problem).....	29
Table 3 Work Information and Schedule.....	32
Table 4 Project Information (continued from Table 1).....	34
Table 5 Optimized results (Maximization Problem)	35
Table 6 Comparison of Optimal Project Sequences	36
Table 7 Project Information (continued from Tables 1 and 3)	37
Table 8 Optimized Results.....	38
Table 9 Network-Level Lock Maintenance Information	43
Table 10 Optimized Results for Network-Level Maintenance Planning.....	45
Table 11 Component-Level Lock Maintenance Information	46
Table 12 Optimized Results for Component-Level Maintenance Planning (Low Traffic)	47
Table 13 Optimized Results for Component-Level Maintenance Planning (High Traffic)	47

List of Figures

Figure 1 Project Funding Accumulation and Construction Time	8
Figure 2 Relations of Project Schedule and Construction Time	10
Figure 3 Time-Cost Tradeoff Relation	11
Figure 4 Paired Representation of Chromosome for Mutually Exclusive Projects	12
Figure 5 Modified Structure of Chromosome for Mutually Exclusive Projects	13
Figure 6 Traffic Demand vs. Impedance Factor	14
Figure 7 Capacity Change during the Lock Closure	15
Figure 8 Proposed Waterway Demand Function	16
Figure 9 Total User Benefit	17
Figure 10 "Smart" Mutation Operators	20
Figure 11 The PGA Procedure with the Hierarchical Model	21
Figure 12 Overall Framework of Basic Waterway Simulation Model	23
Figure 13 Simulation Model with Project Implementation	24
Figure 14 Port Generation Module	25
Figure 15 Dynamic Demand Module	26
Figure 16 Test Network for SIMOPT Extension	27
Figure 17 GA Search Performance (Minimization Problem)	30
Figure 18 Solution Distributions	32
Figure 19 Simulation Outputs w/ and w/o Demand Elasticity	34
Figure 20 GA Search Performance (Maximization Problem)	36
Figure 21 Lock Condition Change with Scheduled Preventive Maintenance	40
Figure 22 Maintenance Cost and Maintenance Schedule	41
Figure 23 Lock Failure Probability and Recovery Cost	42
Figure 24 Lock Deterioration and Maintenance Cost Functions	44
Figure 25 Maintenance Cost and Schedule	45

Abstract

A testbed waterway model (SIMOPT) that combines simulation and optimization has been developed for the Navigation, Economics Technologies (NETS) Program at the University of Maryland. It employs genetic algorithms to solve the problem of evaluating, selecting, sequencing and scheduling waterway improvement projects. Its promising demonstration of simulation-based optimization has been presented in the first phase of GA optimization work completed in April 2006. In order to enhance both the search efficiency of the optimization model and the capabilities for imposing additional constraints, some improvements in investment optimization methods are implemented and tested on SIMOPT.

The improved optimization model is intended to work with the next generation NaSS waterway simulation model which is being developed under the NETS program of the Corps of Engineers. Some enhancements were completed in previous two phases. In this phase, the improvements in the investment model include (1) allowing multiple projects at the same location with different implementation times, (2) considering project construction times and capacity reductions during the construction period with elastic demand responding to the delays, (3) considering tradeoffs between construction time and cost, and (4) network-level and lock component-level maintenance planning and scheduling. With elastic demand, the optimization problem should be to maximize net benefits rather than minimize total costs. Additionally, in order to speed up the optimization process, the feasibility of applying parallel computing is investigated and tested.

Introduction

The U. S. Army Corps of Engineers (USACE) has considerable interest in the problem of selecting, sequencing and scheduling waterway improvement projects. When numerous projects are considered, a massive combinatorial optimization problem results. An investment optimization model based on genetic search algorithms is applied to solve this large and complex combinatorial problem in the SIMOPT, simulation-based optimization model.

In previous phases of this study (Wang and Schonfeld, 2006 NETS Reports Phase I and II), project construction time and capacity reductions during construction were introduced in the SIMOPT model. Mutually exclusive projects at locks are specified in that analysis. Constraints addressing lock precedence relations and regional budgets were also included in the search process. In order to reduce the computation time, the evaluated solutions were recorded to avoid re-simulating them during the genetic search.

The following sections focus on the allowing multiple projects with different implementation times at the same lock location, and considering possible capacity reductions and resulting demand changes during the project construction periods. When considering of capacity reduction during the construction period, the issue of elastic demand response delays (due to partial or full lock closure) arises. In the simulation model, elastic demand (or demand response) can be handled in the trip generation module. Tradeoffs between construction time and cost are also investigated. Since traffic demand and benefits may be significantly affected by the decisions being simulated, it is unreasonable to evaluate or optimize the system merely based on total costs. Benefits to waterway users should be estimated during simulation runs while accounting for the users' responses to lock closures which might significantly affect the travel times.

Enhanced Features in Project Scheduling Problems

According to the Scope of Work drafted for GA enhancement (see Appendix), several tasks are included in phase III, including specifying multiple projects with different implementation times at the same location, considering construction time and capacity reduction with demand elastically responding to delays, and analyzing the tradeoffs between construction times and costs. The option of applying parallel computing in GA optimization is also explored. With multiple processors working on simulation-based evaluations, the time required in the proposed GA search can be reduced in nearly inverse proportion to the number of processors used.

Multiple Projects with Different Implementation Times at the Same Lock

At any specific lock site, several improvement projects or expansion alternatives with discretely specified capacities may be considered. Those projects might be independent of each other, but might also be dependent with interrelated costs.

When considering different expansion projects, two cases project multiplicity may arise. In the case of mutually exclusive projects, only one project among those alternatives at each location could be selected. This one is straightforward since project costs for different alternatives are independent. As been has discussed in the first phase of GA enhancement work, the sequencing problem then determines project timing and size simultaneously.

With non-exclusive multiple projects, several alternatives could be selected for one site but implemented at different times over the planning period. Those alternatives include independent improvement projects as well as dependent expansion projects. There are no cost relations among those independent improvement projects. However, for different expansion projects, if implemented at different times, the project costs and sequence should be carefully defined. For example, expansion project A which increases capacity from a baseline based on capacity expansion ratio of 1.5 should be implemented (if ever) ahead of expansion project B which increases capacity based on capacity expansion ratio of 2. It makes no sense that project B is implemented ahead of project A. In addition, with project precedence, the cost of project B is not the construction cost of project B, but a conditional cost based on the implementation of project A. For example, if \$0.5 million is needed for project A, an extra cost of \$0.8 million is needed for project B after implementing project A.

For different expansion alternatives at different times, a precedence constraint can be applied to restrict the sequence of those expansion projects. Lock precedence constraints have been discussed in the second phase. If projects at two locks L_i and L_j are related by a precedence constraint $L_i \rightarrow L_j$, a project at lock L_i can only be started when a project at lock L_j is funded, or later. In this report, project precedence constraints are considered. At the same lock location, if two projects P_i and P_j are related by a precedence constraint $P_i \rightarrow P_j$, project P_j can only be started when P_i is funded, or later. That is, given an array of integers $\{x_i\}$ where $i = 1, 2, 3, \dots, n$, and n is the number of projects, each element in the array represents the scheduled order of one project. The precedence constraint can be formulated as $x_i < x_j$.

Since precedence constraints define an order of succession among projects, it is important to note that some solutions (i.e., project sequences) would be infeasible and should be prescreened and discarded before being simulated at great expense. To impose the precedence constraints, infeasible solutions which violate any one of the precedence relations should be very unlikely to be selected to reproduce offspring in the next generation. Thus, if a sequence violates the precedence constraints, instead of running the simulation to evaluate its performance, its fitness value is assigned a large number (i.e., 10^{15}) which represents the penalty (Tao 2006) in a minimization problem. In a

maximization problem, a number close to 0 (i.e., 10^{-15}) is assigned as the fitness value for a sequence violating the precedence constraints. Let a binary variable p_i denote the relevant precedence constraints, $i = 1, 2, \dots, k$, if $p_k = 1$, the k^{th} precedence constraint is satisfied; if $p_k = 0$, the k^{th} precedence constraint is violated. Since k denotes the any given precedence constraint, then the objective function is multiplied by a factor of $\prod_k p_k$. In a minimization problem, when $\prod_k p_k = 0$, the fitness value ends with a large number, i.e., 10^{15} . Otherwise when $\prod_k p_k = 1$, the fitness value is the simulated total system cost.

Construction Time and Capacity Reduction

Project construction times have been analyzed in the first phase report (Wang and Schonfeld, 2006) with a conservative assumption that the project construction starts when the funding required for the project is accumulated. However, construction can usually be started whenever there is available budget. Since projects are funded one at a time, their construction periods may actually overlap the funding periods of subsequent project, as shown in Figure 1.

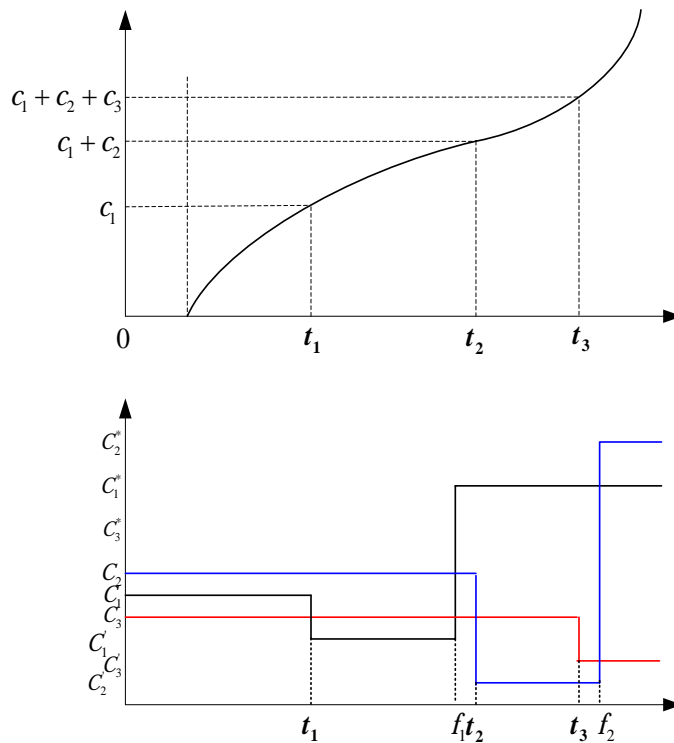


Figure 1 Project Funding Accumulation and Construction Time

However, in the real world, given a budget distributed over time that suffices for several projects, project timing is determined by available funding. Financially, it is desirable to avoid overlaps over time in funding different projects. The proposed model assumes the projects are completed chronologically at the time when sufficient budget is accumulated to cover their construction cost. Additionally, constructability concerns may result in construction overlap when project construction time exceeds than the time required for funding the project. Therefore, if construction overlaps exist, projects become operational after their construction is completed even if the project funding has been fully accumulated earlier. The closure time for construction should be as short as possible. If there are no construction overlaps, projects are started early enough to be completed by the time project funding is fully spent.

An example is shown in Figure 2. Three lock improvement projects are prioritized to increase lock capacities from C_1 , C_2 , and C_3 to C_1^* , C_2^* , and C_3^* , respectively. The project costs are c_1 , c_2 , and c_3 ; the implementation and completion times are t_1 , t_2 , t_3 and f_1 , f_2 , f_3 , respectively. Figure 2 shows that the project construction will decrease the capacities from C_1 , C_2 , and C_3 to C_1' , C_2' , and C_3' during the construction periods of T_1 , T_2 , and T_3 , respectively. After construction, the capacities are increased to the improved levels C_1^* , C_2^* , and C_3^* , respectively. The time between 0 to t_1 is the system warm-up time. If construction overlaps exist, the project operation time $f_i = \max\{t_i + T_i, t_{i+1}\}$; the project implementation time $t_i = \max\{t_{i+1} - T_i, t_i\}$. There are overlaps of construction times T_1 , T_2 , and T_3 , but no overlaps of project funding times B_1 , B_2 , and B_3 .

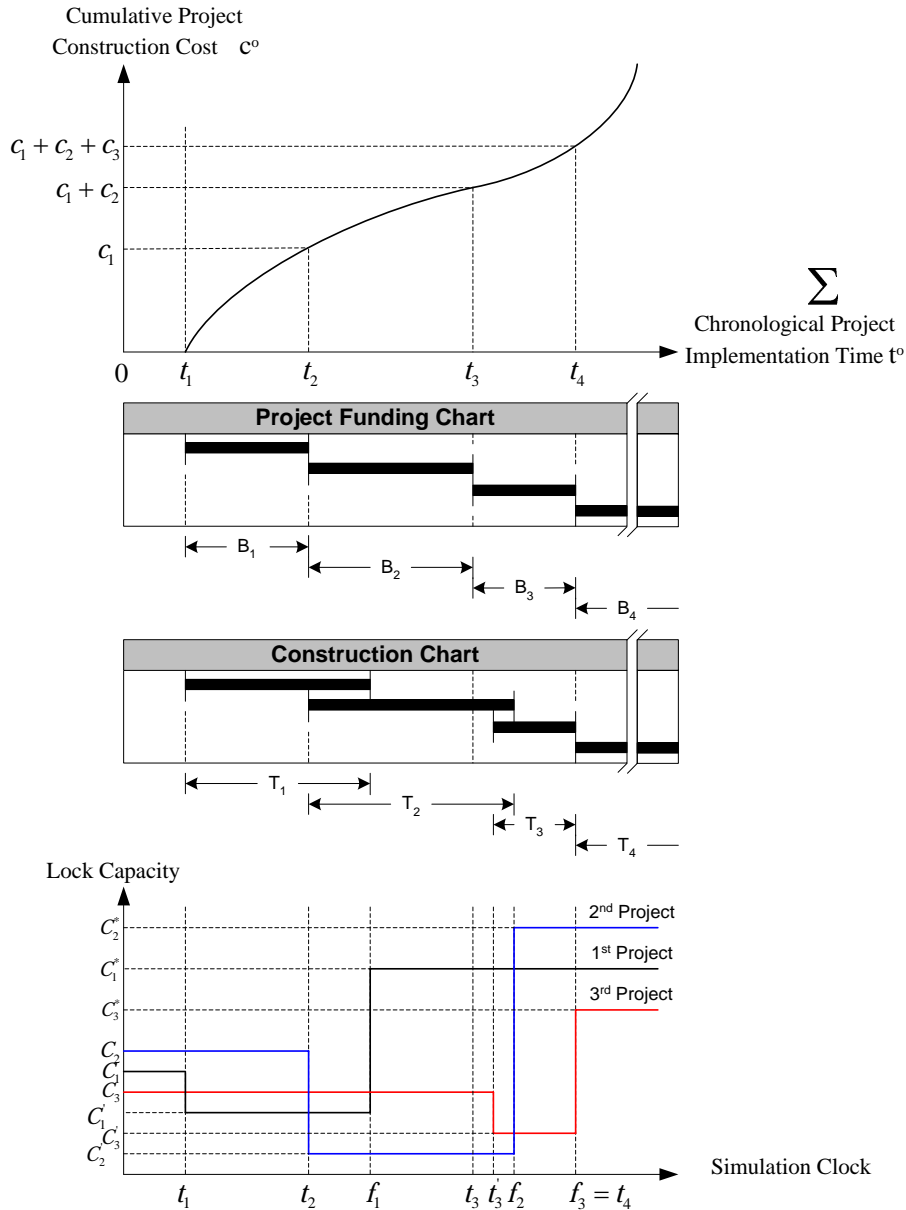


Figure 2 Relations of Project Schedule and Construction Time

Tradeoffs between Construction Times and Costs

For the general construction activities, there may be tradeoffs between construction time and costs. Such time-cost tradeoff relations should be identified and quantified. Various possible combinations of project duration and costs resulting from different procedures and/or resource combination should be considered. From Tien and Schonfeld (2006), the most efficient combinations, such as *a*, *b*, *c* or *d*, define an efficient frontier and are superior in time *T* or cost *C* (or both) to any point above that frontier, as shown in Figure 3. For a project with numerous component activities, the tradeoff frontier may be determined using heuristics and mathematical programming techniques, after analyzing

resource relations with the critical path method. Thus, a time-cost curve could also be approximated, continuously or discretely, to indicate the minimum cost required to speed-up a project to some degree.

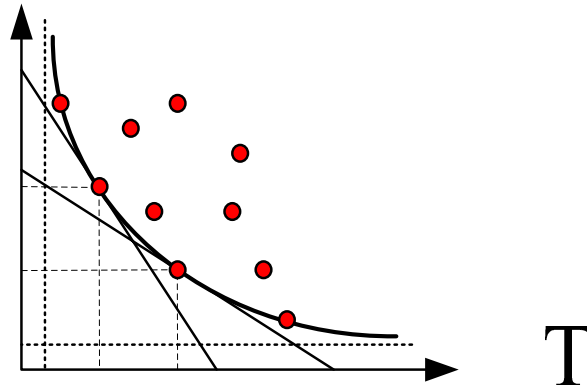


Figure 3 Time-Cost Tradeoff Relation

In a long-term investment planning problem, with a given budget distributed over time, the difference among nearby combination points of time and cost on the efficient frontier curve might not be very significant when an overall evaluation for a large network is pursued. In addition, investment planning tends to determine the best selection, sequence and schedule for candidate improvement projects. When considering a continuous relation between construction time and cost for each single project, it takes more efforts to represent the decision variables since any change between construction time and cost in one project may change the project sequence, and change the solution. Therefore, it is preferable to formulate the time-cost tradeoff relation discretely for several alternative time-cost combinations.

In order to provide alternative time-cost combinations for each project, a tradeoff constraint is considered. Since the tradeoff constraint intuitively provides one combination between two tradeoff variables, it has features of mutually exclusive constraints. That is, with mutually exclusive time-cost combinations for one project, i.e. if only one can be selected, we may consider the inclusion of construction time and cost decisions in the project scheduling problem. When combining construction time, cost, and scheduling problem, the solution space of fully permuted sequences will be further enlarged through the inclusion of all project alternatives at each lock. That is, if there are N lock locations, m_i ($i = 1, \dots, N$) project alternatives, and I_j ($j = 1, \dots, \sum_i m_i$) time-cost combinations for each project, the total number of solution including all possible combinations and permutations would be $N! \cdot \prod_i m_i \cdot \prod_j I_j$. The tradeoff constraint must ensure that only one combination for each project is selected among all available alternatives. Let X_k be a binary variable. If $X_k = 1$, the time-cost combination alternative is selected; if $X_j = 0$, the time-cost combination is not selected. If k denotes

the combination alternatives, then the tradeoff constraints for any project can be formulated as $\sum_k X_k \leq 1$.

As discussed in the first phase (Wang and Schonfeld, 2006), a chromosome used for mutually exclusive projects can be represented with a project ID and a tradeoff alternative ID (as shown in Figure 4). Each project has several discrete time-cost tradeoff alternatives (e.g., project #1, #2, #3..., etc. have 2, 3, 3..., etc. time-cost tradeoff alternatives, respectively.). With this chromosome representation, the proposed GA operators in SIMOPT could still be applied on the mutation and crossover processes without any modification to produce the offspring. As noted in Figure 4, the sequences with full list tradeoffs for all projects are not feasible solutions (as shown in the middle part of the figure). Since only one tradeoff alternative will be included in the implementation sequence, a “refining” scheme embedded to create the feasible solutions is required for simulation evaluation. Thus, instead of sequences with full lists of projects, a shorter sequence whose list of projects has only one project at each lock should be formed after the “refining” procedure (as shown in the lower part of Figure 4).

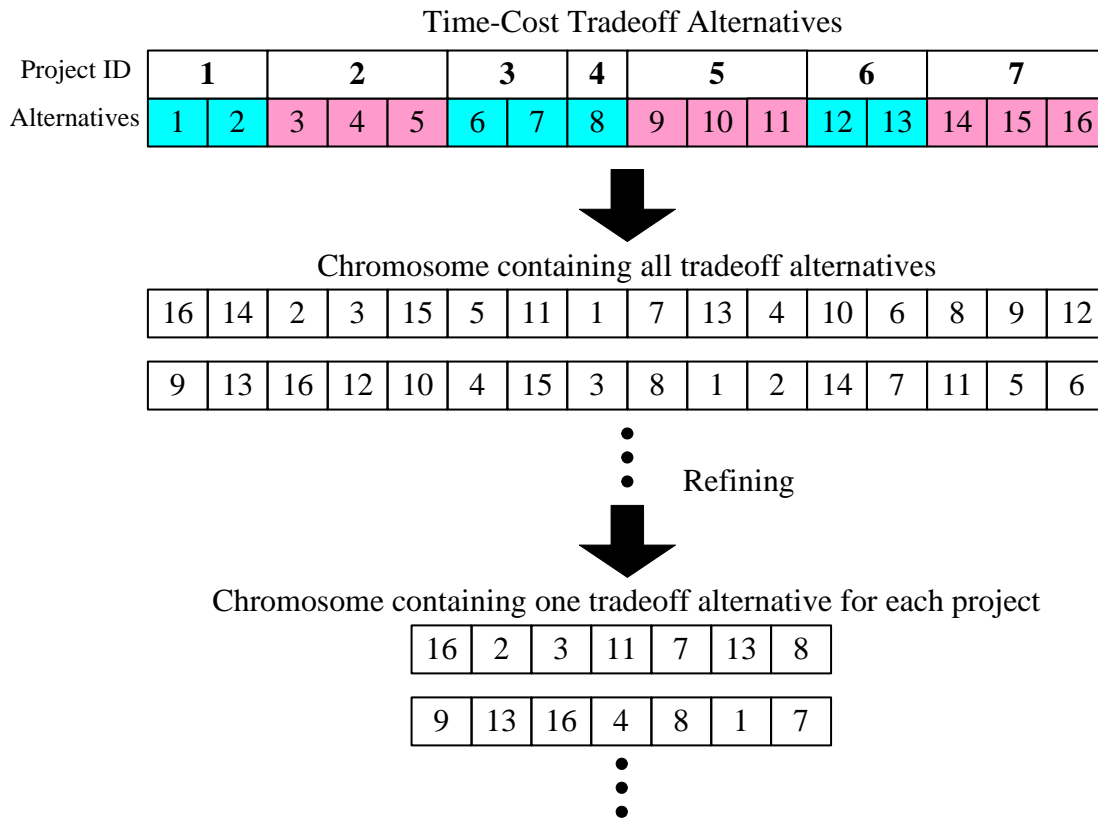


Figure 4 Paired Representation of Chromosome for Mutually Exclusive Projects

A similar “refining” technique (discussed in Wang and Schonfeld, 2006) is applied to discard the other tradeoff alternatives for the same project. As known, all the mutation and crossover operators are applied on the full-list chromosomes, rather than the refined

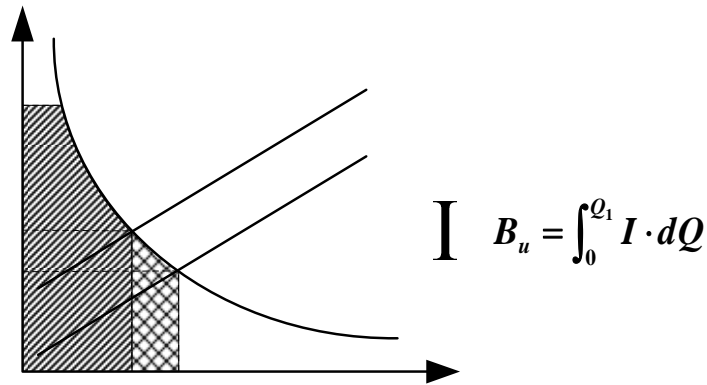
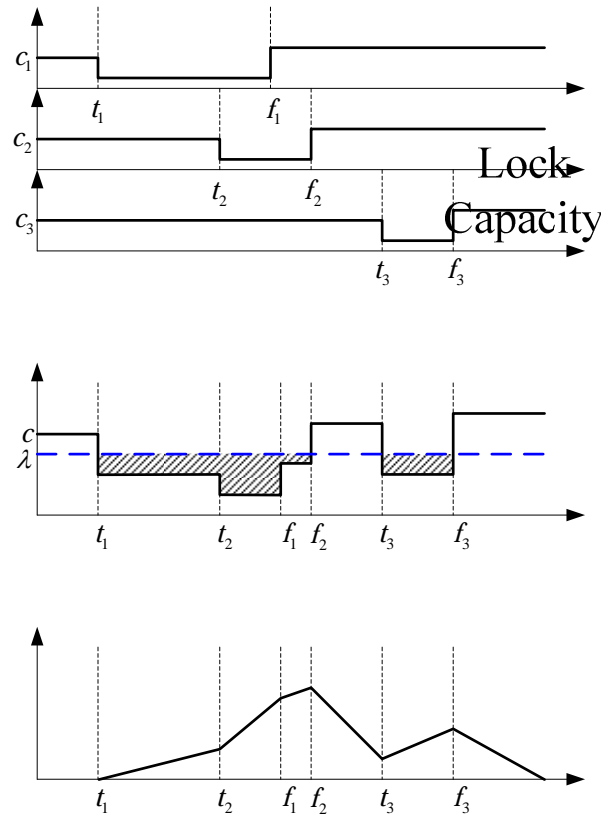


Figure 6 Traffic Demand vs. Impedance Factor

The demand may be limited by various factors determining system capacity, such as chamber dimensions and lockage times. Thus, demand increases as service times and, hence, capacity improves. When impedance decreases from I_1 to I_2 and traffic volume increases from Q_1 to Q_2 , the area of user benefit increases. Similarly, a capacity reduction increases impedance and decreases user benefits.

Demand Function

In Wang and Schonfeld (2007), when lock closures (partial or total) are explicitly considered, the local volume to capacity (V/C) ratios may become very critical, and possibly far above 1.0 for long periods. In Figure 7(a), partial closures are scheduled at times t_1 , t_2 , and t_3 , which greatly reduce lock capacities in periods t_1 to t_1^f , t_2 to t_2^f , and t_3 to t_3^f , respectively. If the V/C ratios exceed 1.0 and the demand level stays unchanged over time, the number of tows accumulating in queues is represented by the shaded area in Figure 7(b). In Figure 7(c), the queue length increases at different rates when inflows exceed lock capacities and decreases when there capacity exceeds inflows (i.e., $c - \lambda$). We must then consider how demand should be adjusted during closure times, i.e., in response to the reduced capacity and resulting delays.



(a)

Figure 7 Capacity Change during the Lock Closure

It is possible that delays may rise rapidly when a local capacity is reduced to zero or near zero during a closure time, if demand cannot respond to the resulting delay. In order to avoid infinite queues, an elastic demand model is used here to account for traffic sensitivity to the total travel time, which is mainly affected by lock service times. For each O/D pair, the demand function is assumed to be a hyperbolic curve, which has a constant elasticity with respect to an impedance factor. In order to normalize the factor of total travel time, the ratio of real travel time (z) to baseline expected travel time (y), z/y , is used as the impedance factor.

When we also consider secular growth in traffic, we let λ_{ij} denote the generation rate in a particular interval, r_{ij} denote the annual growth rate and k_{ij} denote the demand elasticity for each O_i/D_j pair. Then the demand function for each simulation period t can be expressed as

(b)

$$(\lambda_{ij})_t = (\lambda_{ij})_{t-1} \cdot (1 + r_{ij})^{t_p} \cdot \left[\frac{(z_{ij})_{t_p}}{y_{ij}} \right]^{k_{ij}} \quad (1)$$

where t_p duration of simulation interval
 z_{ij} simulated travel time for interval t

y_{ij} expected travel time in the base case simulation

Measurement of User Benefit

If the demand was fixed, i.e., having zero elasticity, then a total cost function (including construction, maintenance, vessel operations and user costs) would suffice to compare scenarios or drive an optimization process. However, if the demand can be affected by simulated decisions, we should maximize a net benefit function rather than minimize total cost. (Otherwise, the optimization might favor decisions that drive traffic, and hence costs, towards zero.) The net present worth (NPW) should be the present worth of total benefits minus the present worth of total costs, with user benefits estimated from the demand functions.

As discussed above, the proposed demand for each O/D pair is a function of continuous impedance and time variables. As shown in Figure 8, (a) and (b) are the projections of (c), an outward hyperbolic demand surface. At any time t , demand function Q_t can be expressed as $Q_t = Q_0 \cdot (I_t)^k \cdot (1+r)^t$.

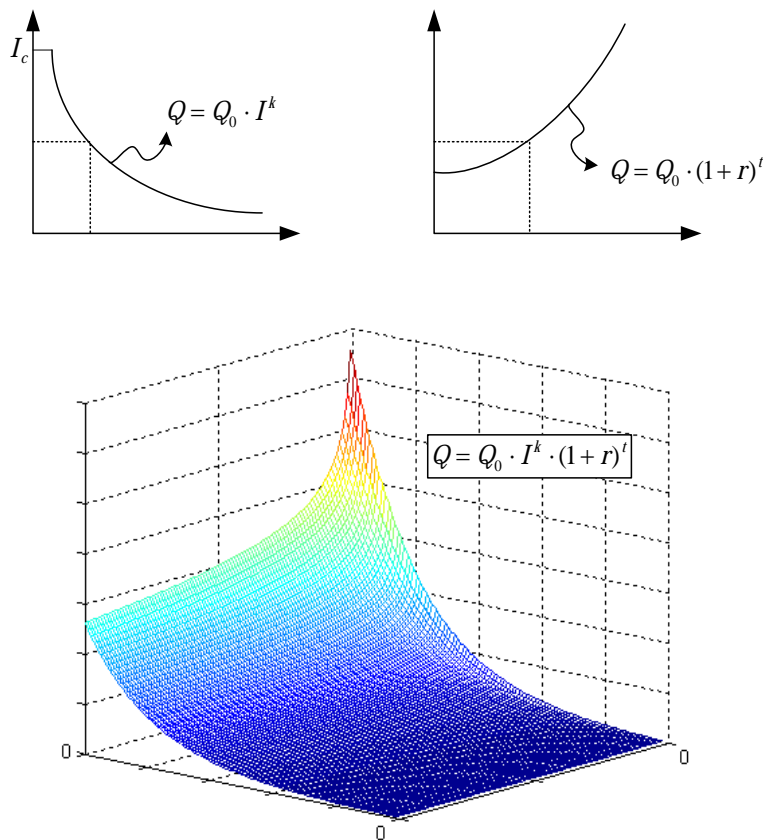


Figure 8 Proposed Waterway Demand Function

R interest rate (per time interval)

Objective Function

The objective function is the present worth of net system benefit NB which is total benefit TB minus total cost TC . To simplify this analysis, only construction costs, user costs and user benefits are considered in the objective function. Operation costs and benefits on the supplier side are not considered here. In this study, user benefits are estimated from the demand function and user costs are estimated from the simulated total travel times, which include cruising times, lock service times, and delay times. Several costs, e.g., for fuel, crew, vessel depreciation, time value of cargo, are combined into an hourly cost v (in \$/tow-hour). This cost also represents the users unit time value, and when multiplied by impedance I , it transforms the impedance and user benefit measures from hours to \$. Therefore, let c_i denote the total travel time in interval i , the net present worth (NPW) is simplified here as the present worth of total user benefit minus total user cost:

$$\begin{aligned} NPW &= B_u - C_u \\ &= \frac{v}{(1+R)^i} \left(\sum_{i=1}^n \left(\int_0^{Q_i} I \cdot dQ \right) - \sum_{i=1}^n (c_i) \right) \end{aligned} \quad (3)$$

If project selection is considered (especially for mutually exclusive projects), the supplier's construction cost C_c cannot be factored out and should also be subtracted from the measured benefit. Let b_i denote the budget spent in the interval i and NPW is found by subtracting the project construction cost.

$$\begin{aligned} NPW &= B_u - C_u - C_c \\ &= \frac{v}{(1+R)^i} \left(\sum_{i=1}^n \left(\int_0^{Q_i} I \cdot dQ \right) - \sum_{i=1}^n (c_i) - \sum_{i=1}^n (b_i) \right) \end{aligned} \quad (4)$$

Improvements to Genetic Algorithms

In our previous work, most GA characteristics are fairly standard, including the creation of solutions, the genetic operators and the computation method. Some improvements are proposed to enhance GAs search performance by creating weighted sequences, developing smarter problem-specific genetic operators and applying parallel computing techniques.

Generation of "Weighted" Sequences

After the first generation of solutions, GAs create further solutions by applying designed genetic operators. However, sometimes we may still need to generate solutions without using any operators, such as in the steps of creating initial population and selecting possible parents. It is clear that all individuals in the initial population are generated without applying any genetic operators. Although all the candidate parents are selected from the current population based on their fitness values or ranks, any specific individual may only be selected a limited number of times in order to prevent “super individuals” from dominating the population. Thus, if an individual has been already selected as candidate parent for a fixed number of times (e.g., two times), whenever it is selected again, a brand new solution should be generated.

Besides, based on the concept of evolution, stronger parents in current generations are more competitive and have a higher chance to produce stronger offspring in the next generations. With different problem characteristics, sequences generated from random selection might be less promising and may then reduce search efficiency. Therefore, it is preferable to have weighted sequences which contain information on problem characteristics in addition to ordinary random sequences.

In the proposed GA, there are two categories of generated solutions: random-order solutions and weighted-order solutions. In random-order solutions, each project in any one of the solution sequences has the same probability to have a particular implementation priority. That is, the sampling process randomly selects a project and leaves the other projects in a sampling space for the next sampling processes. All the projects have the same chance of being selected in any position of a solution sequence. Thus such randomly generated solutions can explore the search space by providing as many variations as possible. On the other hand, weighted-order sequences will favor projects at locks which have special traffic, cost, or benefit characteristics. By considering this prior knowledge, those solutions can help speed up the convergence process.

Different ways may be used to weight the order of projects. The most common consideration for project implementation sequence is the current lock congestion level. Bottleneck-order solutions then include the information about possibly optimal sequences, in which the projects are implemented in the order of the severity of total delays at individual locks. That is, based on individual lock delays, those projects at most congested locks have higher chances to be selected first in a solution sequence. In order to include the senses of delay severity, a baseline simulation run is pursued. In the baseline simulation, the network is evaluated with current traffic and system conditions. No traffic growth or lock improvement projects appear during the simulation.

Development of “Smart” and Problem-Specific Genetic Operator

In the previous section, weighted sequences are generated for the initial population and in the process of selecting candidate parents. A “smart” operator is then used to create more promising solutions in the reproduction process. Those problem-specific operators should be able to produce offspring oriented toward project features such as benefits and locations. Since those considerations are hard to implement in a “crossover” way, two

“smart” mutation operators are proposed, namely project mutation (PM) and geometry mutation (GM).

The PM operator works similarly to the EM (reciprocal exchange mutation, Wang and Schonfeld 2006) operator, but with more than two-point swapping. The number of swapping points depends on the size of problem (e.g., number of projects). Figure 10(a) shows a 3-point PM operator. It swaps the projects in those randomly generated positions with the order of their capacity expansion ratios. Thus, a project with a higher capacity expansion ratio will be shifted forward to an earlier implementation time.

The GM operator considers the network geometry. The number of groups depends on the size of network. It first randomly selects numbers of positions on the chromosome. The adjacent projects are grouped based on the project location shown on the gene. Figure 10(b) shows a 2-group GM operator. It groups adjacent upstream and downstream projects with the selected project.

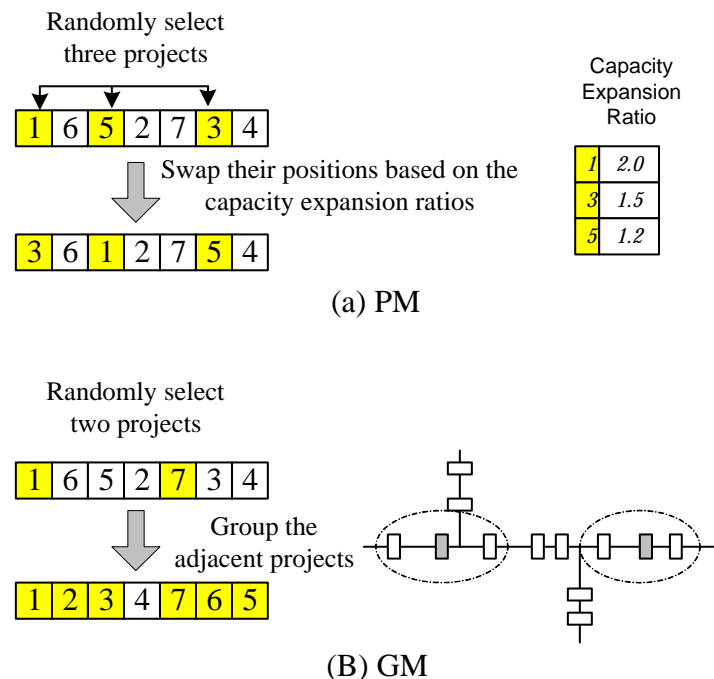


Figure 10 "Smart" Mutation Operators

Parallel Computing with GAs

Adapting the optimization model to parallel computing is a promising approach for speeding up the optimization process. In simulation-based optimization, the evaluation process is the most time-consuming task. If that evaluation process can be distributed among parallel processors, the optimization search time may be reduced almost in inverse proportion to the number of processors, with some additional time for “communication” between processors.

Parallel GAs (PGAs) are relatively easy to implement compared to other parallel computing algorithms. To improve the efficiency of running SIMOPT, we seek to adjust this model to parallel computing without changing the basic structure of the GA applied in it.

According to Yang and Schonfeld (2007), among several conceptual models of the major PGA paradigms, a hierarchical model (also called in the literature a “master-slave” model) is easy to visualize and it is relatively simple to implement. The master processor handles parameters necessary for the objective function evaluation to the slave processors; the slave processors receive the messages and perform the evaluation; objective function values are then returned to the master processor. Figure 11 shows the PGA procedure with the hierarchical model.

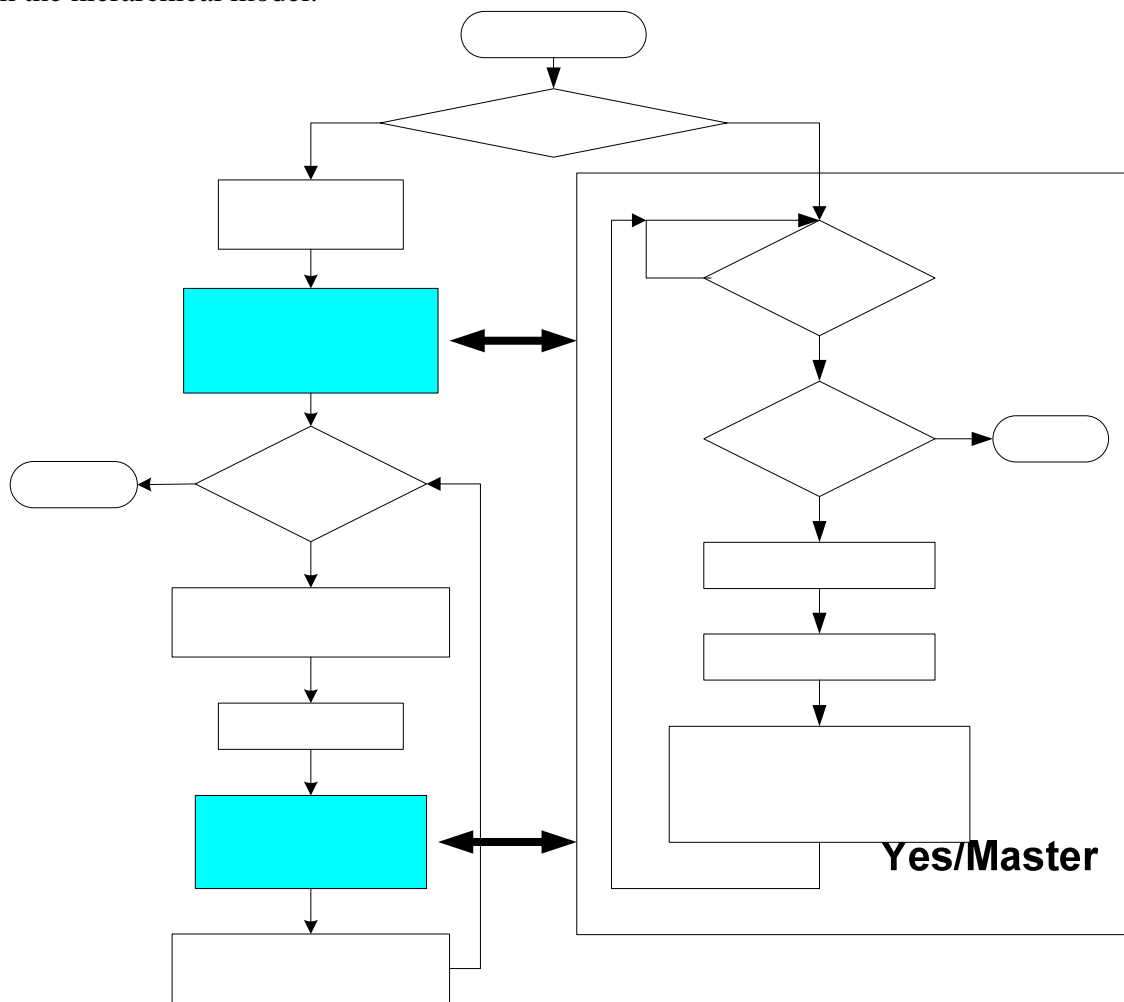


Figure 11 The PGA Procedure with the Hierarchical Model

As shown in Figure 11, in each PGA evaluation step the master processor assigns a subgroup of individuals to each slave processor and receives back their objective function values. Since the fitness evaluations are independent of one another, slave processors only need to communicate with the master processor, without interacting with one

Generate initial population
Evaluate each individual in parallel

another. To reduce idle time and minimize redundant or wasted effort, it is important to design an appropriate task (individual) distribution method which can result in a balanced division of work between contributing processors.

Model Test (Enhanced SIMOPT)

The proposed demand model is incorporated into a generalized waterway simulation model developed by Wang and Schonfeld (2002). The simulation model in SIMOPT is a discrete-time, event-based microscopic simulation model which is developed to analyze trip behavior, lock operations and demand variation, and to evaluate the system performance, and is used here for demonstrating two aspects of demand sensitivity.

Incorporating Dynamic Demand into Simulation Model

In the basic SIMOPT simulation model, there are five operational modules: (1) the *port generation module* where a tow is generated at a port; (2) The *port arrival module* where a tow arrives at a port; (3) the *lock arrival module* where a tow arrives a lock; (4) the *lock departure module* where a tow leaves a lock; (5) the *port exiting module* where a tow ends its trip at a port. All events are invoked by the timing control module, preceded by updating the timing average, and followed by a statistical counting process. The logical organization among its basic event modules is shown in Figure 12. Starting with the timing control scheme and ending with the statistical module, all events (three port events for tows being generated, ending their trips and passing by, plus two lock events for tows being served and leaving) occur at network nodes during the simulation time.

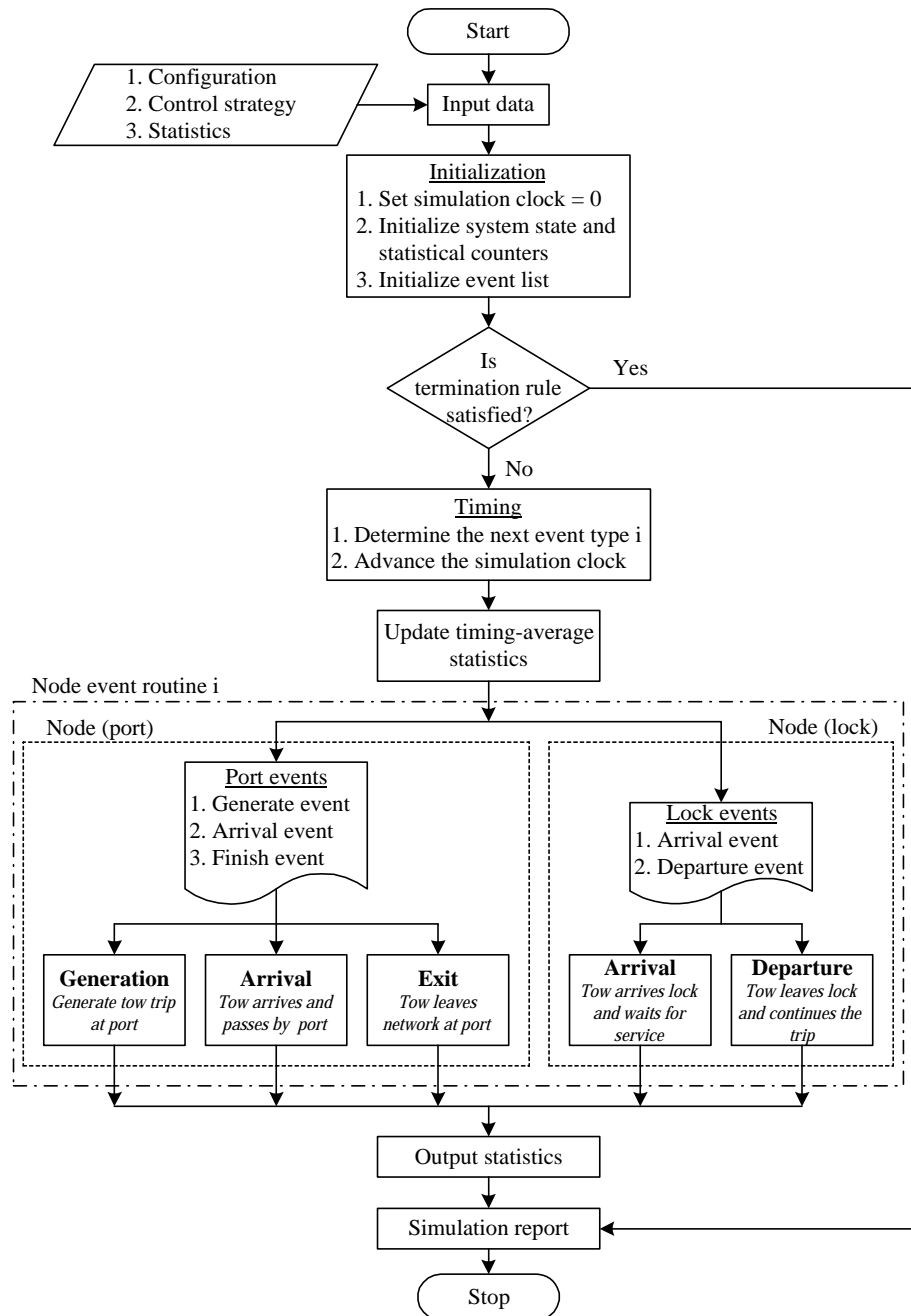


Figure 12 Overall Framework of Basic Waterway Simulation Model

The proposed simulation model is used to evaluate any sequence of projects. In a project scheduling problem, whenever a project sequence is generated by GA, the simulation model is called to evaluate the performance of generated project sequence. With the implementation schedule calculated from the cumulative budgets and project costs, projects are chronologically introduced into the simulation program and implemented immediately. Thus each simulation is run at least for the duration of the planning horizon T . As shown in Figure 13, except for the five timing events at ports or locks (defined in basic simulation framework), there are project implementation events which bring the

project implementation timetable into the simulation and update the system by increasing capacity as well as reducing the service time during the simulation. By extension, if project construction times and capacity reductions are considered, two project implementation events will be included, namely the start of the project and the end of the project. When starting projects, the system is updated by decreasing capacity and increasing service time; when finishing projects, capacity is increased and service time is decreased. During the construction period, demand responds to service level and is elastically changed.

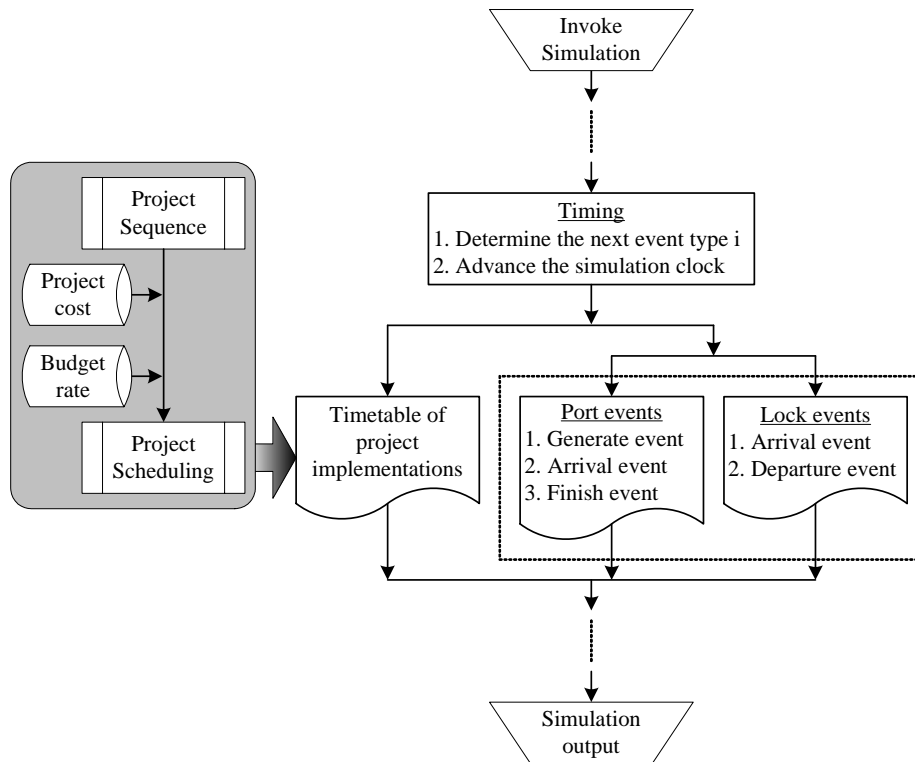


Figure 13 Simulation Model with Project Implementation

If demand is steady, or even seasonal, with unchanged trip rates (e.g., number of trips per day, month, season, or year) along the time axis, all trips can be generated in advance as a complete shipment list from which trips are then fed into the simulation model one by one based on their departure times. However, if demand grows annually or responds elastically to travel delays, as might result from project construction and improvements, a pre-generated shipment list is no longer suitable for the simulation model. In order to incorporate dynamic demand into simulation model, a generation event during the simulation becomes necessary. The generation event is called whenever the simulation clock runs to the instant when a new trip is ready to be generated. Only one trip is generated per generation event. After generating one trip, the next generation event is scheduled based on the most updated traffic level, including O/Ds and travel delays.

Figure 14 presents a flowchart for the generation event. While invoking a generation event, timing control has determined the origin port. Based on the O/D matrix, the tow trip is stochastically assigned a destination port. Meanwhile, the tow's size and travel

speed are generated as part of that tow's data structure. In order to avoid generating extreme speed values, truncations of minimum and maximum speeds must be specified. After associating all the characteristics to the newly generated tow, the generation module sends the tow into the network link, determines its arrival time at the next lock and schedules next generation event based on the updated O/D matrix.

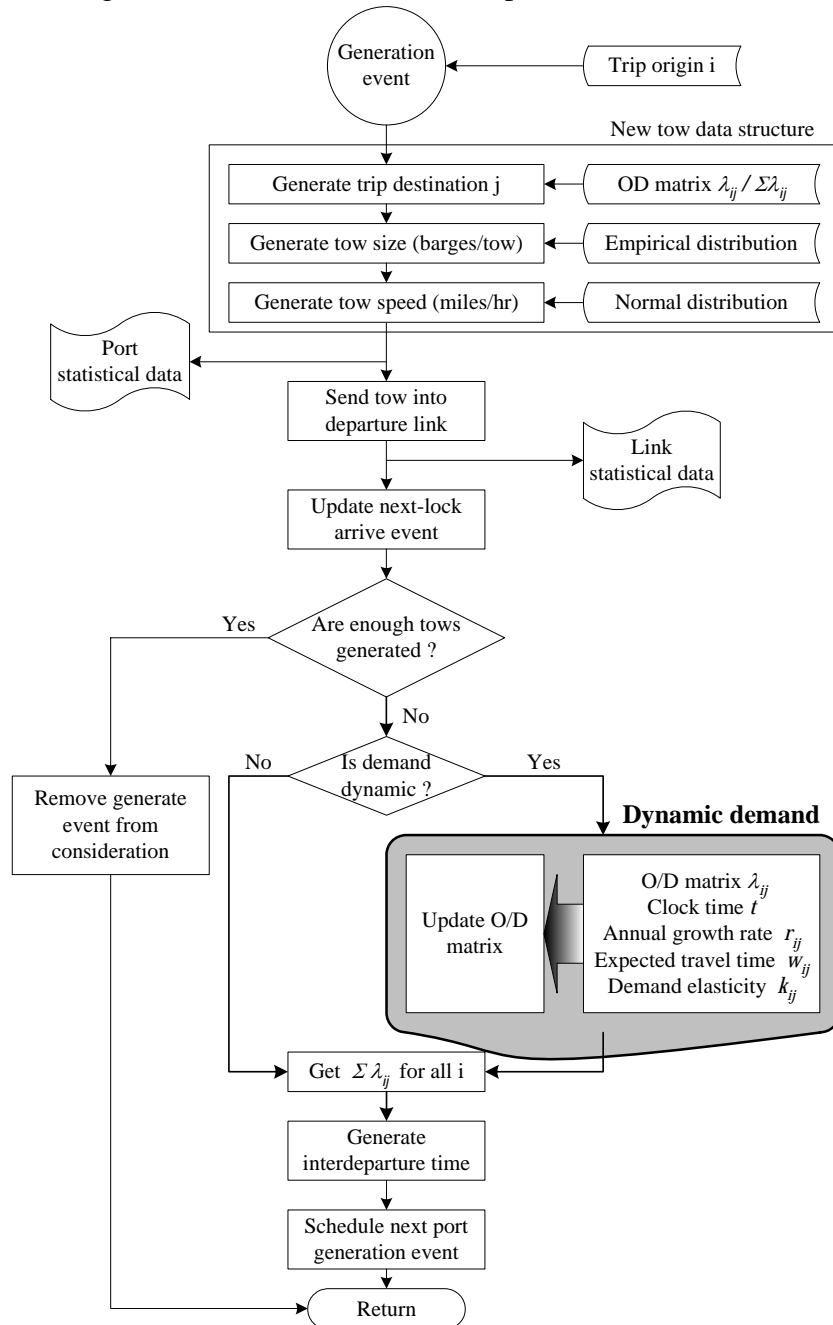


Figure 14 Port Generation Module

During the simulation run, the OD matrix, i.e. the trip generation rate, changes over time. The process of dynamically updating the existing O/D matrix is illustrated in Figure 15. An annual traffic growth rate (r) is first included with an exponential factor of

the time interval (t) between successively generated events, i.e., $(1 + r)^t$. Then the effects of demand elasticity depend on the uncongested O/D travel time from the baseline simulation and on periodic information collected within simulation runs.

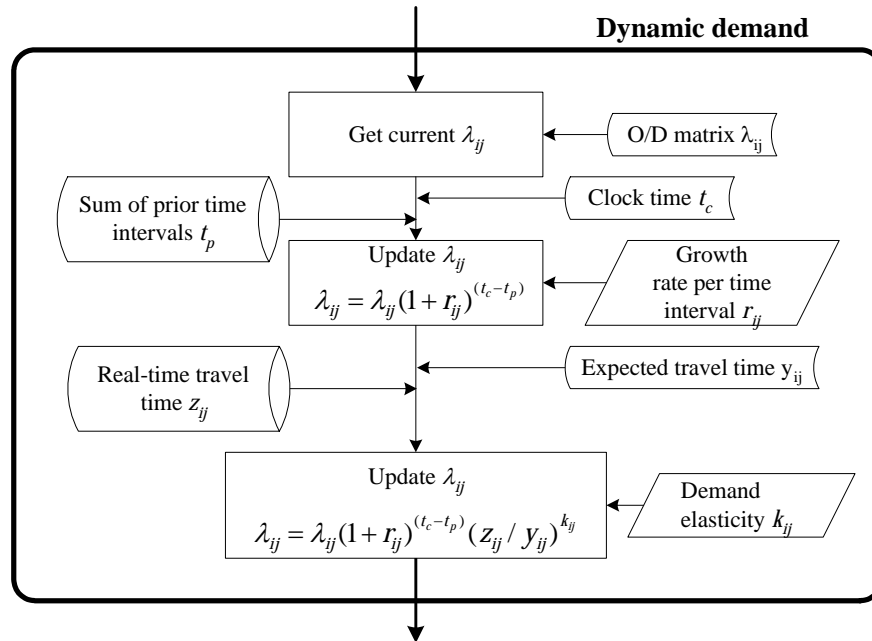


Figure 15 Dynamic Demand Module

Expected O/D travel time is simply acquired from a simulation base case, where a free-flow steady demand is considered over time and the O/D travel time is collected and averaged from all O_i/D_j trips. However, while gathering real-time information, it is possible to not have enough direct O/D travel time data for each O/D pair within a specified time period. Thus, in order to avoid the shortage of statistical data of O/D trips, the information on real O/D travel times is calculated indirectly from the summations of link travel times and lock processing times. Lock processing time includes regular lock service time and delay time in queue, which is the main factor influencing the launching decision for the next tow trip. Through normalization, defined as the ratio of real travel time (z) and base-case expected travel time (w), z/w , the traffic rates (or, equivalently, the time intervals between generated tows) can be updated by the normalized factor $(z/w)^k$, where k is the demand elasticity.

Based on predicted traffic growth, the O/D matrix values increase continuously at annual growth rates which may differ for various O/D pairs. Furthermore, if updated O/D travel times are provided to users during the simulation, the O/D matrix is changed based on the newly updated travel times and applicable elasticities.

Test Network

A simple test network is used here for testing proposed simulation-based optimization model (as shown in Figure 16). There are 3 rivers, 5 ports, and 7 locks (4 single-chamber

locks and 3 double-chamber locks). Locks are numbered with ID's 0, 1, 2, 3, 4, 6, 7. Locks #5 and #8 are dummy locks. (The network configuration is from Wang, 2002.) Not all locks require improvement projects, but all improvement projects are located at real locks. The lock congestion level from baseline simulation is $7 \rightarrow 1 \rightarrow 6 \rightarrow 0 \rightarrow 2 \rightarrow 4 \rightarrow 3$, which is ranked from the highest V/C (volume capacity ratio) to lowest V/C.

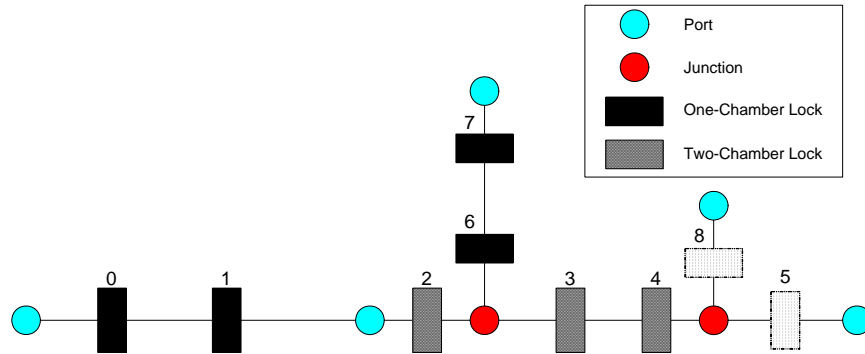


Figure 16 Test Network for SIMOPT Extension

Model Inputs

Simulation inputs include network statistics (O/D trip generation rates, tow size distributions, chamber service time distributions and speed distributions), lock operation (FIFO control, towboats priority, lockage cuts, chamber assignment and chamber bias), demand variables (baseline O/D travel time, annual growth rates), and system variables (simulation period, warm-up period, number of replications) (Wang, 2005). The basic project-relevant inputs include regional budget rate, project ID, costs, capacity expansion/residual ratios, and precedence relations (as shown in Table 1). The regional budget constraints limit the project funds in each region: $\$40 \times 10^6$, $\$70 \times 10^6$, $\$40 \times 10^6$ annually for regions 1, 2, and 3, respectively. The budgets are uniformly distributed within each year. For example, the alternative projects at locks #7, #2, and #6 are funded annually by the 2nd regional budget, 70×10^6 .

There are two kinds of precedence constraints. One limits the sequence of locks receiving improvement projects, and the other restricts the order of projects at the same lock. For example, all the projects at lock #6 should be funded before all the projects at lock #2 and #3. Projects #4, #7 and #12 must follow the completion of project #2, #6 and #11, respectively.

Table 1 Project Information

Project ID	Lock ID	Region Code	Capacity Expansion Ratio	Cost ($\times 10^6$)	Lock Precedence Relations	Project Precedence Relations
1	7	2	1.2	17		
2	7	2	1.5	20		2→4
3	7	2	1.8	23		

4	7	2	2.0	27		2→4
5	1	1	1.2	16		
6	1	1	1.5	20		6→7
7	1	1	2.0	26		6→7
8	6	2	1.5	27	6→3, 6→2	
9	6	2	2.0	33		
10	0	1	1.2	20		
11	0	1	1.5	12		11→12
12	0	1	2.0	29		11→12
13	2	2	1.1	32	6→2	
14	2	2	1.2	35		
15	4	3	1.1	25		
16	4	3	1.2	27		
17	4	3	1.3	31		
18	3	3	1.1	35	6→3	

In order to accelerate the analysis, a high budget flow is specified. 10 replications are used here to complete one simulation evaluation of any candidate solution (i.e., generated project sequence and resulting schedule). The GA population size per generation in this test is set at 500 or 1000 based on the problem size. An interest rate of 4% and an average time value of \$450/tow-hour are assumed. In the evolution process, if the generated sequence violates a constraint, its fitness value is assigned a large cost (or zero benefit) and is unlikely to be selected as a parent for next generation.

The termination rule for GA search is set when the optimized solutions stays unchanged for 50 generations. Mutation and crossover rates are 0.7 and 0.3, respectively. Since parallel computing is tested in this phase, all the tests are run in parallel on several Pentium IV processors with 3.2 or 3.6 GHz CPU, and 1 or 2 GB memory, depending on the availability of computer resources.

Test Results

Adding Constraints (Multiple Projects with Different Implementation Time)

In this test, multiple projects are considered at some lock locations, and all projects will be funded at different times. Therefore a full implementation sequence with 18 projects is sought in this test: 4 alternatives at lock #7, 3 alternatives at lock #1, 2 alternatives at lock #6, 3 alternatives at lock #0, 2 alternatives at lock #2, 3 alternatives at lock #4, and 1 alternative at lock #3. Without mutual exclusivity constraints for projects at some locks, the solution space is $18! = 6,402,373,705,728,000$. However, with 2 lock precedence constraints and 3 project precedence constraints, the solution space is further reduced to $(C_7^{18} \times 7! \times 3! \times 2!) = 1,924,715,520$.

Due to increased problem size, restricted memory and search time within one computer are of concern after searching through several generations. Thus PGAs are used in these tests in order to alleviate the memory loads for each computer and also reduce the search time for a near optimal solution.

In this test, each feasible solution is simulated 10 times with different random seeds. A fitness value is calculated by averaging those 10 evaluations. Penalties (e.g. large costs) are directly assigned to the infeasible solutions (i.e. those that violate constraints) before any simulation is used to evaluate them. For any generation, parents are selected based on the ranks of their fitness values. Individuals with large cost are less likely to be selected to produce offspring. For GA, since the solution space is huge, population size for each generation starts with 500 and the overall search is ended when optimized solution stays unchanged for 100 generations.

With those pre-specified parameters, the optimized results of 20 GA search processes with different random seeds are shown in Table 2. The inherited stochastic features in GA result in various values in the search process, such as number of generations required to locate optimized solution, number of total generated sequences in any search, and number of evaluated sequences which go through simulations. The optimized results from different GA searches are also slightly different (approximately 1% difference between \$647,830,771, \$655,890,781, \$655,902,872, and \$655,916,715) but should be very close to the lower-cost tail of the distribution of solutions. The lowest cost found as \$647,830,771 is found from 5 GA searches. The optimal sequence for these 5 GA searches is 8 → 5 → 2 → 16 → 11 → 4 → 6 → 9 → 18 → 14 → 7 → 15 → 13 → 3 → 12 → 17 → 1 → 10.

Approximately 3.7 ~ 3.8 hours are required for completing one generation on 6 parallel computers (Pentium IV 3.2 or 3.6 GHz, 1 or 2 GB memory). Total search times vary for different GA searches and are based on the number of generations required to find their optimized solutions. Significant improvements in the time needed to obtain results from simulation-based optimization process result from applying parallel computing. Without PGAs, more than a week might be required for each GA search for this problem. The larger the problem, the more valuable the PGAs become.

Table 2 Optimized Results (Minimization Problem)

GA Search	# of Gen.	# of Generated Sequences	# of Evaluated Sequences	Optimal Total Cost (\$)	Search Time (sec)
1	132	126,463	4,265	655,916,715	75,714
2	226	216,368	6,370	647,830,771	118,622
3	136	130,245	4,382	655,902,872	77,704
4	141	135,242	3,676	647,830,771	50,332
5	169	161,628	4,731	647,830,771	61,476
6	111	106,343	3,389	664,294,640	51,666
7	138	132,360	4,313	655,902,872	64,808
8	134	128,106	4,330	657,931,927	64,566

9	147	140,863	4,105	653,778,575	60,811
10	140	133,988	3,964	655,902,872	60,041
11	158	151,415	4,028	647,830,771	60,510
12	120	114,987	3,766	655,902,872	56,039
13	159	152,350	4,830	657,931,927	72,601
14	223	213,243	7,569	655,916,715	113,584
15	218	208,326	6,663	655,890,781	99,610
16	126	120,793	3,650	672,879,681	55,085
17	148	141,731	4,291	647,830,771	64,208
18	202	193,169	6,038	655,890,781	91,451
19	150	143,759	5,026	655,916,715	75,019
20	239	228,611	6,968	664,294,640	104,802

The evolution of objective values from 4 GA searches (searches #3, #14, #15 and #18) which have more than 200 generations is plotted in Figure 17. Though four searches converge with slightly different optimized solutions (approximately 1% difference), the optimized solutions improve relatively quickly in early generations and converge at the end of genetic search.

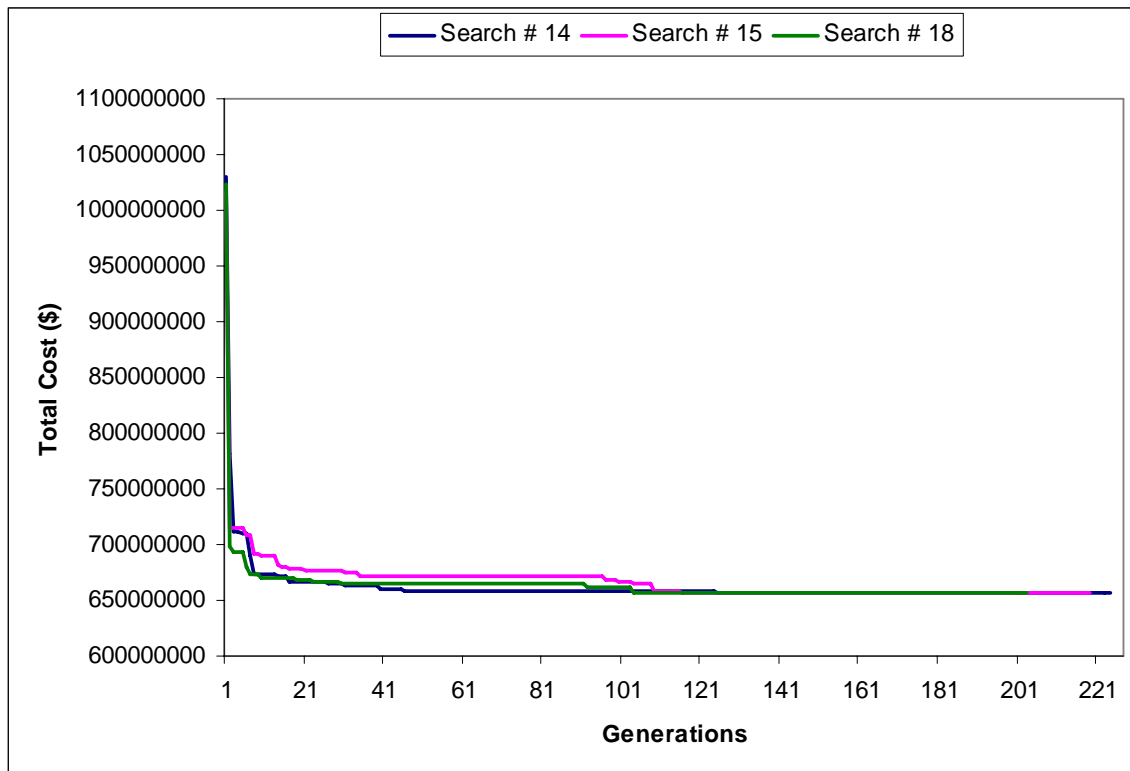
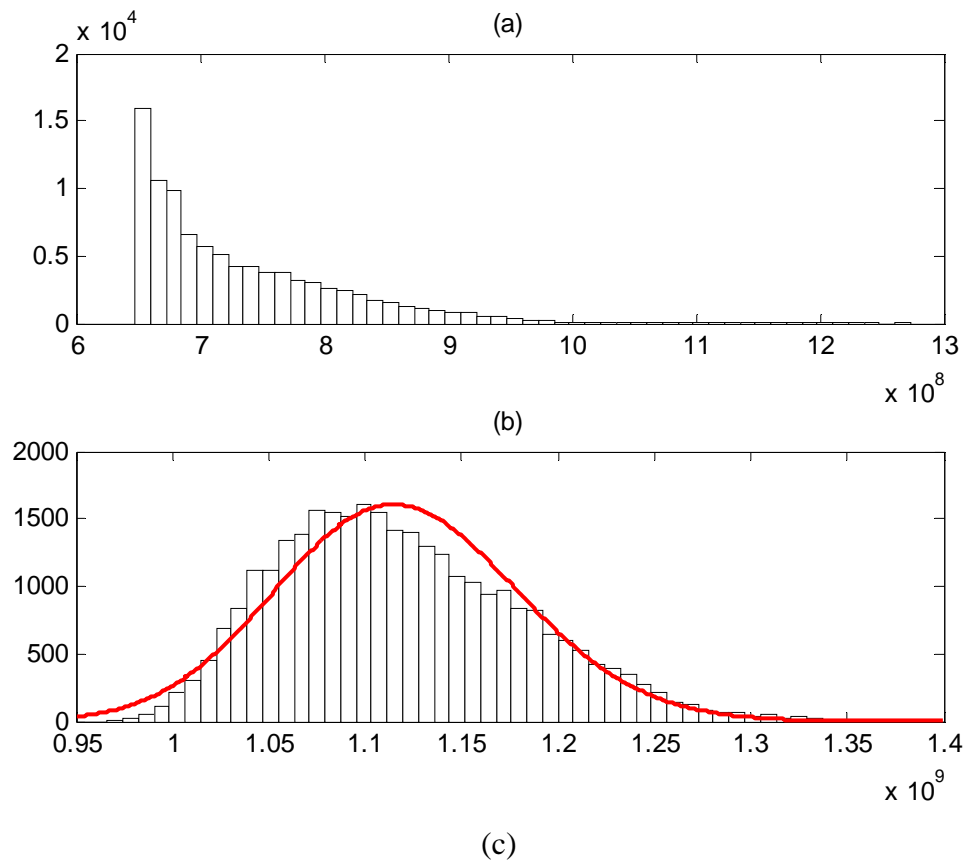


Figure 17 GA Search Performance (Minimization Problem)

Figure 18(a) shows the solution distributions (i.e. histogram of solutions) throughout the GA search process. A total of 93,774 feasible solutions are generated from 20 GA searches with a mean of 7.3122×10^8 and standard deviation of 7.7979×10^7 . In each GA procedure, in addition to solutions created in the initial population, new solutions are all

created as offspring from selected parents from previous generations and specified mutation/crossover operators. Thus, except for the solutions in initial population which are generated randomly, the newly generated solutions from reproduction process are no longer created randomly in the solution space. The created offspring are highly related to the selected parents who have better fitness values and higher chances to survive in the evolution process. Compared with the solution distribution (shown in Figure 18(b)) based on 30,547 randomly generated feasible solutions (out of 1,000,000 random solutions), the GA changes the random search to a smarter search which search solutions in the domain which contain solutions with better fitness values. Thus, the GA process should have already directed toward on the search more efficiently to optimal solution.

Figure 18(c) further jointly shows density functions for two solution distributions. The histograms on the left and right sides are for the solutions produced in GA search and in random search, respectively. As can be seen, the GA process directs the search into the domain with lower cost with a mean of 7.3122×10^8 . Very conservatively, based on the fitted normal distribution with a mean of 1.1182×10^9 and standard deviation of 6.303×10^7 , the mean of GA solution set is located in the tail far away from the mean of random solution set (more than 6 standard deviations). The optimal solutions found from different GA searches are further away in the tail. It is estimated that the probability of finding a solution better than optimal solutions found by the GA is extremely low, i.e., very close to zero.



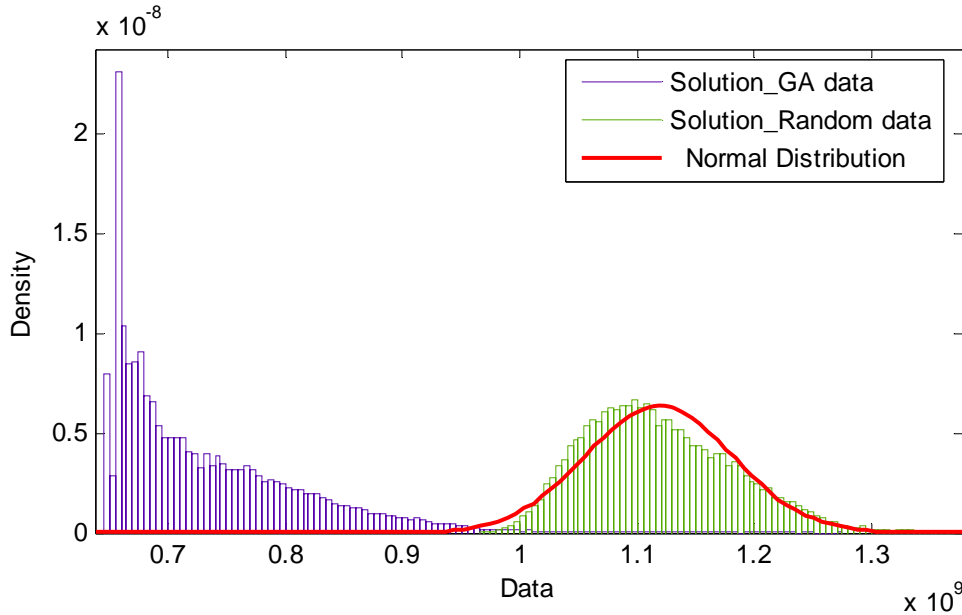


Figure 18 Solution Distributions

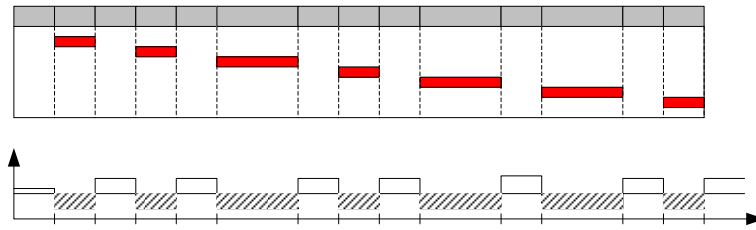
Measuring Net Present Worth with Dynamic Demand

Table 3 shows the information on scheduled work (such as construction projects or maintenance tasks which require partial lock closures) at locks, including work schedule, closure duration, residual capacity ratio during the closure period, and improved capacity ratio after the work completion. Lockage rates vary and lockage times vary in SIMOPT inversely with the residual ratio. Thus, if the residual capacity ratio is 0.5, the service time will double. In this case, closures for different projects occur at different times. A two-year period is simulated, after running a one-year warm-up period to populate the network with traffic and approach a steady-state. With a given schedule of lock closures, O/D traffic responds to the simulated service level based on the given elasticity coefficients. Thus, the total user benefit and total costs are computed from simulation outputs. Throughout the simulation (for each weekly period), user travel times (including delays) and user benefits (integrated from demand functions) are recorded so that aggregate performance measures can be computed at the end of the simulated period by summing individual movements. By tracking individual movements, total costs are summed at the end of simulation.

Table 3 Work Information and Schedule

Lock ID	Work Schedule (yr)	Work Duration (yr)	Residual Capacity Ratio	Improved Capacity Ratio
0	0.1	0.1	0.5	1.2
1	0.3	0.1	0.5	1.2
2	0.5	0.2	0.7	1.5
6	0.8	0.1	0.5	1.2
3	1.0	0.2	0.7	1.5

4	1.3	0.2	0.7	1.5
7	1.6	0.1	0.5	1.2



Four designed scenarios are tested: with or without capacity reductions (i.e., closures) during construction work, and with or without demand elasticity. The capacity reductions during closures are expected to greatly increase costs. During such periods, service rates should greatly decrease and queuing delays should greatly increase. Projects that increase lock capacity would reduce delays and, if demand is elastic, increase subsequent traffic.

#2

Figure 19 shows the simulated cost and benefit outputs from four different scenarios with a summary table on the top. The elasticity coefficient k is 0.1 for all for scenarios that consider elasticities. Figure 19(a) shows the cumulative costs over the simulation time for the four scenarios. Scenarios with closures have much higher total costs than those without. Since work projects reduce the impedance to traffic, scenarios with elasticity have greater traffic after the work and hence greater total costs (but also greater benefits). Figure 19(b) shows monthly changes in average cost based on the first scenario, considering closure and demand elasticity. Early in the simulation period, user cost may increase due to closures. As more completed projects add capacity at locks, traffic experiences less impedance and incurs less cost. Figure 19(c) compares the cumulative benefits of scenarios with and without demand elasticity. Those with elasticity yield lower benefits by having traffic respond to travel times. Along the simulation time, traffic grows as more works are completed. Figure 19(d) shows the monthly benefits over the simulation time based on the first scenario.

0.7 0.8

Scenarios	Simulation Outputs		
	Total Tows in System	Total Cost (\$)	Total Benefit (\$)
(1) w/ closure, w/ elasticity	804,529	2.03×10^9	1.26×10^{10}
(2) w/ closure, w/o elasticity	732,561	1.69×10^9	2.64×10^{10}
(3) w/o closure, w/ elasticity	672,947	1.25×10^9	1.27×10^{10}
(4) w/o closure, w/o elasticity	554,299	6.66×10^8	2.64×10^{10}

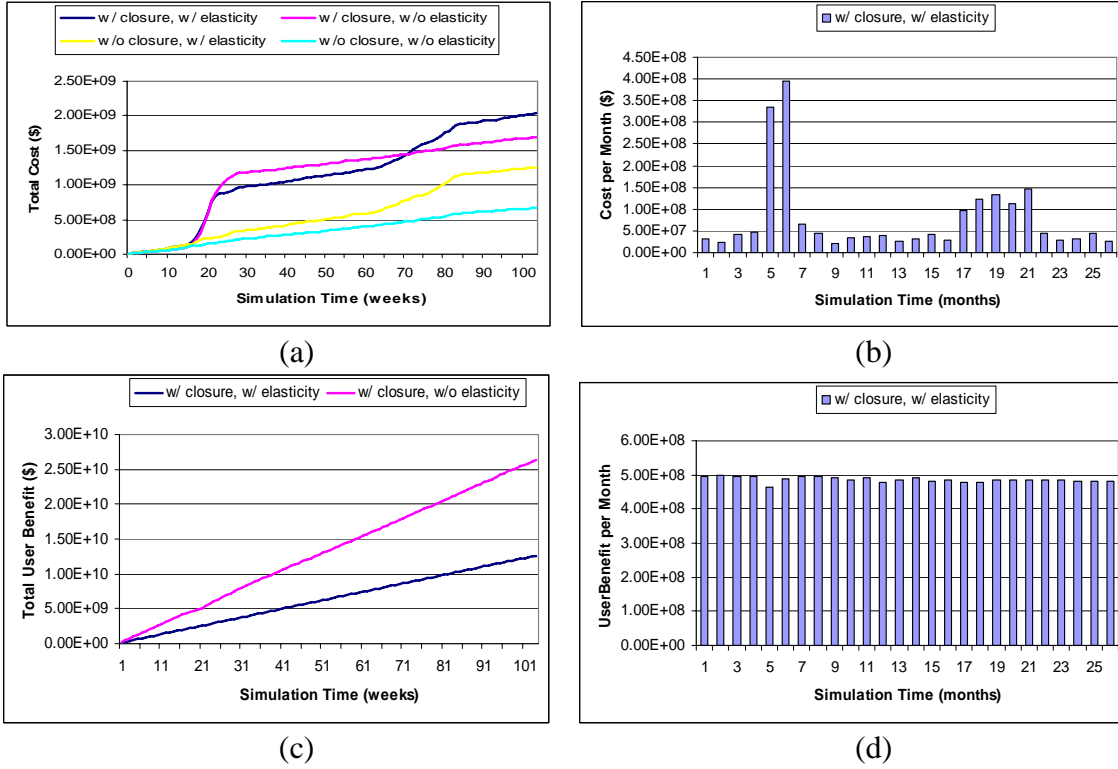


Figure 19 Simulation Outputs w/ and w/o Demand Elasticity

Including Construction Time and Capacity Reduction

Construction time and residual capacity ratio are included in the project information shown in Table 4. Some construction requires total or partial lock closures. That is, during the construction period, capacities at some locks decrease based on the relevant residual capacity ratios. Afterwards, the capacities increase based on capacity expansion ratios when improvement projects are completed. The tests are still subjected to all the project precedence and lock precedence constraints shown in Table 1.

Table 4 Project Information (continued from Table 1)

Project ID	Lock ID	Capacity Expansion Ratio	Cost ($\times 10^6$)	Construction Time (year)	Residual Capacity Ratio
1	7	1.2	17	0.09	0.8
2	7	1.5	20	0.10	1.0
3	7	1.8	23	0.13	0.8
4	7	2.0	27	0.17	0.2
5	1	1.2	16	0.04	0.8
6	1	1.5	20	0.05	1.0
7	1	2.0	26	0.09	0.5
8	6	1.5	27	0.10	0.8
9	6	2.0	33	0.12	1.0

10	0	1.2	20	0.09	0.8
11	0	1.5	12	0.10	1.0
12	0	2.0	29	0.11	0.5
13	2	1.1	32	0.03	0.8
14	2	1.2	35	0.05	0.8
15	4	1.1	25	0.01	1.0
16	4	1.2	27	0.05	0.5
17	4	1.3	31	0.09	0.2
18	3	1.1	35	0.04	0.5

As discussed above, since more traffic delays are expected when lock capacity is reduced, dynamic demand should be estimated in the simulation model to avoid infinite queues during the construction periods. Therefore, in this scenario, a net benefit maximization approach is formulated to solve this optimization problem. Fitness values measured from simulation model are the net benefits (as shown in previous section), rather than total costs. In this analysis, the construction costs need not be explicitly subtracted from the benefits (in order to obtain net benefits) because the same construction costs as limited by the budget constraints, are spent over a given analysis period, regardless of the project sequence that is evaluated.

In a minimization problem, large penalty values are assigned to the infeasible solutions which violate any of constraints. In a maximization problem, zero benefits are assigned to those infeasible solutions. Based on the ranks of fitness values, individuals with zero benefits still have very slight chances of being selected as parents to produce offspring for next generation.

The optimized results and evolution processes from 5 searches are shown in Table 5 and Figure 20. The optimal sequence shown in first GA search, $2 \rightarrow 6 \rightarrow 15 \rightarrow 8 \rightarrow 11 \rightarrow 9 \rightarrow 16 \rightarrow 3 \rightarrow 7 \rightarrow 4 \rightarrow 17 \rightarrow 14 \rightarrow 12 \rightarrow 13 \rightarrow 18 \rightarrow 10 \rightarrow 1 \rightarrow 5$, is the best one among these 5 searches with largest net benefits.

Table 5 Optimized results (Maximization Problem)

GA Search	# of Gen.	# of Generated Sequences	# of Evaluated Sequences	Optimal Total Net Benefit (\$)
1	165	158,067	4,358	9,445,148,835,840
2	290	277,410	6,267	9,428,852,275,200
3	254	242,991	5,264	9,450,640,465,920
4	161	154,075	3,685	9,443,086,110,720
5	147	140,805	3,137	9,427,986,063,360

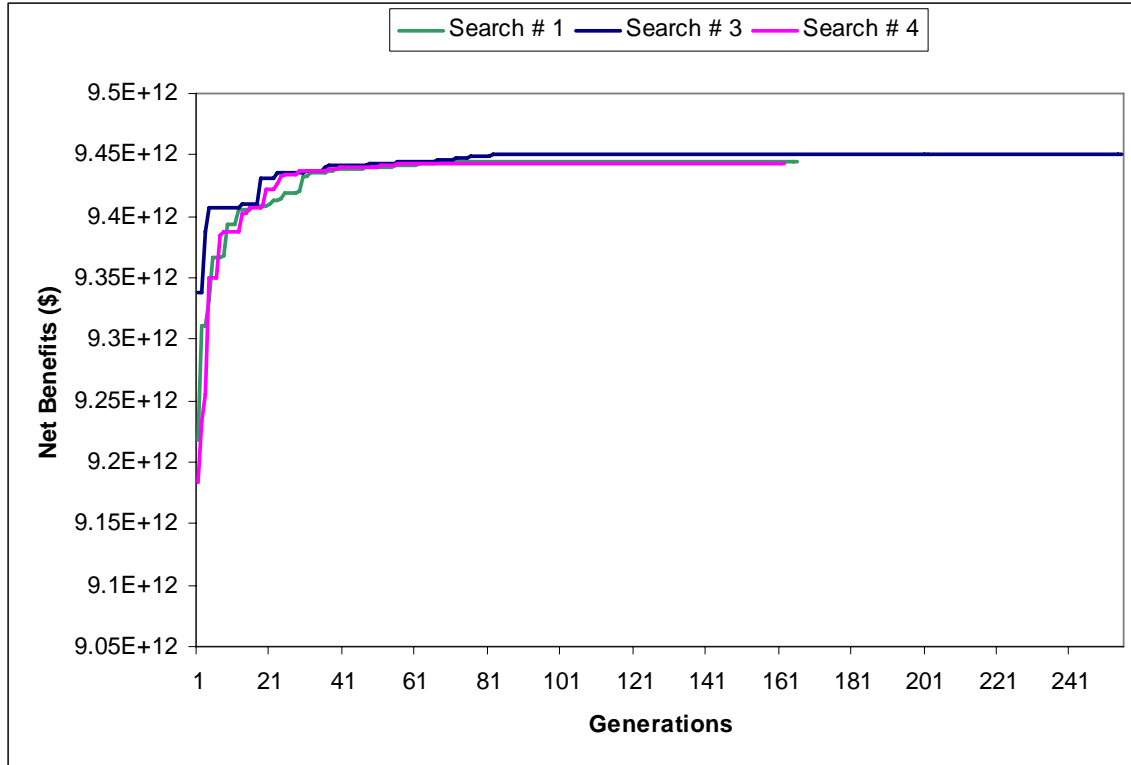


Figure 20 GA Search Performance (Maximization Problem)

The new optimal sequence is entirely different from that found in the previous scenario that does not consider construction closure and capacity reduction during the construction periods, as shown in Table 6. It is important that the implementation decision for improvement projects is strongly based on the total benefits as well as the total costs. The shippers’ response to any possible service interruption has significant effects on overall network performance and resulting optimal project sequence.

Table 6 Comparison of Optimal Project Sequences

CT & CR	Optimized Sequences
w/o	8→5→2→16→11→4→6→9→18→14→7→15→13→3→12→17→1→10
w/	2→6→15→8→11→9→16→3→7→4→17→14→12→13→18→10→1→5

* CT: construction time; CR: capacity reduction

Tradeoffs between Construction Times and Costs

If the tradeoffs between construction times and costs are considered, more project information is required, such as detailed ID information (including alternative ID, project ID and lock ID), and tradeoff alternatives among construction costs and times (as shown in Table 7). When construction times are considered, the effects of partial lock closures with residual capacity ratios must also be considered. Shorter closure times would usually require higher construction costs.

As discussed above, tradeoff alternatives between construction times and costs can be considered as mutually exclusive alternatives for any project (for example, project #1 has 2 construction cost/time alternatives, project #2 has 3 construction cost/time alternatives, etc). That is, only one alternative is selected for any single project. In this case, 18 out of 42 alternatives are selected for 18 projects. After prescreening the generated solutions based on the precedence constraints, the simulation model is used to evaluate the feasible solutions and zero benefits are directly assigned to infeasible solutions.

Table 7 Project Information (continued from Tables 1 and 3)

Project ID	Alternative ID	Cost ($\times 10^6$)	Time (years)		Project ID	Alternative ID	Cost ($\times 10^6$)	Time (years)
1	1	17	0.09		10	23	20	0.09
1	2	15	0.10		10	24	30	0.06
2	3	20	0.10		11	25	25	0.10
2	4	15	0.13		11	26	20	0.13
2	5	10	0.20		11	27	30	0.08
3	6	23	0.13		12	28	29	0.11
3	7	20	0.15		12	29	35	0.09
4	8	27	0.17		12	30	40	0.08
4	9	20	0.23		13	31	32	0.03
4	10	30	0.15		13	32	48	0.02
5	11	16	0.04		14	33	35	0.05
5	12	12	0.05		14	34	44	0.04
6	13	20	0.05		15	35	25	0.01
6	14	25	0.04		15	36	20	0.02
6	15	30	0.03		16	37	27	0.05
7	16	26	0.09		16	38	35	0.04
7	17	20	0.12		17	39	31	0.09
7	18	30	0.08		17	40	27	0.10
8	19	27	0.10		18	41	35	0.04
8	20	30	0.09		18	42	42	0.03
9	21	33	0.12					
9	22	40	0.10					

In this test, there are two categories of solutions, random-order solutions and weighted-order solutions. That is, in the initial population, one half of the sequences are generated with random order and the other half are generated based on projects' priorities which are defined as lock congestion levels. Projects at the same lock are assumed to have the same priorities. In the selection process, new solutions, if necessary, are also generated with the projects' priorities. If multiple projects are considered at the same lock, the same priorities are assigned to those projects. Additionally, two "smart" mutation operators, PM and GM, designed for this specific problem (as discussed in previous section) are added to the process of creating offspring, to further refine some of the offspring based on specified probabilities. It is assumed that the prioritized individuals and "smart" operators help expedite the search process.

The optimized results from one single search (i.e., one random seed) are shown in Table 8 based on “smart” GA and “standard” GA, respectively. The resulting optimal sequences and schedules are presented with listed alternative IDs and their relevant project IDs and lock locations. As can be seen from this single search, “smart” GA by adapting weighted sequences and problem-specific operators can find better solution, with higher net benefits, than “standard” GA does. Again, the optimal sequence found in this scenario is entirely different from that found in the previous scenario without tradeoff alternatives. This indicates that the implementation decision changes if available resources (e.g. time and cost) change.

Table 8 Optimized Results

	Number of Generation	Optimized Total Net Benefit (\$)
“Smart” GA	272	9,521,229,404,160
“Standard” GA	273	9,506,448,046,080

“Smart” GA			“Standard” GA		
Alternative ID	Project ID	Lock ID	Alternative ID	Project ID	Lock ID
15	6	1	24	10	0
2	1	7	12	5	1
20	8	6	20	8	6
28	12	0	5	2	7
5	2	7	13	6	1
12	5	1	21	9	6
21	9	6	39	17	4
26	11	0	26	11	0
42	18	3	10	4	7
6	3	7	36	15	4
17	7	1	16	7	1
36	15	4	34	14	2
8	4	7	32	13	2
32	13	2	41	18	3
33	14	2	28	12	0
38	16	4	6	3	7
40	17	4	1	1	7
24	10	0	37	16	4

Other GA Applications for Waterway Operations

The optimization based on evaluating objective functions with simulation is becoming feasible but computation time is crucial. With the advantage of advanced computer resources (e.g. faster CPU) and techniques (e.g. parallel computing), other applications of simulation-based optimization for waterway operations becoming feasible, such as

network-level or lock component-level maintenance planning, in addition to the capital investment discussed earlier

In order to apply the current methodology on waterway maintenance planning, modifications in the objective function and cost structure are required. Again, since the optimization method can be fully separated from the simulation model, the development efforts for these two processes can proceed concurrently. Both of them should be able to handle specific characteristics of maintenance problem.

Network Level Maintenance Planning and Scheduling

Ideally, a general objective of the maintenance planning process should be maximizing overall net benefits, including the costs and benefits associated with system failures and the performance of maintenance and repairs. Due to lock deterioration in waterway network, in addition to have capital investment on improvement projects, it is also critical to have timely maintenance to preserve navigability and safety with good lockage service. Lock stalls (e.g. downtimes) affect the waterway traffic by reducing lock capacity, increasing operation costs and interfering with lockage services. In order to lower the traffic impact over time, it is important to have scheduled maintenance to keep the condition above the threshold and provide the minimum acceptable level of service. If budgets are constrained, it is necessary to optimize maintenance scheduling over a multiyear planning period.

With scheduled maintenance, the change of lock condition over time is shown in Figure 21(a). The cyclic lock condition shows that lock deteriorating continuously over time at increasing deterioration rates. The lock condition is recovered after the maintenance is carried out. A minimum allowable condition, i.e., threshold condition, is set as the lowest tolerable lock condition, under which the lockage service is still acceptable for waterway users. If a lock's condition is below the threshold, that lock might lose its functionality and maintenance cost might possibly exceed the replacement cost. If the condition reaches 0, end of the life cycle, further maintenance will not help increase the condition to serviceable level but require reconstruction or rehabilitation. Figure 21(b) shows the change of lock condition if the maintenance durations are considered.

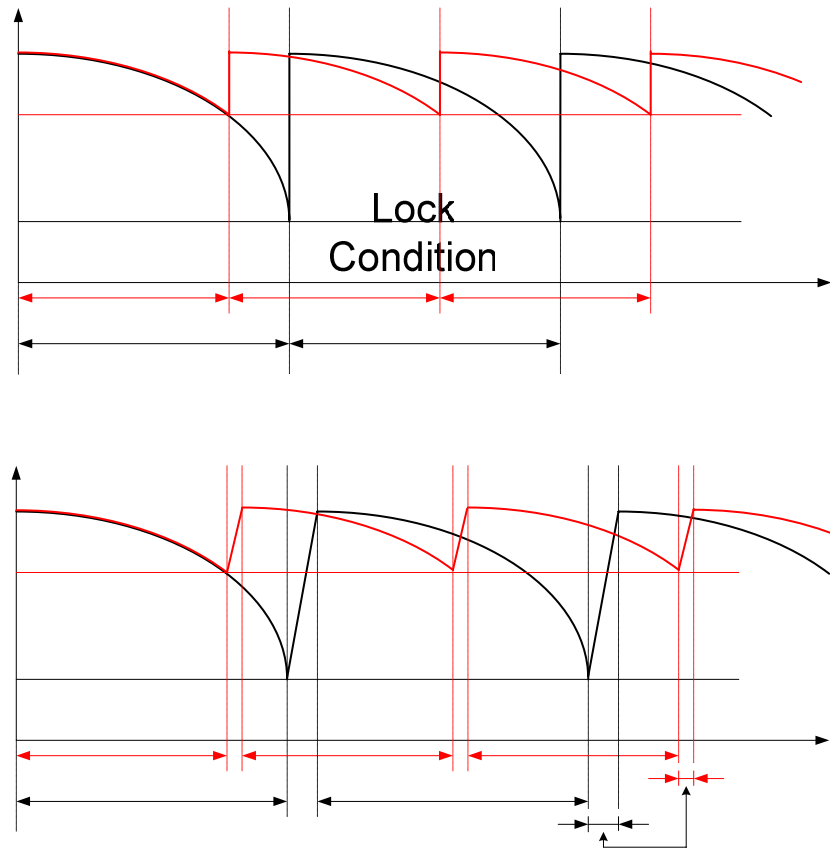


Figure 21 Lock Condition Change with Scheduled Preventive Maintenance

There may be different maintenance cycles associated with different lock conditions. With a shorter cycle, a shorter maintenance duration is needed due to the lower deterioration, thus resulting in less traffic impact. However, it is undesirable to have very frequent maintenance, that is, with very short maintenance cycle, since there is a fixed cost associated with each maintenance project.

Since the intent of preventive maintenance is to improve the locks from a lower condition to higher one, the cost for preventive maintenance, that is, routine maintenance, increases over time due to the severity of deterioration at locks. As shown in Figure 22(a), scheduled preventive maintenance cost generally consists of an initial cost and a variable cost which may be proportional to the recovery level from the current lock condition to original lock condition. The variable cost increases with increasing slopes. Since we have a maintenance budget flow (\$ per year), the maintenance schedule for each single lock may be determined based on the expected maintenance cost and the cumulative maintenance budget. As shown in Figure 22(b), for any single lock, its maintenance schedule is determined when the cumulative maintenance budget is available for this lock and equals the maintenance cost at that time.

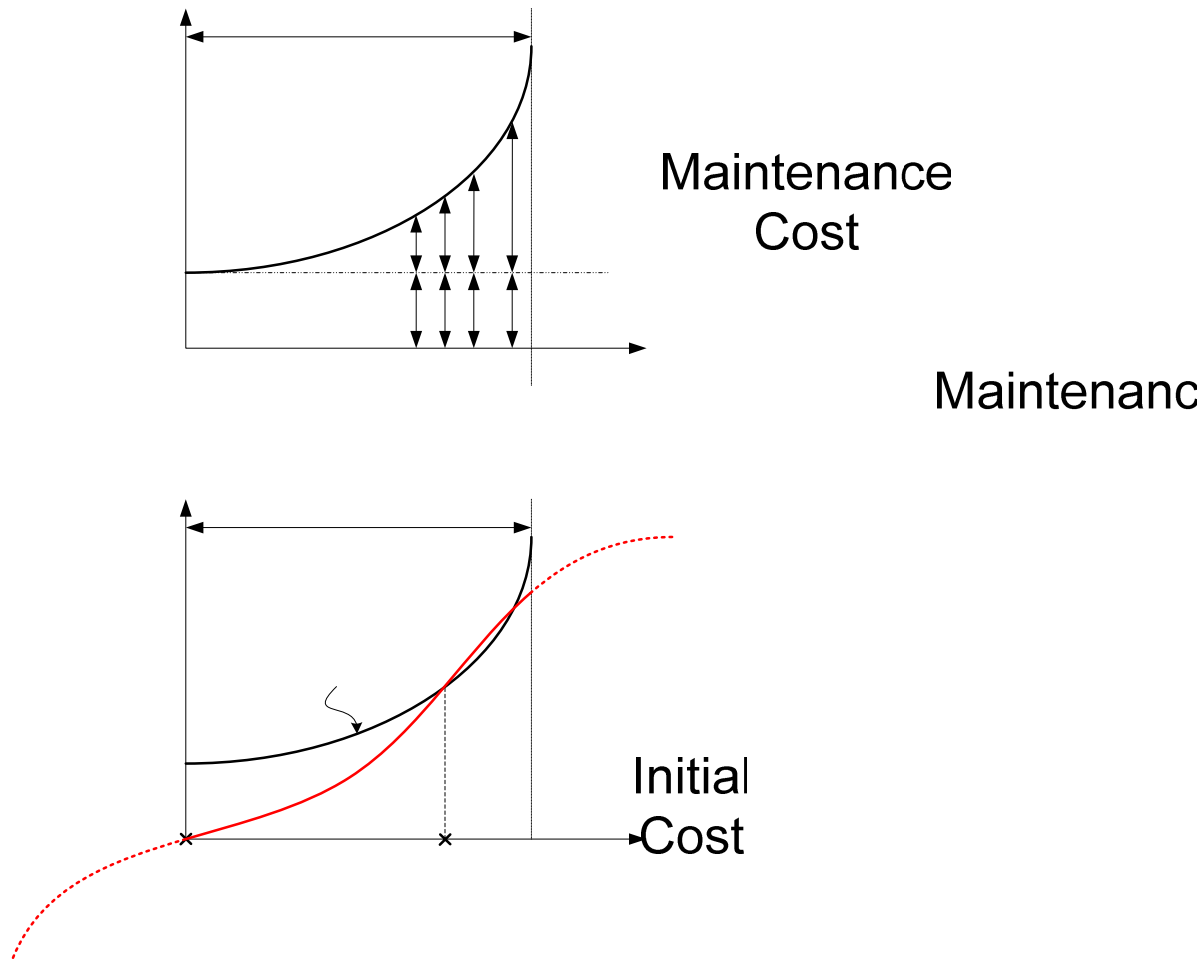


Figure 22 Maintenance Cost and Maintenance Schedule

If the i^{th} maintenance cost is function of time, $f_i(t)$, plus its initial cost $(C_{IC})_i$, for a given maintenance sequence, the time at which each maintenance task is finished can be obtained by comparing the available maintenance budgets and required maintenance costs if budget constraints are binding. Then let o_i denote the i^{th} maintenance task to be implemented in chronological order and t_i^o denote the time at which o_i is finished. Then

t_i^o can be determined by solving the equation, $(C_{IC})_i + f_i(t) = \int_{t_{i-1}^o}^{t_i^o} b(t) dt$, to get time schedule t . The maintenance cost $f_i(t)$ is then determined by t . Although there may be more than one point where the two curves cross, the first intersection is selected for the maintenance schedule when budget constraints are binding.

In addition to normal deterioration over time due to natural wear and tear at locks, such as decreasing channel depths, rusting elements, crumbling guide walls, etc., it is possible to have operational failures due to mechanical or electrical failures on opening/closing valves, gates, pumping water, etc. Those random failures are related to the reliability

problems. There is a tradeoff between scheduled preventive maintenance and unscheduled corrective maintenance, e.g., recovery from random failures. With earlier or more frequent preventive maintenance, the lock failures are less likely. Thus, the failure frequency and expected restoration effort are related to the lock condition. As shown in Figure 23(a) and (b), failure probability and expected failure recovery cost increases over time during the maintenance cycle. When the lock condition decreases to 0, the failure probability is 1 and it is time for reconstruction or rehabilitation. The values and curves of failure probability and expected restoration cost will be reset for each maintenance cycle.

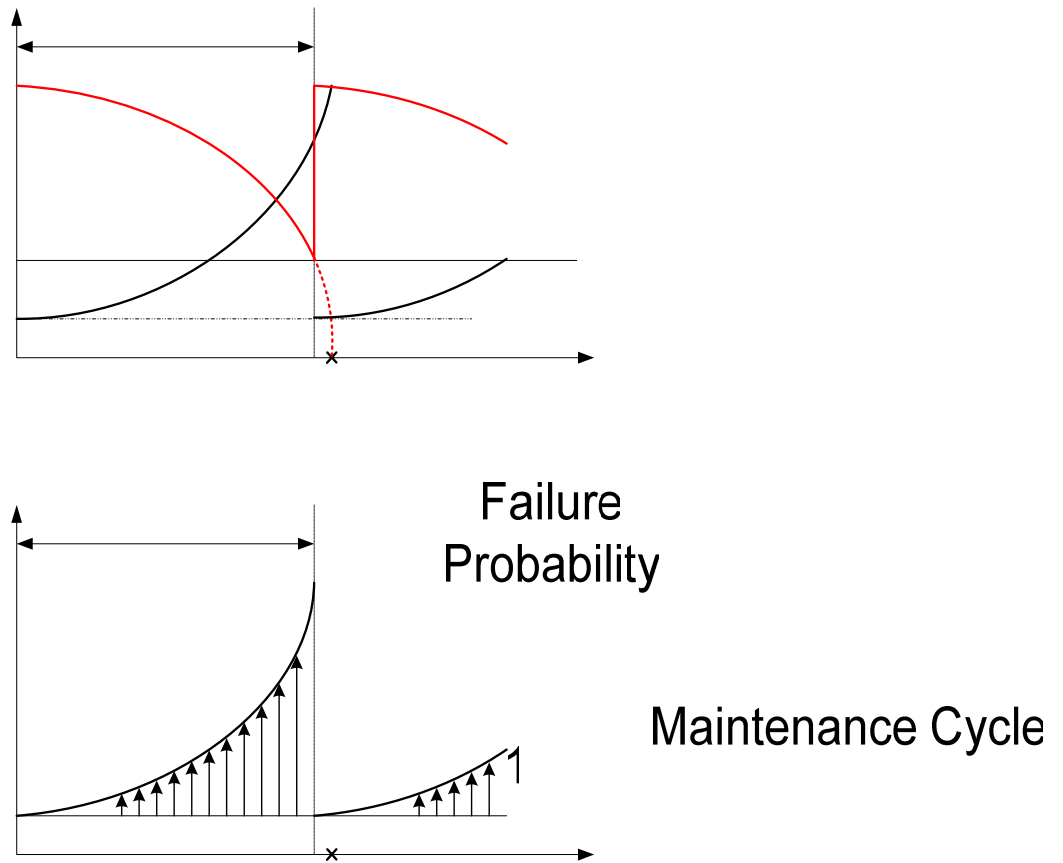


Figure 23 Lock Failure Probability and Recovery Cost

Since a simulation model is used to evaluate the maintenance plan in this study, some modifications in SIMOPT are necessary. First, the simulation model used for network-level lock maintenance should be able to handle the increasing service times due to the condition deterioration at locks, e.g. decreasing capacity. Besides, it is expected that locks/chambers must close for a certain period, i.e., lock/chamber capacity decreases to zero, if there are scheduled maintenance tasks. Since capacity changes at locks affect service quality, impacts on traffic demand should be included in the simulation model.

Minimum
Allowable
Condition
0

Time for
or

Finally, since there are risks of facility failures which result from insufficient preventive maintenance, the simulation should model random failures and the relevant traffic impacts. The required restoration cost will definitely take a fraction of the regular maintenance budget and change the maintenance plan. In order to simplify the maintenance application at the current stage, random failures related to the lack of maintenance are not yet considered.

A simple test is provided here to demonstrate how the optimized maintenance schedule is determined with SIMOPT. Usually network-level maintenance scheduling is performed for a specified period. In this scenario, the smallest unit considered for maintenance work is “chamber”. Locks with parallel chambers require two separate maintenance tasks, respectively. Table 9 shows the information provided for network maintenance. The proposed maintenance planning covers one maintenance task for each individual chamber. All chambers have their initial conditions at the beginning of planning period. With the depreciation function, chamber acquires maintenance work before its condition reaches threshold value. Thus, threshold conditions are set as constraints which enforce the maintenance to be completed before reaching the minimum operational stage.

Table 9 Network-Level Lock Maintenance Information

Maintenance ID	Lock ID	Chamber ID	Initial Condition	Threshold Condition	Restored Capacity Ratio	Life Cycle (year)
1	0	0	0.9	0.2	1.0	15
2	1	0	1.0	0.2	1.0	15
3	2	0	0.7	0.2	1.0	10
4	2	1	0.8	0.2	1.0	10
5	3	0	0.7	0.2	1.0	10
6	3	1	1.0	0.2	1.0	10
7	4	0	0.8	0.2	1.0	10
8	4	1	0.9	0.2	1.0	10
9	6	0	0.9	0.2	1.0	12
10	7	0	0.7	0.2	1.0	12

Maintenance ID	Lock ID	Chamber ID	Initial Cost ($\times 10^6$)	Maintenance Duration (year)	Residual Capacity Ratio
1	0	0	0.9	0.02	0
2	1	0	0.7	0.02	0
3	2	0	1.0	0.02	0
4	2	1	0.8	0.02	0
5	3	0	1.0	0.02	0
6	3	1	0.8	0.02	0
7	4	0	1.0	0.02	0
8	4	1	0.8	0.02	0
9	6	0	0.9	0.02	0
10	7	0	0.7	0.02	0

Chamber closures are required for almost all the maintenance tasks. For single-chamber locks, chamber closure results in total lock closure and there is no lockage service during the closure period. For double-chamber locks, a lock is still operational even one chamber is closed for maintenance. Since the maintenance is done one by one, two chambers will not be closed at the same time. During the closure period, traffic demand is elastically responding to the delays, as discussed in previous section.

A polynomial deterioration function, $c = 1 - t^3 / L^3$, is used determine chamber condition in this test, where c is current condition, t is time lag from the first installment, L is life cycle (as shown in the upper part of Figure 24). The deterioration rate is increasing over time and chambers are completely deteriorated at the end of their life cycles. Chamber service time then varies inversely with the chamber condition. That is, along the simulation time, lock service time increases as chamber condition decreases. Whenever a lockage is performed, the required service time reflects the chamber condition at that time.

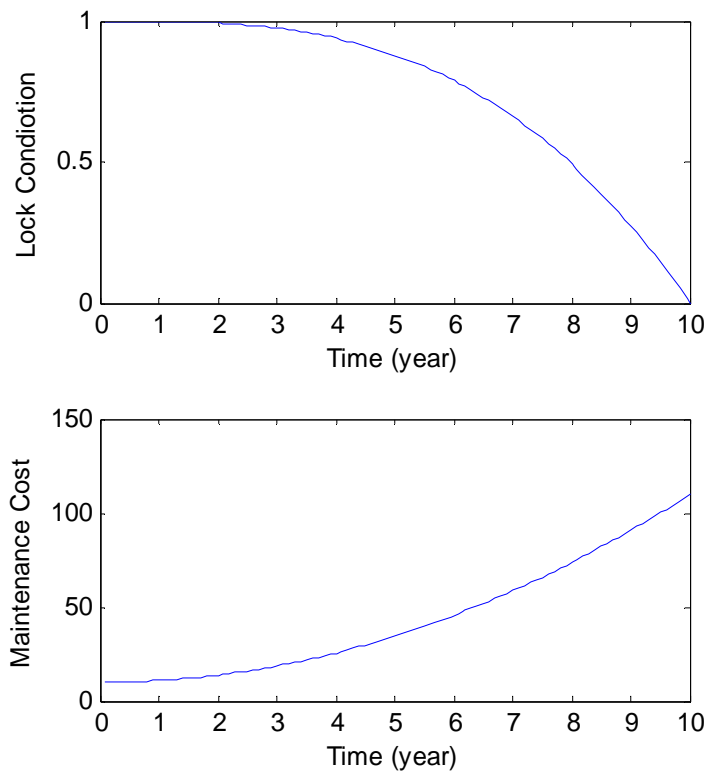


Figure 24 Lock Deterioration and Maintenance Cost Functions

A parabolic function, $C = C_{IC} + t^2$, is used for maintenance cost, where C is total maintenance cost, C_{IC} is initial cost and t is the time lag (as shown in the lower part of Figure 24). The initial cost is required for performing any maintenance task, and the marginal maintenance cost is increasing over time.

In the proposed genetic algorithm, generated sequences are the candidate solutions for maintenance planning. Whenever a sequence is generated, the maintenance schedule is then determined chronologically when the available budget for the current chamber covers its required maintenance cost. As shown in Figure 25, with binding budget, maintenance schedule for any single lock is determined when maintenance cost curve first intersect with cumulative budget curve. That is, the cumulative budget is able to cover the maintenance work at that time.

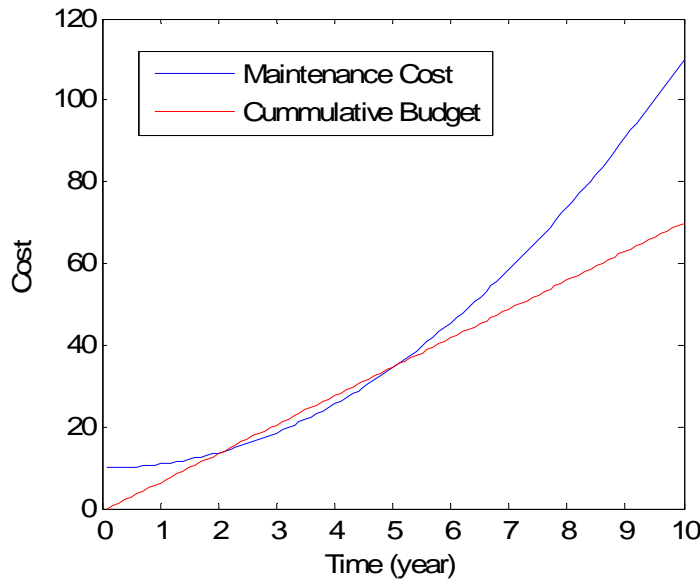


Figure 25 Maintenance Cost and Schedule

In addition, threshold constraints for each chamber are used to check a solution's feasibility. With a determined schedule, chamber conditions can be calculated based on their deterioration functions which are the functions of elapse times and initial conditions. Solutions violate the threshold constraints if any one of the chamber conditions is below its threshold condition when maintenance work is performed. Zero benefits are then assigned to all the infeasible solutions.

The optimized results from one single search are shown in Table 10. The resulting optimal sequence and schedule are presented with maintenance IDs and their relevant lock IDs and chamber IDs. Chamber conditions are described with I.C. (initial condition), C.C. (current condition), and T.C. (threshold condition). Based on the proposed maintenance schedule, required maintenance cost and current deterioration condition can be determined. As can be seen, when maintenance is scheduled, current conditions for all chambers are still above threshold conditions.

Table 10 Optimized Results for Network-Level Maintenance Planning

# of Gen.	# of Generated Sequences	# of Evaluated Sequences	Optimal Total Net Benefit (\$)
134	470	1763	1,237,038,336,000

Maintenance	Lock	Chamber	I.C	Schedule	Cost	C.C	T.C
-------------	------	---------	-----	----------	------	-----	-----

ID	ID	ID		(year)	(\$)		
4	2	1	0.8	0.38	0.9444	0.7584	0.2
10	7	0	0.7	0.70	1.19	0.6145	0.2
3	2	0	0.7	1.20	2.44	0.5080	0.2
7	4	0	0.8	1.70	3.89	0.5700	0.2
5	3	0	0.7	2.20	5.84	0.2964	0.2
8	4	1	0.9	2.57	7.4049	0.6249	0.2
6	3	1	1.0	2.95	9.5025	0.9743	0.2
1	0	0	0.9	3.39	12.3921	0.6713	0.2
9	6	0	0.9	3.82	15.4924	0.5209	0.2
2	1	0	1.0	4.15	17.9225	0.9788	0.2

Lock Component Level Maintenance Planning and Scheduling

Unlike network-level maintenance planning for locks/chambers, component-level maintenance planning is conducted for single locks in order to keep the functional and operational infrastructure elements of locks, such as gates, valves, and walls. Similarly, components have their life cycle and require periodic maintenance to sustain the level of service. Thus the relevant maintenance concepts about deterioration functions, initial/threshold conditions, and restoration costs applied in network-level maintenance planning can be employed here. Maintenance requires chamber closures for some components, but not others.

A simple test for a single lock is provided here to demonstrate how the optimized maintenance schedule is determined with SIMOPT. Table 11 shows the information provided for single lock maintenance. For any single lock, 10 components are assumed to be scheduled for maintenance.

Table 11 Component-Level Lock Maintenance Information

Component ID	Initial Condition	Threshold Condition	Restored Capacity Ratio	Initial Cost ($\times 10^6$)	Maintenance Duration (year)	Residual Capacity Ratio
1	1.0	0.5	1.0	0.9	0.005	0
2	1.0	0.3	1.0	0.7	0.007	0
3	1.0	0.4	1.0	1.0	0.003	1
4	1.0	0.5	1.0	0.8	0.004	1
5	1.0	0.2	1.0	1.0	0.005	0
6	1.0	0.3	1.0	0.8	0.002	1
7	1.0	0.4	1.0	1.0	0.008	0
8	1.0	0.5	1.0	0.8	0.007	1
9	1.0	0.2	1.0	0.9	0.003	1
10	1.0	0.3	1.0	0.7	0.005	0

At the opening of a lock, initial conditions for all components are 1.0, perfectly new conditions. The threshold conditions, maintenance cost and maintenance durations vary

among different components. Some components, such as gates and valves, play key roles in lockage process, thus requiring lock closures for maintenance work. Some components may partially or not affect lockage service and resulting lock capacity. In this test, component deterioration functions and maintenance cost functions are similar to those used in previous section.

The optimized results from 10 searches for component-level maintenance planning are shown in Table 12. All sequenced are ended with maximum net benefits of \$1,443,639,744,000. Since some component maintenance does not require any service interruption, their positions in scheduled sequence do not affect the overall evaluated system performance. In addition, if traffic is low, some very short closure for component maintenance will not affect the travel delay and benefit measurement as well. Therefore the positions of some short-term closures in a sequence are not significantly important.

Table 12 Optimized Results for Component-Level Maintenance Planning (Low Traffic)

#1	#2	#3	#4	#5	#6	#7	#8	#9	#10
2	2	2	2	2	2	2	2	2	2
10	10	10	10	10	10	10	10	10	10
5	8	6	9	1	6	5	6	8	9
3	1	5	5	8	5	6	8	9	6
4	4	8	3	4	8	4	7	7	7
8	3	9	1	3	3	3	9	3	1
9	5	7	7	9	7	1	3	4	5
6	7	1	6	6	4	8	5	6	8
1	9	3	8	5	9	9	4	1	3
7	6	4	4	7	1	7	1	5	4

A higher traffic is applied to retest this scenario. Table 13 shows the optimized results from 10 searches for component-level maintenance planning under higher traffic. All sequences are ended with maximum net benefits of \$1,443,639,744,000. As discussed above, since no service interruption is required for some component maintenance, their positions in scheduled sequence do not affect the overall evaluated system performance. Short-term closures do not affect sequences as well.

Table 13 Optimized Results for Component-Level Maintenance Planning (High Traffic)

#1	#2	#3	#4	#5	#6	#7	#8	#9	#10
2	2	2	2	2	2	2	2	2	2
10	10	10	10	10	10	10	10	10	10
5	9	6	6	8	6	3	9	3	6
3	6	5	5	1	5	5	7	7	7
4	3	8	3	6	8	6	4	1	3
8	7	9	7	3	3	8	1	6	8
9	4	7	4	9	7	7	5	9	9
6	8	1	9	5	4	1	6	5	5
1	5	3	8	7	9	9	3	4	1
7	1	4	1	4	1	4	8	8	4

Conclusions

The development of NETS methods for evaluating, prioritizing and scheduling waterway projects is continuing at the University of Maryland. A testbed waterway model (SIMOPT) that combines simulation and optimization has been developed. It employs simulation to evaluate project implementation schedules found through an evolutionary search process by Genetic Algorithms. Thus it solves the problems of evaluating, selection, sequencing and scheduling waterway improvement projects, and provides a promising demonstration of simulation-based optimization. Since the developments of simulation and optimization components are largely separable, this testbed model can be used to quickly test optimization improvements without running more detailed and longer-running simulations.

In order to enhance the search efficiency of the optimization model and consider additional constraints, some improvements in investment optimization methods are tested in SIMOPT. The improved optimization models are intended to work with the next generation NaSS waterway simulation model which is developed under USACE's NETS program. As a testbed, SIMOPT was first (in Phase I) modified to consider project construction time and capacity reductions during construction, to avoid duplicate simulations of similar or identical solutions ("solutions" consist here of project implementation schedules) and to consider mutually exclusive projects within any locks. Secondly in Phase II, additional constraints on project precedence and regional budgets can now be imposed. A simple evaluator was proposed to replace complex and time consuming simulation model while investigating search efficiencies among different genetic operators and their combinations.

In the current phase (Phase III), pre-screening rules are also used to avoid expensive simulation of unpromising or infeasible solutions. Recent improvements allow the investment model to consider multiple projects at the same location with different implementation times as well as consider project construction time and capacity reduction during the construction period, with demand elastically responding to the service quality. With elastic demand, the optimization problem is changed to maximize net system benefits rather than minimize total cost. In addition, tradeoffs between construction time and cost are considered while sequencing and scheduling project alternatives.

When considering multiple projects, which could be independent improvement projects as well as dependent expansion projects, at the same location with different implementation times, the cost relations among dependent projects should be considered. In order to cope with dependent projects, project precedence constraints, similar to lock precedence constraints, are applied to restrict the sequence of those expansion projects. With two kinds of precedence constraints, project and lock precedence constraints, which define an order of succession among projects, there are large fractions of infeasible solutions which are prescreened and discarded before being simulated.

When considering project construction time and capacity reduction during the construction, the “events” of starting and completing the projects are defined to update the system capacity during the simulation. The simulation model also considers the possibility of queue “explosion” if capacity decreases significantly during construction periods. Traffic demand is thus designed to be sensitive to the service level and adjusted automatically during the trip generation. If demand is fixed, a total cost function would suffice to compare scenarios or drive an optimization process. However, if the demand can be affected by simulated decisions, an objective function of maximizing a net benefit rather than minimizing total cost is used. Different results show how shippers’ response to any possible service interruption due to capacity reduction during the construction time has significant effects on overall network performance and resulting optimal project sequence.

When considering tradeoffs between construction time and cost, mutually exclusive constraints for combination of construction time and cost are developed. That is, only one combination of construction time and cost can be selected if there are mutually exclusive tradeoffs for the same project. Thus the newly defined chromosome contains a full list of mutually exclusive tradeoffs. Solutions with full lists of projects are not feasible when we allow at most one combination per project. Therefore, a “refining” technique is applied to create feasible solutions with lists of tradeoffs having at most one tradeoff per project. The modified SIMOPT is able to solve the problem of sequencing and scheduling project with tradeoff consideration among construction time and cost.

The simulation-based optimization method is also being applied to analyze other waterway problems, such as network-level and component-level maintenance planning. With appropriately defined project costs and performance changes resulting from projects, the modified SIMOPT is now able to optimize network or lock maintenance schedule.

GAs search performance may be improved by creating weighted sequences, developing smarter problem-specific genetic operators and applying parallel computing techniques. The feasibility of applying parallel computing to speed up the optimization process has been tested on various scenarios for scheduling waterway improvement projects. The value of parallel computing in simulation-based optimization increases significantly as the problem size and complexity increase. It greatly reduces the time needed to obtain solutions as well as the memory load for any individual computer.

References

Wang, S. and Schonfeld, P. (2002), "Development of Generalized Waterway Simulation Model for Waterway Operations", Transportation Research Board 2002 Annual Meeting (CD-ROM 02-2194)

Wang, S. and Schonfeld, P. (2005), "Scheduling Interdependent Waterway Projects Through Simulation and Genetic Optimization", ASCE Journal of Waterway, Port, Coastal, and Ocean Engineering, May/June 2005, Vol. 131, No. 3, pp. 89-97

Wang, S and Schonfeld, P., "Genetic Algorithms for Selecting and Scheduling Waterway Projects (Phase 1)", NETS Report Phase I, April 2006

Wang, S and Schonfeld, P., "Genetic Algorithms for Selecting and Scheduling Waterway Projects (Phase 2)", NETS Report Phase II, November 2006

Yang, N and Schonfeld, P., "Parallel Computing in Waterway Optimization", TSC Report, University of Maryland

Tao, X. and Schonfeld, P. (2006), "Selection and Scheduling of Interdependent Transportation Projects with Island Models", Transportation Research Record

Wang, S. and Schonfeld, P. (2007), "Demand Elasticity and Benefit Measurement in a Waterway Simulation Model", Transportation Research Board 2007 Annual Meeting (CD-ROM 07-2579)

Tien, S. and Schonfeld, P. (2006), "Duration versus Costs Tradeoffs in Work Zone Optimization", Transportation Research Board 2006 Annual Meeting (CD-ROM 06-2579)

Appendix GA Phase 3 Scope of Work

In the Design Document development phase, a “testbed” simulation-optimization model was used to demonstrate the feasibility of using simulation and GA optimization to determine optimal solutions to problems requiring simulation as the objective function evaluation tool. During that demonstration, several needed enhancements to the GA optimization capabilities were identified. The following tasks describe those activities which are related to enhancing the capabilities of the GA optimization model. Two extra subtasks (Task 1.3 and Task 2.2) were added during the contract period.

Task 1 Genetic algorithm

- 1.1 Create “smart” operators specific for NaSS problem
- 1.2 Explore parallel processing options
- 1.3 Create “weighted” sequences during search process

Task 2 Evaluation / Simulation model

- 2.1 Store results and prescreen alternatives to avoid repeated simulation near previous searches
- 2.2 Estimate total use benefit from simulation model

Task 3 Project selection / sequencing / scheduling

- 3.1 Consider multiple alternatives at the same location which may be implemented at different times
- 3.2 Consider the tradeoffs between construction time and cost
- 3.3 Consider construction times and capacity reductions during construction periods

Task 4 Other applications

- 4.1 Adapt GA for network level maintenance planning and scheduling
- 4.2 Adapt GA for lock component maintenance planning and scheduling

Task 5 Continued participation on NaSS team

5.1 Continue to participate in teleconferences and face-to-face meetings. At the time of scope development it is anticipated that bi-weekly teleconferences will continue throughout the period of this scope. In addition, at least one face-to-face meeting between team members is anticipated. (Phases 2.2 and 3)

5.2 Specific assignments. It is anticipated issues and activities will arise during the period of this scope for which CEE-UMD will be tasked. If the level of effort involved requires significant additional time and resources, this scope may be modified to provide additional funds and time to CEE-UMD. (Phases 2.2 and 3)

Responses of Species–Rich Low–Salinity Tidal Marshes to Sea Level Rise: a Mesocosm Study

Basic Information

Title:	Responses of Species–Rich Low–Salinity Tidal Marshes to Sea Level Rise: a Mesocosm Study
Project Number:	2007MD143B
Start Date:	3/1/2007
End Date:	2/29/2008
Funding Source:	104B
Congressional District:	5th &8th Congressional District of Maryland
Research Category:	Biological Sciences
Focus Category:	Wetlands, Ecology, Climatological Processes
Descriptors:	
Principal Investigators:	Andrew Baldwin, Peter James Sharpe

Publication

Annual Report FY 2007

Responses of Species-Rich Tidal Freshwater Wetlands to Sea Level Rise: a Mesocosm Study



Reporting period: March 1, 2007-February 28, 2008

Project duration: March 1, 2007-February 28, 2009

Prepared for:

Maryland Water Resources Research Center

Principal Investigator:

Andrew H. Baldwin
baldwin@umd.edu
301-405-7855

Co-PI:

Peter J. Sharpe

Prepared by:

Peter J. Sharpe (Ph.D. Candidate) and Dr. Andrew H. Baldwin
Department of Environmental Science and Technology
1423 Animal Science Building
University of Maryland
College Park, MD 20742

Submitted June 18, 2008

TABLE OF CONTENTS

	<u>Page</u>
Introduction	1
Methods.....	4
Results.....	10
Discussion of Results.....	20
Project Status Update and Products	22
Literature Cited	22

LIST OF TABLES

Table 1. Overall Type Three Test of Fixed Effects Model Output	10
Table 2. Plant Species Indicator and p-values by Group Membership	10

LIST OF FIGURES

Figure 1. Plant Species Richness in 1000m ² plots	2
Figure 2. Experimental Treatments in Plan View Layout (Greenhouse).....	5
Figure 3. Profile Drawing of Mesocosms within a trough.....	6
Figure 4. Image of topsoil homogenization	6
Figure 5. Nanticoke River Salinities	7
Figure 6. Patuxent River Salinities.....	8
Figure 7. Average Cover versus Salinity <i>Amaranthus Canabinus</i>	12
Figure 8. Average Cover versus Salinity <i>Echinochloa walteri</i>	12
Figure 9. Average Cover versus Salinity <i>Leersia oryzoides</i>	13
Figure 10. Average Cover versus Salinity <i>Mikania scandens</i>	13
Figure 11. Average Cover versus Salinity <i>Phragmites australis</i>	14
Figure 12. Average Cover versus Salinity <i>Pilea pumila</i>	14
Figure 13. Average Cover versus Salinity <i>Pluchea purpurascens</i>	15
Figure 14. Average Cover versus Salinity <i>Polygonum arifolium</i>	15
Figure 15. Average Cover versus Salinity <i>Polygonum punctatum</i>	16
Figure 16. Average Cover versus Salinity <i>Spartina patens</i>	16
Figure 17. NMS two dimensional graph	17
Figure 18. Redox Potential Graph (5 cm Depth)	18
Figure 19. Redox Potential Graph (20 cm Depth)	19
Figure 20. Redox Potential Graph (30 cm Depth)	19

APPENDICES

Appendix A – Experiment Photographs



Introduction

Statement of Critical Regional or State Water Quality Problem

Sea level rise is threatening coastal wetlands worldwide. Increases in sea level may cause shoreward movement of salt-tolerant species such as *Spartina alterniflora* (Donnelly and Bertness 2001) or conversion of coastal wetlands to open water (Baumann et al. 1984). In the Chesapeake Bay, where the relative rate of sea level rise since 1900 has been 2.5-3.6 mm/year (Lyles et al. 1988; Stevenson and Kearney 1996), extensive marshes such as those at Blackwater National Wildlife Refuge on Maryland's eastern shore have been lost (Stevenson et al. 1985; Kearney et al. 1988). Much of the research on effects of sea level rise on coastal wetlands has focused on brackish and salt marshes, where increases in relative water level due the combined effects of land subsidence and eustatic (background) sea level rise have been implicated as a dominant factor in loss of these wetlands (Stevenson et al. 1985, 1986; Morris et al. 2002). However, little is known about the effects of sea level rise on low-salinity tidal wetlands, which include the species rich, high-productivity tidal freshwater and intermediate or oligohaline marshes (Tiner and Burke 1995). In addition to increases in water level, the salt-sensitive vegetation of low-salinity wetlands also is likely to exhibit stress or mortality due to saltwater intrusion from sea level rise (McKee and Mendelssohn 1989; Baldwin and Mendelssohn 1998). Therefore, sea level rise arguably poses a greater risk to low-salinity wetlands than to salt and brackish marshes.

The Chesapeake Bay contains one of the greatest concentrations of tidal low-salinity marshes in the United States, covering about 16,000 hectares in Maryland alone (Tiner and Burke 1995; Mitsch and Gosselink 2000). Extensive low-salinity tidal marshes are associated with many of the rivers flowing into the Bay, including the Patuxent, Choptank, Wicomico, and Pocomoke Rivers in Maryland and the James, York, and Rappahannock Rivers in Virginia (Tiner and Burke 1995). These wetlands are of tremendous importance to the Chesapeake Bay ecosystem. Due to their low salinity, the plant communities of tidal freshwater marshes are considerably more diverse than those of salt and brackish marshes. Additionally, tides and river flooding supply abundant nutrients, generating primary productivity as high as any ecosystem on earth, including agroecosystems (Tiner 1993; Mitsch and Gosselink 2000). The combination of high plant diversity and productivity and low salinity stress supports diverse and abundant fish and wildlife populations. For example, almost 300 bird species have been reported in tidal freshwater marshes, and the majority of commercially important fish species rely on tidal low-salinity wetland for some phase of their lifecycle (Odum et al. 1984; Odum 1988). These include the rockfish or striped bass, *Morone saxatilis*, a multimillion dollar fishery industry in Maryland. Reportedly 90% of east coast rockfish are spawned in the tidal fresh and oligohaline portions of tributaries of the Chesapeake Bay, where their larvae congregate in and along the edges of low-salinity marshes (Berggren and Lieberman 1977; Odum et al. 1984). In addition to supporting plants, fish, and wildlife, tidal low-salinity wetlands are used heavily for hunting, fishing, and nature observation by humans, and act to protect shoreline properties from coastal erosion and storm surges (Mitsch and Gosselink 2000).

Clearly, the loss of tidal low-salinity marshes, or their conversion to brackish or salt marshes, in the Chesapeake Bay due to sea level rise would have dramatic socioeconomic and ecological consequences. While sea level rise itself cannot be readily controlled, measures can be taken to stabilize or restore coastal wetlands. These include addition of sediment to increase elevation, a technique that has been used in coastal Louisiana to mitigate wetland loss due to sea



level rise (Ford et al. 1999), and which is being considered for restoration of wetlands at Blackwater National Wildlife Refuge.

While the broad responses of vegetation to increases in salinity and soil waterlogging are understood, the potential for vegetation dieback or changes in species composition in tidal low-salinity marshes of the Chesapeake Bay and other Atlantic Coast estuaries in response to changes in salinity and waterlogging acting together has not been studied. Because of their position in the estuary, these marshes may experience increases in salinity, but not waterlogging if sedimentation patterns continue to provide adequate accretion to keep pace with increases in water level (Kearney et al. 1988). Alternatively, salinity and water level both may increase. Currently little quantitative information exists upon which to base predictions of changes in species diversity or composition in tidal low-salinity marshes, or even whether vegetation will die back under different projected sea level rise scenarios (IPCC, 2001). Because of the ecological and socioeconomic significance of tidal low-salinity marshes of the Bay and elsewhere, quantitative information and predictive models are invaluable tools for understanding how coastal wetlands will respond to increases in sea level and in designing mitigative measures or wetland restoration projects in the face of sea level rise.

Preliminary Research

During 2006 we studied patterns of plant diversity and composition across low-salinity tidal marshes in the upper estuaries of the Patuxent and Nanticoke Rivers in Maryland. Vegetation cover was described in 1000 m² plots located across an approximately 50-km gradient at roughly 5-km intervals, extending across tidal freshwater and oligohaline marshes into the brackish marsh zone in both estuaries. Sampling used the module method for non-destructive sampling, which combines large-scale sampling (1000 m²) with nested plots of 100 m², 10 m², 1 m², 0.1 m², and 0.01 m² (Peet et al. 1998). This methodology is a powerful but rapid method that provides composition data across a relatively large area of marsh and allows comparison of species richness at different spatial scales.

Preliminary results show a species richness peak occurring in areas 15-25 km downstream from the uppermost tidal freshwater marshes. In these reaches salinity periodically increases of 2-5 ppt (mddnr.chesapeakebay.net) during periods of low river discharge, which typically occur in late summer during drought years; our springtime 2006 measurements also detected salinity (Fig. 1). This observed peak in plant species richness occurs within the fresh-brackish transition (oligohaline zone) of both rivers and

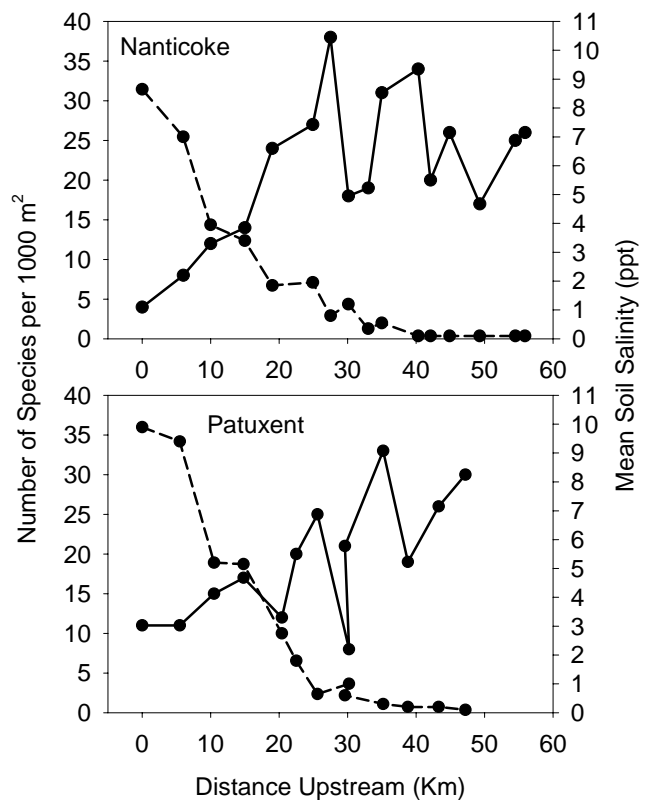


Fig. 1. Plant species richness in 1000 m² plots (solid lines, left axis) and porewater salinity (dashed lines, right axis) in tidal marshes in the upper Nanticoke and Patuxent Rivers, Maryland (May/June 2006).



challenges the popular belief that plant species richness is uniformly and inversely related to salinity in tidal marsh ecosystems (Anderson et al. 1968; Tiner 1995; Odum 1988). We hypothesize that the principal abiotic mechanisms controlling the observed plant species richness peak is periodic salinity stress, which reduces the competitive advantages afforded many freshwater plant species and allows less competitive brackish marsh plants to survive in this transition zone.

These preliminary results document the considerably higher plant diversity in low-salinity tidal marshes and that increases in salinity associated with sea level rise will reduce the diversity of these wetlands. Furthermore, if marshes are unable to migrate landward, as is expected in many regions due to coastal steepening, the low-salinity marshes may succumb to the so-called “coastal squeeze” between saline marshes and uplands (Taylor et al. 2004).

While these preliminary findings demonstrate correlation between salinity and plant diversity in coastal wetlands, stronger cause-and-effect relationships can be examined using manipulative experiments than is possible in observational studies. Questions not addressed by this preliminary research are: 1) how do increases in salinity concentration alter species richness and composition in low-salinity coastal marshes?; and 2) does soil waterlogging, also predicted to increase due to sea level rise, reduce or interact with changes in salinity? These questions are the subject of our proposed research.

Nature, Scope, and Objectives of the Project

Our overall goal for the research proposed here is to understand how changes in salinity and water level will influence diversity and ecosystem function of these tidal low-salinity marshes. Specifically, our objectives are to:

- 1) Create experimental wetland mesocosms containing species from tidal oligohaline and freshwater marshes
- 2) Subject mesocosms to a factorial arrangement of salinity and inundation treatments
- 3) Relate changes in plant communities and indices of ecosystem function to potential changes in water level and salinity predicted under various sea level rise scenarios

Through these objectives we will test the following hypotheses, developed based on literature discussed previously and later in the Related Research section:

H1: Increases in salinity will tend to reduce plant diversity (species richness and diversity index) and indices of ecosystem function (biomass, nutrient pools, and soil respiration), but maximum diversity will occur at low salinity rather than in fresh water.

H2: Increases in salinity will result in a shift toward salt-tolerant species.

H3: Increases in soil waterlogging will reduce plant diversity and growth of all species.

H4: Salinity and waterlogging will interact in a synergistic manner to reduce diversity and ecosystem function.

The probability of rejecting the null construction of these hypotheses (no treatment effect) will be tested statistically. If the null hypothesis is rejected at a specified level of probability, the



alternative hypothesis (a treatment effect exists) will be accepted. The magnitude and direction of treatment effects will be examined by looking at means and trends.

Methods

The principal objectives of this study were to determine the importance of salinity and flooding frequency on plant community richness and biomass using constructed marsh mesocosms in the University of Maryland greenhouse complex. Additionally we wanted to assess the potential seed bank variability in collected marsh topsoils from brackish, transitional, and fresh marsh sites.

To examine the potential future responses of low-salinity marsh vegetation to sea level rise; we developed a greenhouse experiment subjecting marsh mesocosms (the experimental unit) to a range of salinity and soil flooding conditions. The experiment tests the effects of various salinity and flooding regimes on species richness, species composition, and indices of ecosystem function (above ground biomass, nutrient pools, and soil respiration). Specifically, we subjected synthetic plant communities to three levels of soil flooding and five levels of salinity (0, 1.5, 3, 6, and 12 parts per thousand or ppt) in a 3 x 5 factorial treatment arrangement. For reference, the salinity of ocean water is about 35 ppt, and the salinity classification of coastal marshes is <0.5 ppt for freshwater, 0.5-5 ppt for oligohaline or intermediate marshes, 5-18 for mesohaline or brackish marshes, and >18 for polyhaline or salt marshes (Cowardin et al. 1979).

Mesocosm Configuration

Because of possible gradients in light, temperature, or humidity across greenhouse benches, as well as greenhouse space limitations, experimental units were arranged in a split-plot randomized complete block design (i.e., there are two blocks of 15 mesocosms, with each mesocosm in a group randomly receiving a different one of the 15 salinity x flooding treatment combinations – see Figure 2).

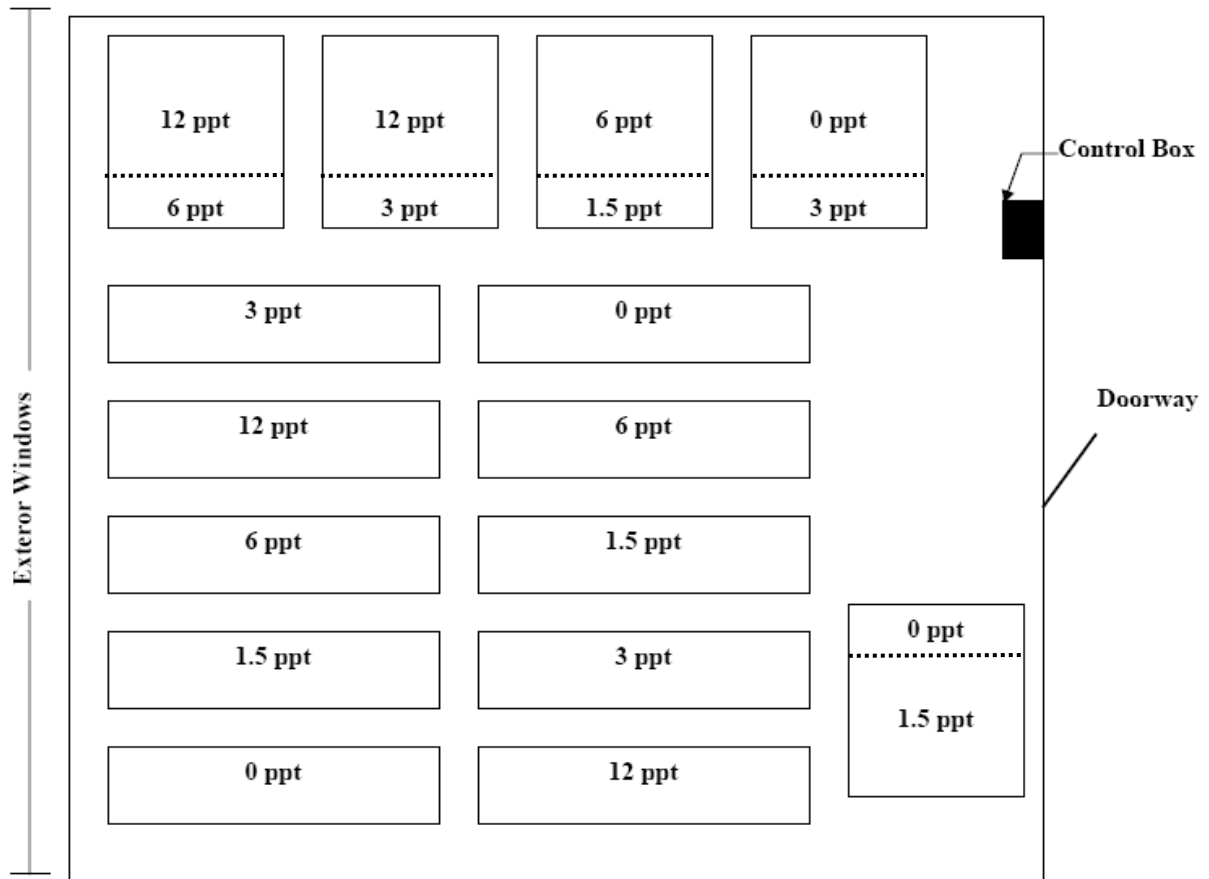


Figure 2. Experimental treatments and plan view layout for the greenhouse mesocosm study of effects of sea level rise on diversity, composition, and ecosystem function of low salinity coastal marshes (total experimental units = 30).

The mesocosms consisted of a container-in-container design that allows control of water level and supply of salinity and nutrients. The mesocosm itself was a 56 x 44 x 44 cm (h x l x w; 151.4 L), Rubbermaid square brute container with sixteen 1.3 cm diameter perforations along the bottom to allow for exchange of water within the watering trough. Each mesocosm also had mesh screens installed at the bottom of each mesocosm over the drainage holes to prevent soil loss. The screens were made from plastic and had a 4 mm² pore size. The watering troughs were made from pressure treated lumber and were (61 x 196 x 56 cm, 666 L). The troughs were designed to house three mesocosms and were fed by a dedicated reservoir randomly assigned to that particular trough. The reservoirs were constructed from pressure treated lumber and were (56 x 117 x 117 cm, 767 L) and were randomly located within the greenhouse. To prevent water loss and leaking the troughs and reservoirs were lined with 45 mil thick black Firestone Pond Liners (Figure 3). Submersible pumps (Little Giant 115 Volt) were placed in the reservoirs and troughs to move water into and out of the system. The pumps were attached to a circuit board and timing mechanism set to a six hour interval rate. The six hour pumping cycle was established to simulate the natural tidal cycles of marshes within the Chesapeake Bay. Target salinity levels were achieved through the addition of

Instant Ocean Sea Salt to our targeted treatment level and verified through the use of a handheld YSI-30 SCT meter.

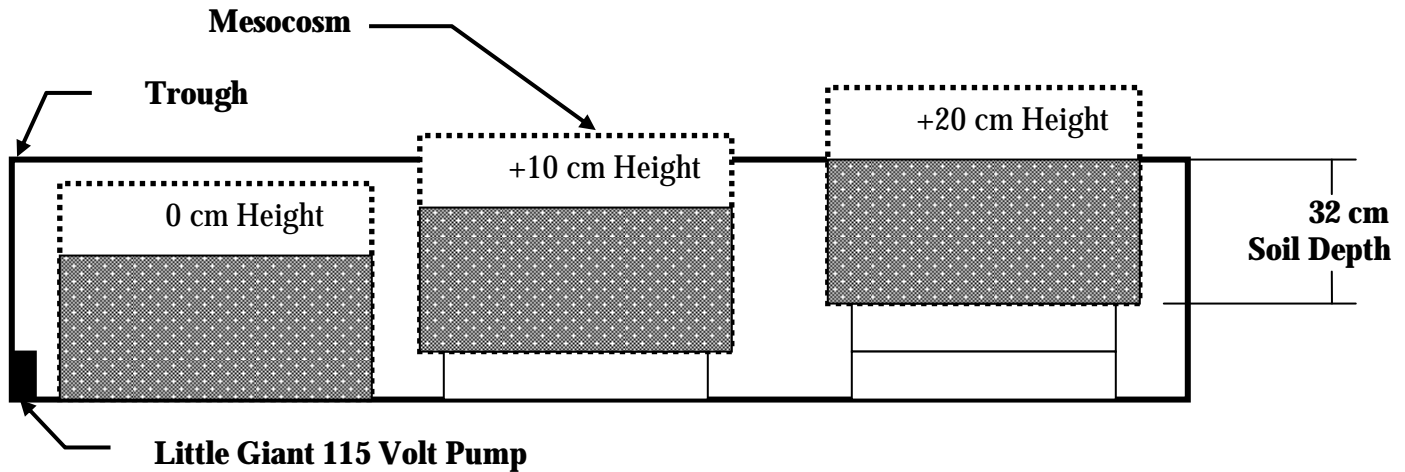


Figure 3. Profile drawing showing a conceptual layout of the marsh mesocosms within a trough.

Experimental Plant Community – Mesocosm and Seedbank Studies

Marsh topsoil was collected from four marsh locations (two freshwater sites, one transitional site, and one brackish site) along the Patuxent River on March 19-21, 2007. Marsh soils were collected by hand using 5 x 4.75 cm (h x d) corers. A total volume of 38 L (of the top five centimeters of topsoil) was collected from each of the four sites. An additional freshwater marsh site was needed due to concern that a sufficient number of freshwater annual plants would not germinate from a single site. As commercially grown wetland annuals are difficult to obtain, the additional fresh marsh site was included to ensure adequate representation of each salinity class in our mesocosms. The collected marsh topsoil was stored in 19 L buckets and placed in refrigerated conditions until April 17, 2007 when the soils were homogenized.

Each sites topsoil samples were homogenized in a cement mixer and five (284 cm³) samples from each of the four marsh topsoil collections were extracted and spread in a uniform 1 cm thick layer on top of a 2 cm thick layer of Sunshine LC1 potting soil mix within 4 x 14 x 20.3 cm aluminum pans. The homogenization of the collected topsoil across all four marsh locations was accomplished by placing one bucket of topsoil from each marsh type into a cleaned and rinsed cement mixer. The cement mixer was run for seven minutes and the resulting mixture was placed back into the four



Figure 4. Image showing topsoil homogenization process in the UM Greenhouse complex.



empty buckets. This process was repeated for the remaining four topsoil sample buckets. Next, two buckets from each of the mixed sets were chosen haphazardly (four buckets total) and mixed again for five minutes and poured back into the empty buckets. This process was repeated for the remaining four buckets. This process of mixing and re-mixing of the collected topsoil samples was utilized to achieve a homogeneous soil mixture (Figure 4).

Five 284 cm³ volumes of soil were extracted from the homogenous mix and placed in the aluminum pans as part of the seed bank variability component of this study. The seedbank trays were randomly placed on a misting bench in the University of Maryland Research Greenhouse Complex and emerging seedlings counted by species. Soil seed banks contain seeds of several dominant annual species in low-salinity marshes, including *Polygonum* spp., *Impatiens capensis*, *Bidens* spp., and *Pilea pumila* (Baldwin and DeRico 1999; Peterson and Baldwin 2004). Application of a homogeneous soil sample is an effective way to introduce these species, many of which cannot be purchased from nurseries and for which seed collection would be necessary throughout the year. I anticipated that between the planted perennials and plants recruited from the seed bank we will approach stem densities similar to those of natural marshes later during the experiment (e.g., 250 stems/m² in July and 150 stems/m² in August; Darke and Megonigal 2003).

Upon completion of topsoil homogenization and seedbank study set-up, mesocosm containers were filled with 30 cm of SUNGRO Professional Blend potting soil and inoculated with a 2 cm thick layer of collected marsh topsoil. The resulting mesocosms were put on a freshwater drip-line irrigation system, placed outside and then moved into the greenhouse and allowed to acclimate to greenhouse conditions until July 11, 2007 when the mesocosms were placed into our tidal system. Perennial wetland plants (two inch plugs) purchased from Environmental Concern, Inc. (St. Michaels, MD) were randomly planted at each of 16 positions within each marsh mesocosm on May 31, 2007. The perennial plants were selected based on availability and relative indicator value and cover from the previous observational study (Phase 1 of this proposal). The plant species were: *Acorus calamus*, *Distichlis spicata*, *Leersia oryzoides*, *Spartina alterniflora*, *Typha angustifolia*, *Spartina patens*, *Phragmites australis*, and *Spartina cynosuroides*. *P. australis* and *S. cynosuroides* were grown in the greenhouse from rhizomes harvested along the Patuxent River as these two species were not commercially available. All of the aforementioned perennial species were from Maryland ecotypes and two of each species were randomly placed into each mesocosm with the exception of *S. cynosuroides*. The *S. cynosuroides* rhizomes did not successfully generate enough viable plants for more than one of that

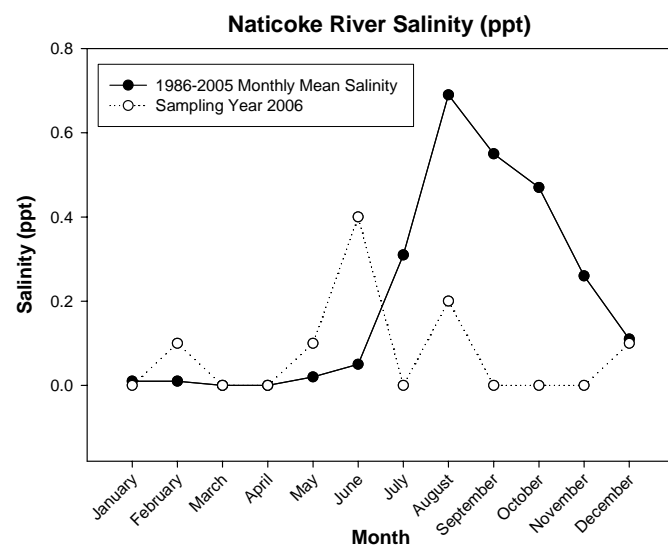


Figure 5. Nanticoke River Salinities Measured at Maryland DNR surface water quality station ET6.1 – Sharpetown, Maryland (near plot N35W) showing the mean monthly salinities measured from 1986-2005 and the mean monthly salinities from the 2006 sampling effort.



particular species to be planted per mesocosm.

The rationale for including some species of brackish marshes was to provide a source of vegetative material that will allow plant communities to potentially shift from salt-intolerant to salt-tolerant communities if environmental conditions are appropriate, as occurs in coastal wetlands experiencing high rates of relative sea level rise that do not convert directly to open water (Boesch et al. 1994; Perry and Hershner 1999). Previous research has used sections of marsh soil and vegetation collected intact from wetlands rather than synthetic plant communities proposed here (Baldwin and Mendelssohn 1998; Baldwin et al. 2001). However, we decided to use synthetic plant communities because we wish to assemble a diverse suite of propagules and vegetative material from a range of coastal wetland types to better understand how the diversity and composition of wetland vegetation will respond to increases in salinity and soil flooding. Synthetic plant communities also have the added benefit of reducing variation between experimental units, allowing reduced numbers of replicates, and therefore greater numbers of treatment factor levels, than would be possible with more variable soil-vegetation sections.

Mesocosm Operation

After the May 31, 2007 perennial planting event the mesocosms were maintained on a freshwater drip line system, the planted perennials were censused and dead planted perennials were removed and replaced prior to salinity treatment initialization on July 27, 2007. Salinity was altered by creating solutions of reconstituted sea water using Instant Ocean® sea water mix. After salinity treatments began for all reservoirs (except for the two fresh water systems), final reservoir salinities were gradually ramped up over a period of twelve days. The initial salinity treatment brought reservoir salinity concentrations up to 0.75 ppt initially, followed by increases every other day, to levels 1.5, 3.0, 6.0, 9.0 and finally 12.0 ppt. For those treatments whose target salinities were less than 12.0 ppt, no further salts were added to the system once the target salinity level was reached, except where necessary to maintain the treatment salinity level. The salinity levels were raised gradually to avoid shocking the plant communities with high salt concentrations. Historic salinity data from the Nanticoke and Patuxent River (Figures 5 and 6) also show that salt concentrations tend to spike in late July and August, so this procedure was employed to mimic field conditions on these two river systems (Maryland DNR “Eyes On The Bay Program, 2007). Apart from simulating natural salinity increases, this procedure also prevented inhibition of early season

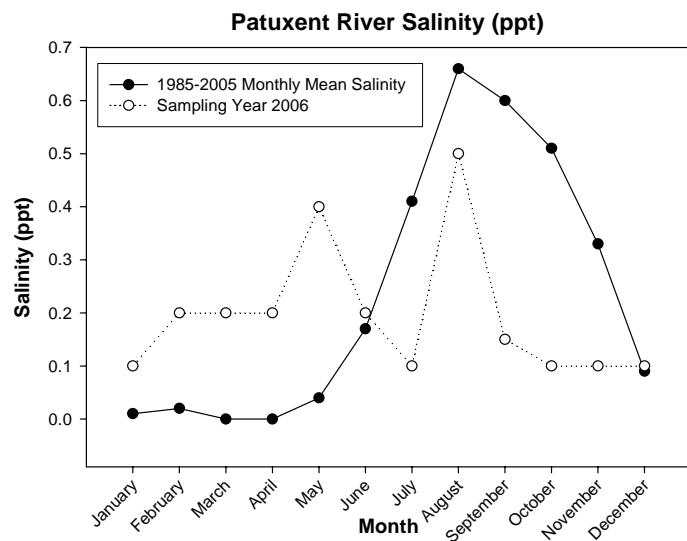


Figure 6. Patuxent River Salinities Measured at Maryland DNR surface water quality station TF1.5 at Nottingham, MD (near plot X30E) showing the mean monthly salinities measured from 1985-2005 and the mean monthly salinities from the 2006 sampling effort.



germination due to salinity (Odum et al. 1984 and Baldwin et al. 1996)

The mesocosms will be run from the middle of the growing season (July 2007) to the end of August 2008. Water salinity and temperature levels are monitored twice a week during this time. Due to evapo-transpiration losses the water within each mesocosm system is replaced, on average, once per week. Flooding regimes in the mesocosms were maintained 10 cm below the soil surface for 2 weeks so that plants could acclimate, after which water levels were adjusted to their appropriate experimental treatment levels (0cm, +10 cm, and +20 cm).

Vegetation and Environmental Measurements

Vegetation in mesocosms is censused non-destructively by using species presence/absence determinations and by estimating percent cover of each plant species type using the North Carolina Vegetative Survey protocol (Peet et al. 1998). This census was performed at the beginning of the salinity/flooding treatments in July 2007 and again in September 2007, and is being repeated throughout the life of the project (at least two more census events planned for Spring and Summer 2008). The purpose of the initial monitoring was to describe variation in the initial structure of plant communities between mesocosms and track potential treatment effects within and between the mesocosms. Light measurements using a Li-Cor 250A light meter were also taken under full sun and partial sun (70% cloud cover) at three locations within the greenhouse to quantify any potential light gradients.

Experimental treatment water is periodically analyzed for salinity, pH, and temperature using portable meters. Treatment water samples will also be analyzed periodically for ammonium, nitrate, and ortho-phosphate using a portable spectrophotometer. Soil oxidation-reduction potential (Eh) will be measured at 10 cm during the study using platinum electrodes and a pH/mV meter (Faulkner et al. 1989, Patrick et al. 1996). Interstitial sulfide concentrations will be measured using sulfide needle electrodes (Hotes et al. 2005).

At the conclusion of the experiment, the aboveground biomass will be harvested, separated by species, dried to a constant mass at 60°C, and weighed. Biomass of all species will then be combined for aboveground components, homogenized, and a subsample analyzed for total nitrogen, phosphorus, and carbon (by combustion or microwave digestion, as appropriate, at the University of Delaware Soil Testing Laboratory).

Data Analysis

Species richness was calculated for this preliminary report using September 2007 data. Upon completion of the experiment the analysis will include species richness from July 2008 surveys (number of species), Shannon-Wiener diversity index (Peet 1974), and root-shoot ratios will be calculated from biomass data. Total above and belowground nutrient pools will be calculated from biomass and nutrient concentration data. These variables and biomass of individual species and environmental parameters will be analyzed as dependent variables in two-way analysis of variance (ANOVA). If initial plant species richness or any other measured environmental parameter differed significantly between experimental units, they will be included as covariates. Two separate ANOVA models will be used. One model will treat flooding frequency and salinity level as categorical variables. This will allow treatment means to be calculated and means separation procedures to be applied. The second model will treat salinity as a continuous variable and flooding frequency as a categorical variable. Statistical analyses will be conducted using the SAS System for Windows (SAS Institute, Cary, NC) and Sigma Plot.



Regression models developed will be used to predict changes in diversity, composition, and ecosystem function for a range of sea level rise predictions (IPCC 2001). For each predicted value of sea level rise, the effect of a range of salinity values will be examined to quantify the best and worst-case scenarios for vegetation change and wetland loss in Chesapeake Bay low-salinity tidal marshes.

Results

As the experiment is still currently ongoing the results and subsequent discussion will be focused on the preliminary (September 2007 plant species data). The overall Split-Plot ANOVA analysis of the preliminary September 2007 plant species richness and cover data yielded no significant results regarding the level of variance explained by salinity, inundation, or salinity*inundation (Table 1).

Table 1. Overall Type III Test of Fixed Effects using Plant Species Richness (September 2007) as the response variable and salinity, flooding frequency, and salinity*flooding frequency as independent variables.

Table with 5 columns: Effect, Num DF, Den DF, F Value, Pr > F. Rows include Salinity, Inun (Flooding Frequency), and Salinity*Inun.

Marsh mesocosms did show excellent recruitment of plant species from the collected marsh sediments (Table 2), indicating successful construction and operation of the tidal marsh system.

Table 2. Overall Marsh Mesoscom Plant Species List (2007 Preliminary Data)

Table with 3 columns: Species, Volunteer From Seedbank (Yes/No), Planted (Yes/No). Lists various plant species like Acorus calamus L., Amaranthus cannabinus L., etc.



Species	Volunteer From Seedbank (Yes/No)	Planted (Yes/No)
<i>Distichlis spicata</i> (L.) Greene	N	Y
<i>Echinochloa walteri</i> (Pursh) Nash	Y	N
<i>Echinochloa</i> sp.	Y	N
<i>Eleocharis parvula</i> (R.&S.) Link	Y	N
<i>Eupatorium</i> sp.	Y	N
<i>Galium tinctorium</i> L.	Y	N
<i>Galium palustre</i> L.	Y	N
<i>Hibiscus moscheutos</i> L.	Y	N
<i>Hibiscus</i> sp.	Y	N
<i>Impatiens capensis</i> Meerb.	Y	N
<i>Juncus</i> sp.	Y	N
<i>Kosteletzkya virginica</i> (L.) Presl	Y	N
<i>Leersia oryzoides</i> (L.) Sw.	Y	Y
<i>Lythrum salicaria</i> L.	Y	N
<i>Nasturtium officinale</i> R. Br.	Y	N
<i>Mikania scandens</i> (L.) Willd.	Y	N
<i>Murdannia keisak</i> (Hasskarl) Hand.-Mazz.	Y	N
<i>Peltandra virginica</i> (L.) Schott & Endl.	Y	N
<i>Phragmites australis</i> (Gav.) Trin.	N	Y
<i>Pilea pumila</i> (L.) Gray	Y	N
<i>Pluchea purpurascens</i> (Sw.) DC.	Y	N
<i>Polygonum arifolium</i> L.	Y	N
<i>Polygonum punctatum</i> Ell.	Y	N
<i>Polygonum sagittatum</i> L.	Y	N
<i>Polygonum</i> sp.	Y	N
<i>Rorippa islandica</i> (Oeder) Borbas	Y	N
<i>Schoenplectus</i> sp.	Y	N
<i>Senecio</i> sp.	Y	N
<i>Sonchus</i> sp.	Y	N
<i>Spartina alterniflora</i> Loisel.	N	Y
<i>Spartina cynosuroides</i> (L.) Roth	N	Y
<i>Spartina patens</i> (Ait.) Muhl.	N	Y
<i>Typha angustifolia</i> L.	N	Y
<i>Zizania aquatica</i> L.	Y	N

Of the plant species observed in the marsh mesocosms 84% of them volunteered from the seed bank of the mesocosms with the remaining 16% (8 species) being composed of species which we planted randomly within each mesocosm.

Figures 7-16 show the top ten most abundant plants species across all 30 mesocosms based on percent cover for September 2007 and arranged by the categorical variable flooding frequency. The preliminary analysis of the Split-plot ANOVA of the September (2007) data showed few significant relationship between the top ten most abundant plant species and salinity, flooding frequency, and the interaction between the two treatments (salinity*flooding frequency). These results were consistent with our overall findings of no significant treatment effects on plant species richness across all mesocosms based on the preliminary plant species/cover data (September 2007).

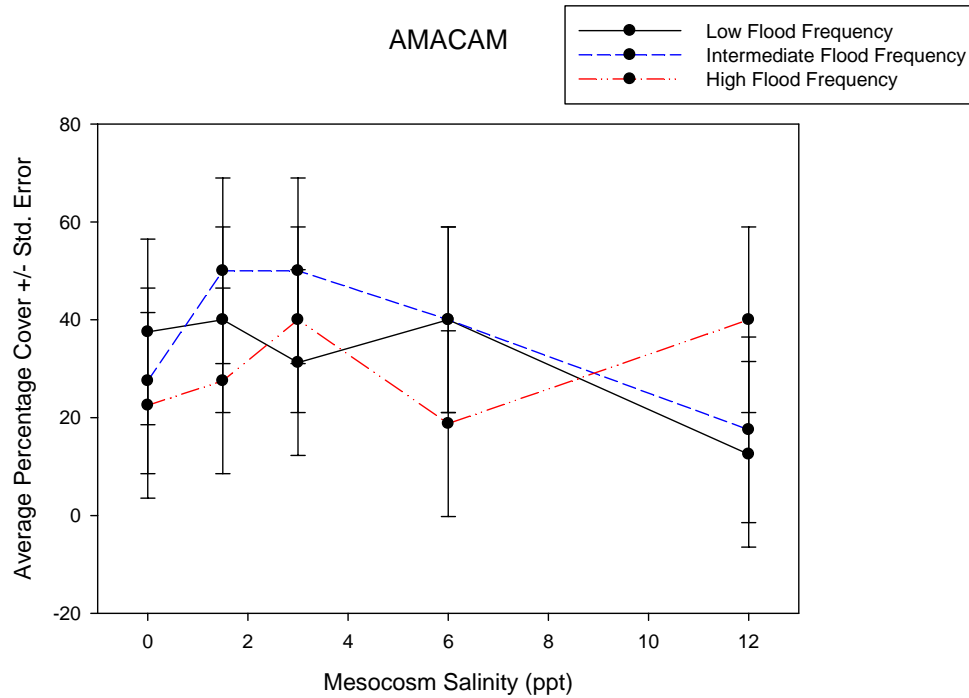


Figure 7. Average cover of *Amaranthus cannabinus* L. across all mesocosms from September 2007. No significant relationships were found for Salinity, Flood Freq., or Salinity/Flood Freq. interaction treatments.

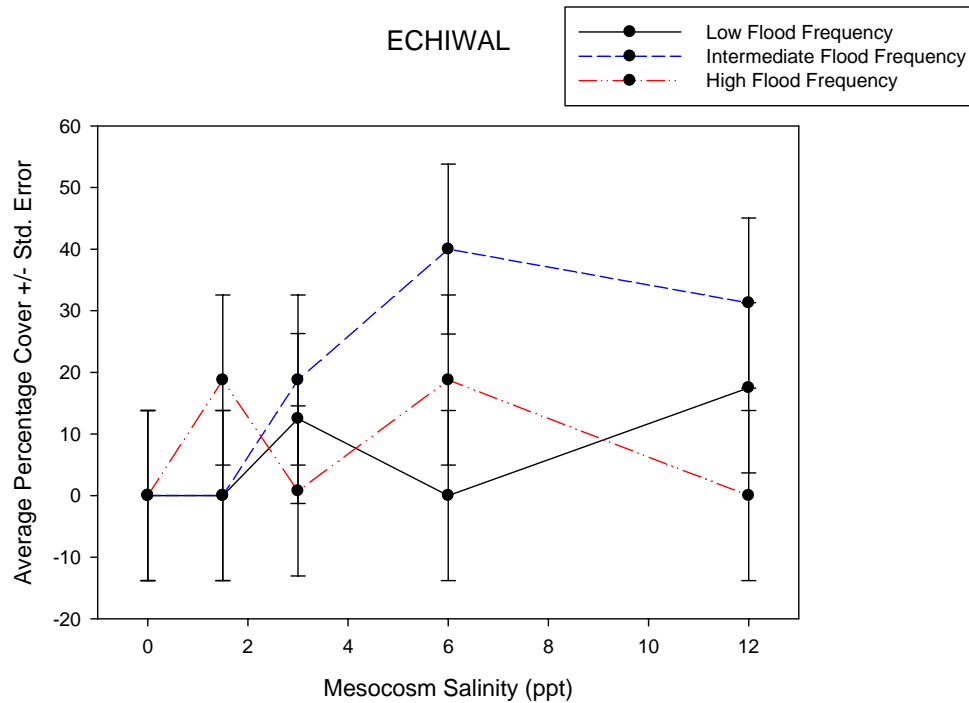


Figure 8. Average cover of *Echinochloa walteri* (Pursh) Nash across all mesocosms from September 2007. No significant relationships were found for Salinity, Flood Freq., or Salinity/Flood Freq. interaction treatments.

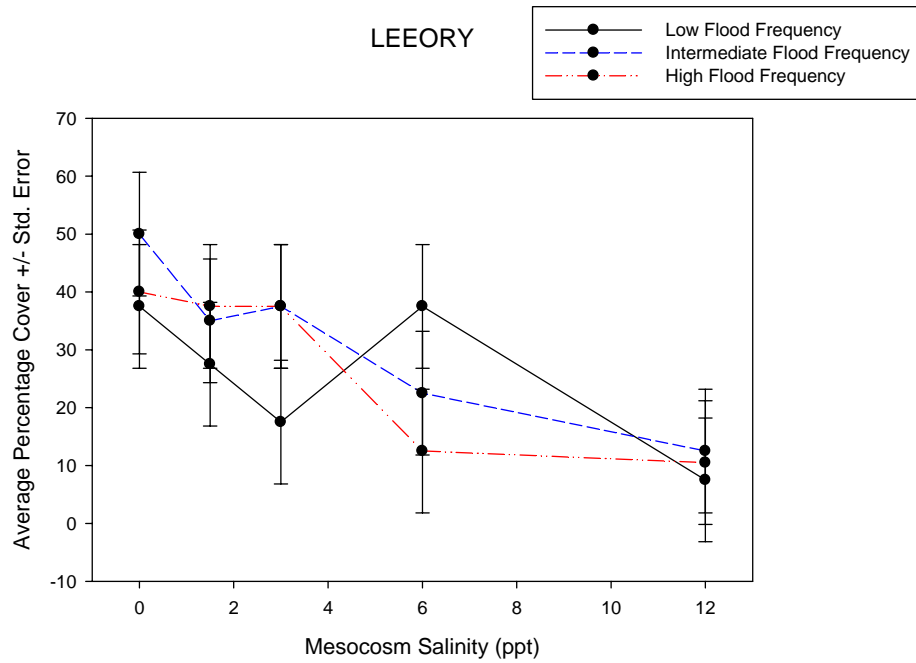


Figure 9. Average cover of *Leersia oryzoides* (L.) Sw. across all mesocosms from September 2007. Salinity displayed a significant relationship ($p = 0.0269$) across these treatments.

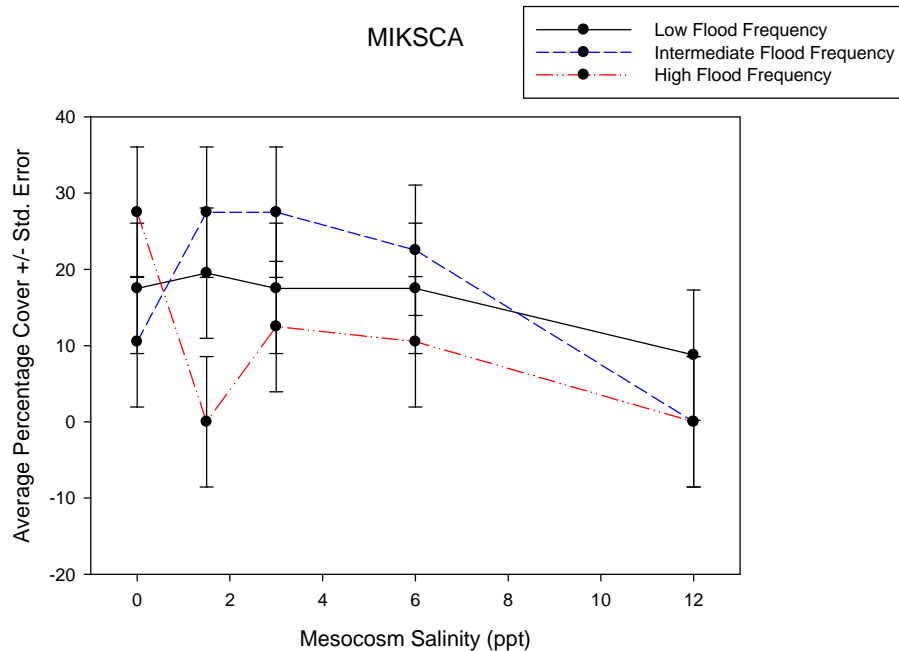


Figure 10. Average cover of *Mikania scandens* (L.) Willd. across all mesocosms from September 2007. No significant relationships were found for Salinity, Flood Freq., or Salinity/Flood Freq. interaction treatments.

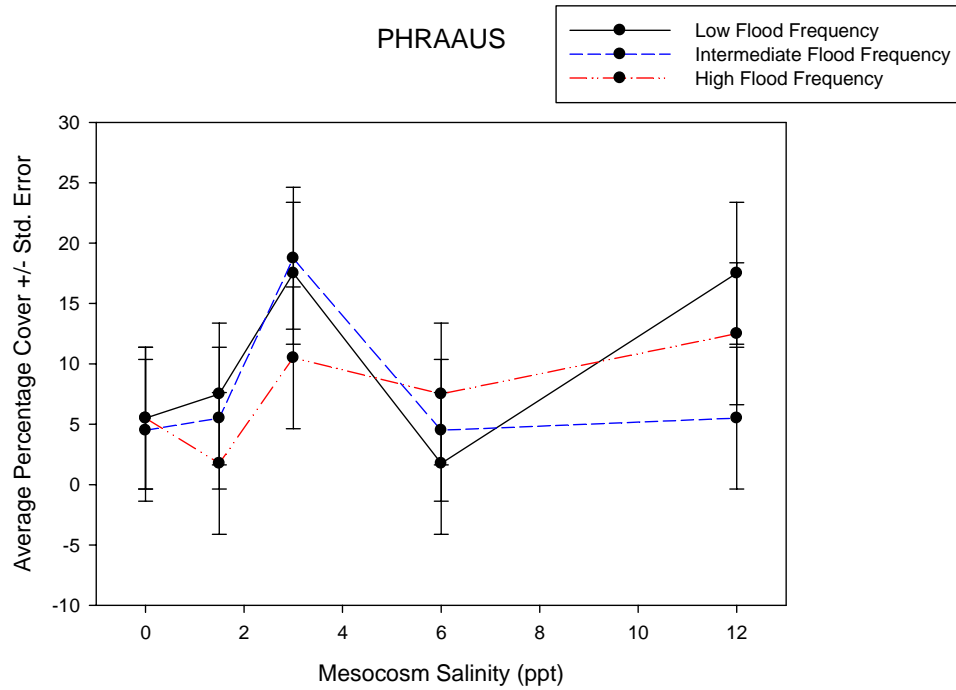


Figure 11. Average cover of *Phragmites australis* (Gav.) Trin. across all mesocosms from September 2007. No significant relationships were found for Salinity, Flood Freq., or Salinity/Flood Freq. interaction treatments.

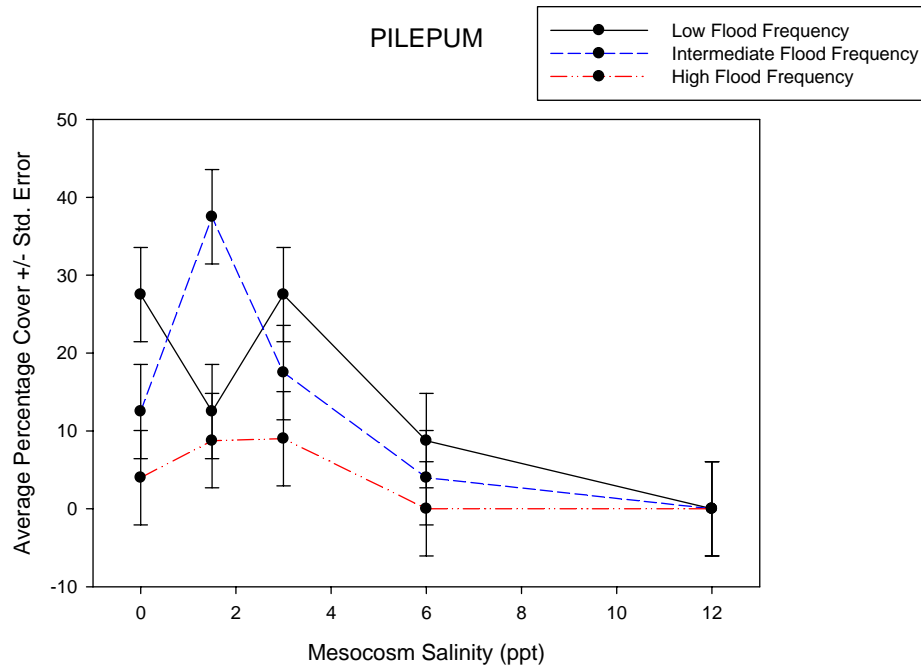


Figure 12. Average cover of *Pilea pumila* (L.) Gray across all mesocosms from September 2007. Flooding Freq. displayed a significant relationship ($p = 0.0142$) across these treatments.

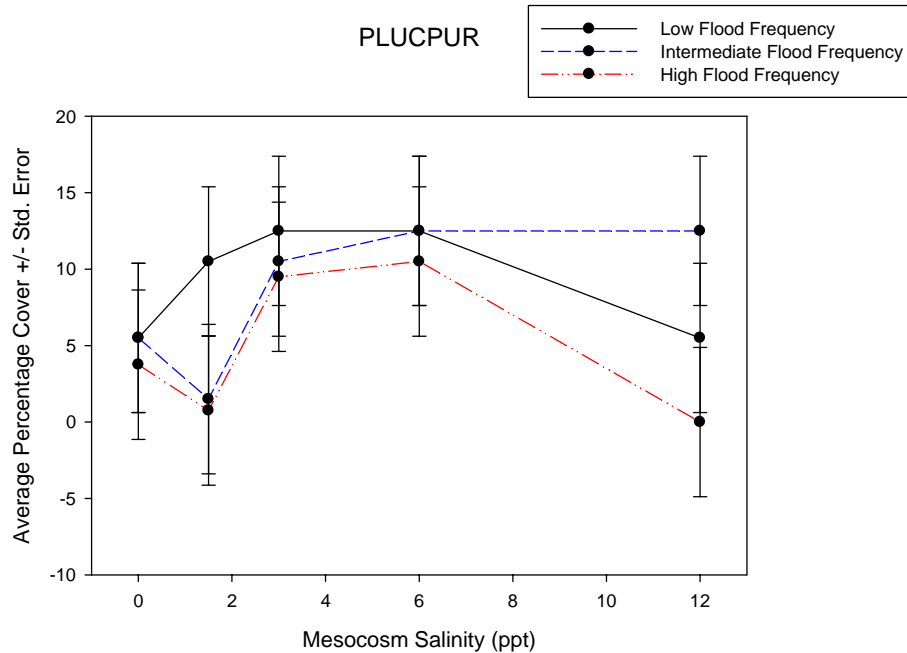


Figure 13. Average cover of *Pluchea purpurascens* (Sw.) DC. across all mesocosms from September 2007. No significant relationships were found for Salinity, Flood Freq., or Salinity/Flood Freq. interaction treatments.

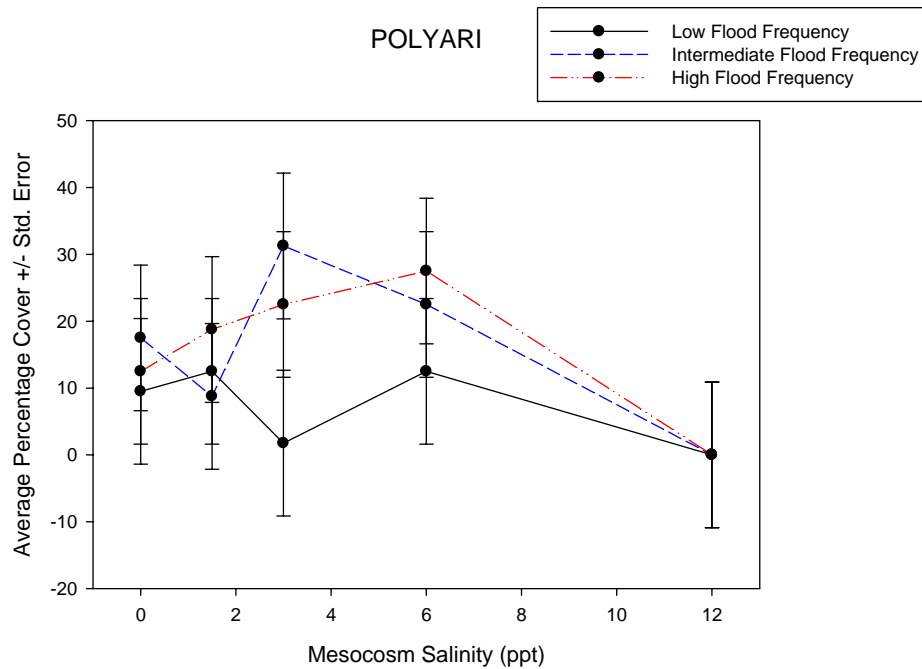


Figure 14. Average cover of *Polygonum arifolium* L. across all mesocosms from September 2007. No significant relationships were found for Salinity, Flood Freq., or Salinity/Flood Freq. interaction treatments.

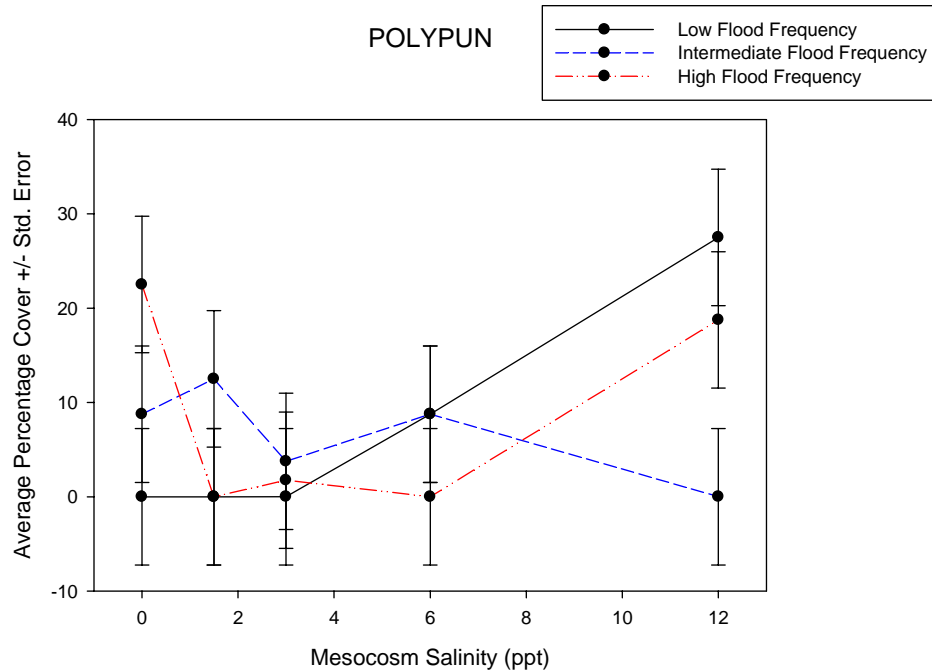


Figure 15. Average cover of *Polygonum punctatum* Ell. across all mesocosms from September 2007. No significant relationships were found for Salinity, Flood Freq., or Salinity/Flood Freq. interaction treatments.

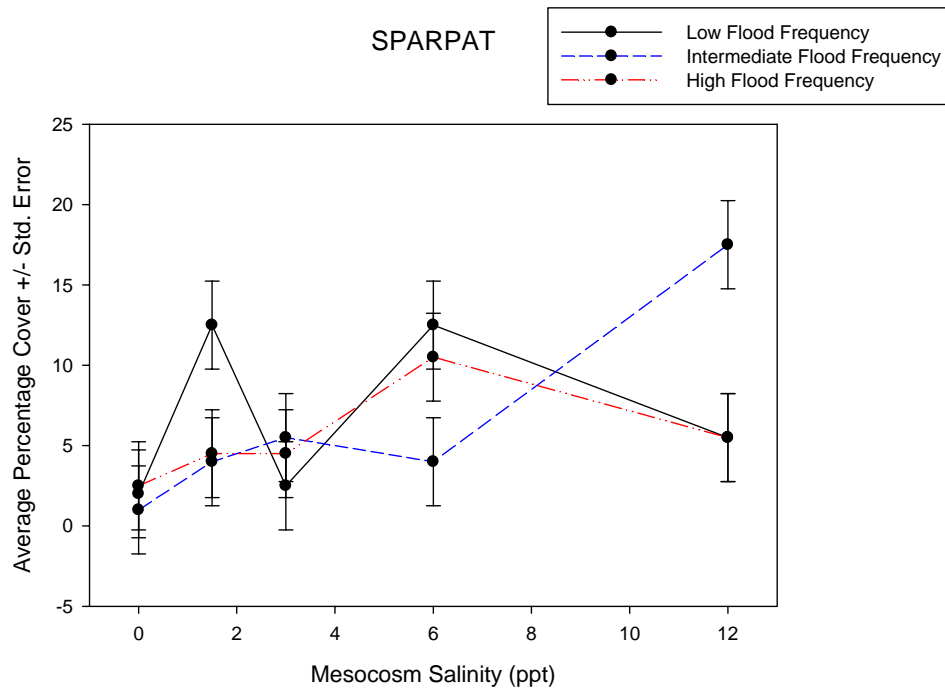


Figure 16. Average cover of *Spartina patens* (Ait.) Muhl. across all mesocosms from September 2007. The interaction of Salinity and Flooding Freq. displayed a significant relationship ($p = 0.0005$) across these treatments.

Of the figures shown previous only *Leersia oryzoides*, *Pilea pumila*, and *Spartina patens* plant cover showed significant responses to the treatment regimes. Each one of the aforementioned species reacted differently to the treatments with *Leersia oryzoides* showing a negative relationship with increasing salinity (Figure 9), *Pilea pumila* reacting strongly to increased flooding frequency (Figure 12), and *Spartina patens* showing a strong reaction to the interaction between flooding frequency and salinity stress.

Figure 17 displays the results of Non-metric multi-dimensional scaling analysis performed in PC-ORD. The main axis in Figure 7 is composed of the covers for each individual plant species across all 30 mesocosms, the secondary axis was the salinity and flooding frequency parameters. Using the preliminary plant species cover data yielded no discernable relationships within or between salinity groups.

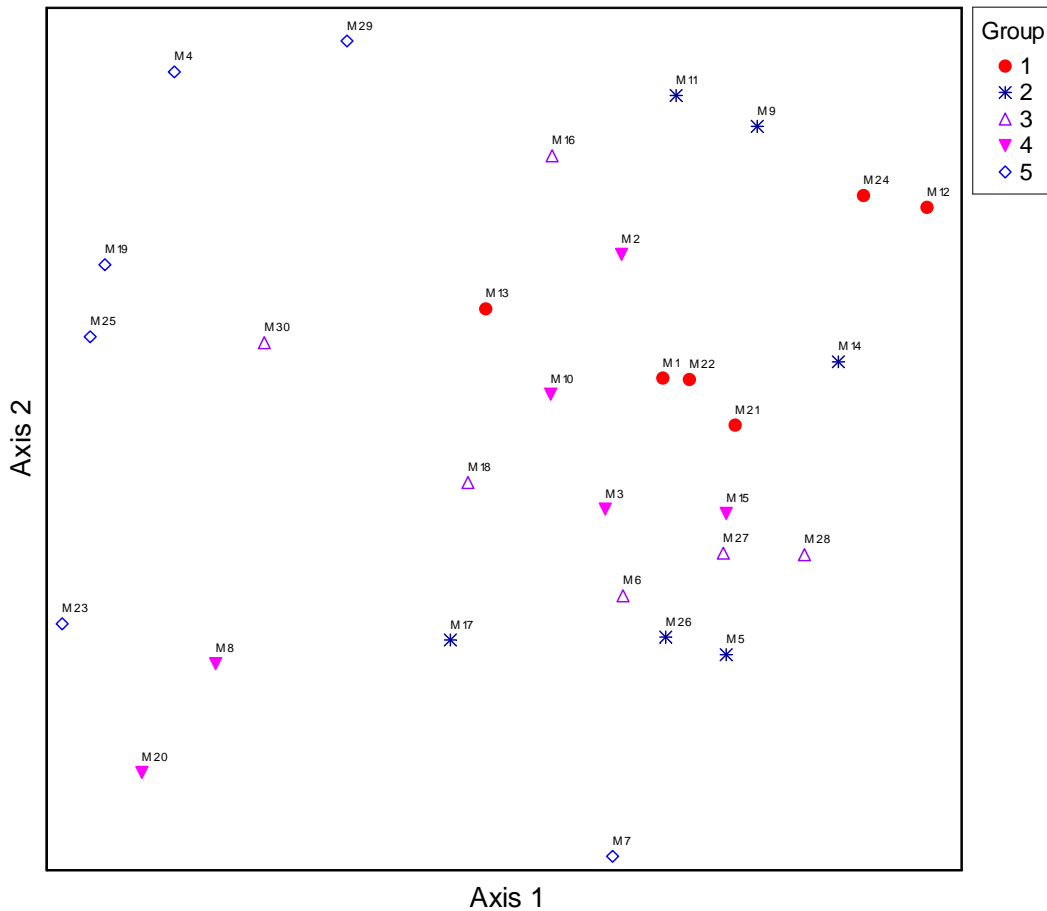


Figure 17. NMS two dimensional graph showing the Mesocosm plant species cover data (main matrix) versus salinity and flooding frequency parameters (secondary matrix). The groups are arranged by salinity treatment with Group 1 = 0 ppt, Group 2 = 1.5 ppt, Group 3 = 3 ppt, Group 4 = 6 ppt, and Group 5 = 12 ppt.



The soil redox potential was assessed at three depths (5 cm, 20 cm, and 30 cm) for each mesocosm in November 2007. The data are presented in Figures 18-20 and show Redox potentials within the mesocosms to range from ≈ 122 to 309 mV at 5 cm depth. The Redox potentials generally tended to decrease as one would expect further down into the mesocosm soil profile with ranges from 140 – 335 mV at 20 cm depth and 105 – 301 mV at 30 cm depth. The graphs also show the mesocosms grouped by their respective flooding frequency category. The preliminary Redox data shows a general tendency for the most frequently flooded mesocosm to display the lowest redox potential as one would expect with Figure 18 showing the clearest separation at 30 cm depth.

Redox Potential (5 cm Depth) by Flood Frequency

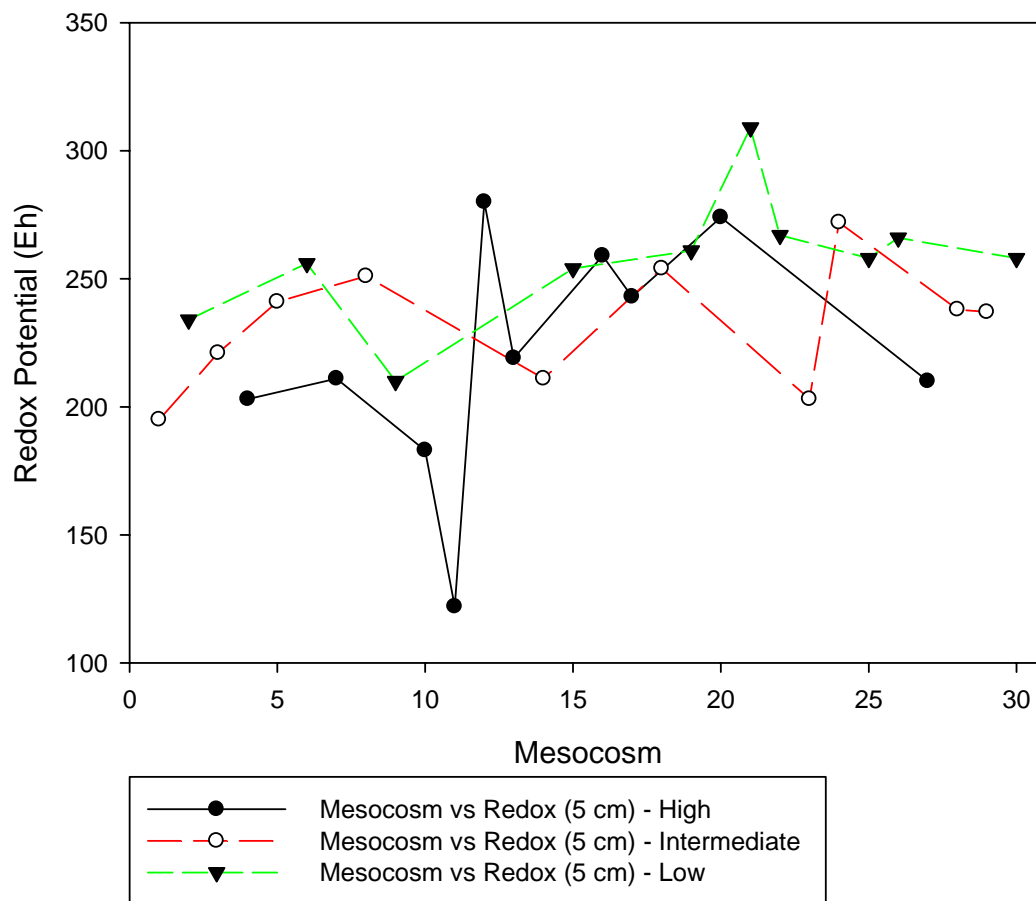


Figure 18. Redox potential Data across all mesocosms measured in November 2007 and separated by flooding frequency for the 5 cm Depth.

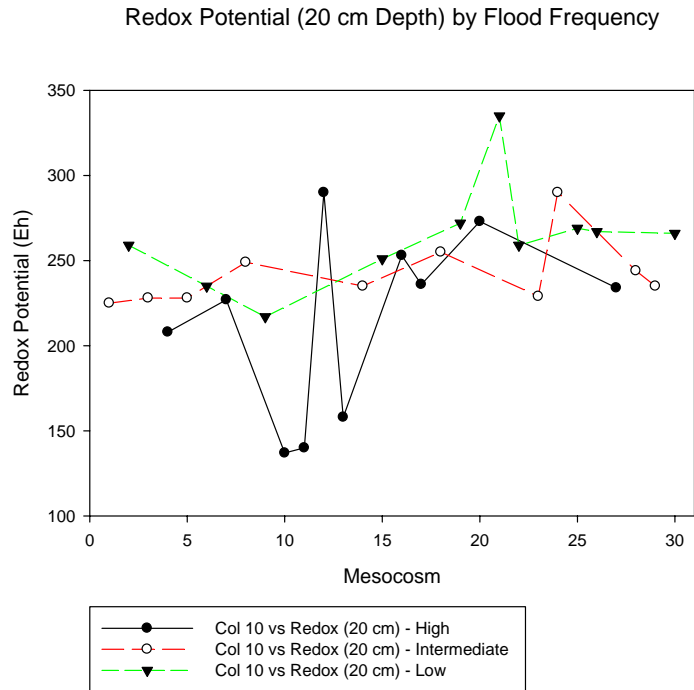


Figure 19. Redox potential Data across all mesocosms measured in November 2007 and separated by flooding frequency for the 20 cm Depth.

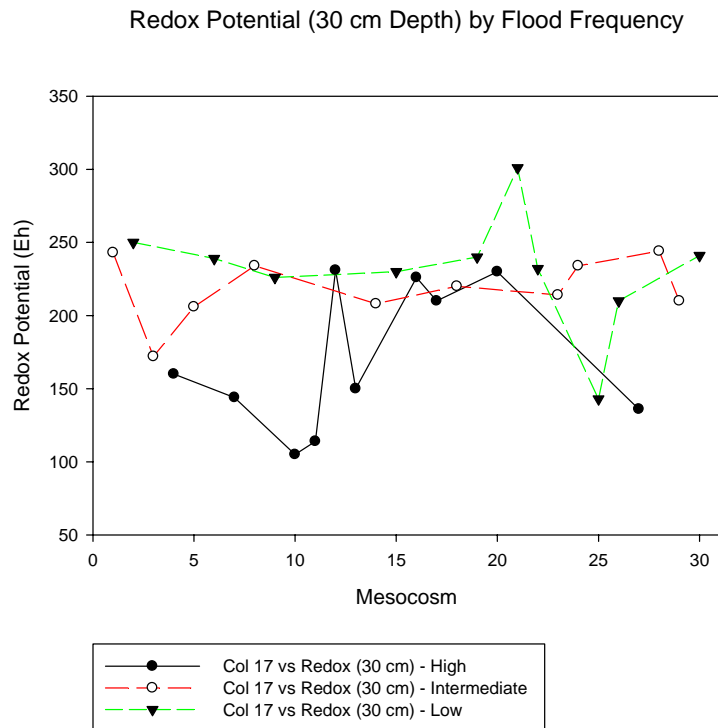


Figure 20. Redox potential Data across all mesocosms measured in November 2007 and separated by flooding frequency for the 30 cm Depth.



Discussion of Results

Considerable research has been conducted on how salt and brackish marshes will respond to sea level rise (Mitsch and Gosselink 2000; Morris et al. 2002; Turner et al. 2004). Much of this research has focused on the responses of the ability of salt marshes to accrete vertically at sufficient rates to keep pace with sea level rise, and the role of macrophytes in marsh stability or loss (Kearney et al. 1994; Roman et al. 1997; Day et al. 1999), or on the responses of marsh vegetation to increases in salinity and water level or soil waterlogging (Mendelssohn et al. 1981; Pezeshki et al. 1993; Broome et al. 1995; Naidoo et al. 1997; Gough and Grace 1998). These and other studies have demonstrated the importance of mineral sediment and organic matter deposition, which are critical to maintaining elevation (Reed 1995), and tolerance of marsh vegetation to increases in salinity and water logging (Kozlowski 1997). In general, growth and survival of salt and brackish marsh vegetation is reduced by increases in soil waterlogging, such as those that may occur due to sea level rise (e.g., Webb et al. 1995; Mendelssohn and Batzer 2006). Loss of salt and brackish marshes in areas such as the Mississippi River delta plain (Louisiana) and the Chesapeake Bay is believed to primarily be the result of an inability of marsh elevation to keep up with relative sea level, which increases soil waterlogging and anoxia, stressing or killing salt marsh plants (Stevenson et al. 1985; Boesch et al. 1994).

In contrast to salt and brackish marshes, responses of tidal low-salinity marshes to sea level rise have received little attention, with the exception of those in the Louisiana delta plain. Research in Louisiana has shown that increases in salinity, as well as soil waterlogging, due to high rates of relative sea level rise result in vegetation dieback and wetland loss (McKee and Mendelssohn 1989; Boesch et al. 1994; Flynn et al. 1995; Webb and Mendelssohn 1996). These findings suggest that low-salinity marshes in other estuaries are similarly sensitive to increases in both relative water level and salinity. In the Chesapeake Bay, Kearney et al. (1988) found that marsh losses in the Nanticoke River estuary since the 1920s had occurred primarily in the lower portions of the estuary; tidal freshwater marshes remained relatively stable, probably because they occur in the sediment-trapping portion of the estuary. However, it is likely that as sea level continues to rise, the salt wedge and the zone of major sediment deposition will move farther upstream (Meade 1972; Officer 1981), resulting in vegetation dieback or conversion to salt-tolerant species.

While excessive salinity can cause stress and dieback of marsh vegetation, occasional saltwater intrusion events may maintain or increase plant diversity which was the principal research hypothesis of this study. Our preliminary results using the September 2007 plant species richness and cover data do not support our research hypothesis. Salinity, frequency of flooding, and the interaction between the two variables did not prove to be significant predictors of plant species richness during the preliminary phase of this experiment, nor was a significant shift in the plant species composition of the marsh mesocosms observed. It should be noted however that the experimental treatments did not begin until well after the marsh mesocosm plant communities had had ample time (four months) to establish themselves under ideal growing conditions. The effects of salinity and increased flooding frequency are likely to manifest themselves early in a plants developmental stages, when the seeds/seedlings are at their most vulnerable to environmental perturbation. It is highly probable that under the current flooding frequency and salinity treatment regime (July 2007 – July 2008) the marsh mesocosm plant communities are likely to respond in a manner more supportive of our research hypothesis.

Despite the challenges associated with the reduced treatment schedule in Spring-Summer 2007 the fresh, transitional, and brackish marsh indicator taxa *Pilea pumila*, *Leersia oryzoides*, and *Spartina patens* did show significant individual reactions to either salinity, flooding stress, or the interaction of the variables. These results suggest that given a full tidal/salinity treatment regime



from the time of seed germination to plant maturity additional support for the research hypothesis may be attained. Additional soil redox potential data is currently being collected and will add further clarity to the preliminary redox potential results provided in Figures 18-20. At 30 cm depth soil redox potentials did appear to be consistently lower for the most frequently flooded groups which are what was expected, further redox data should make these differences more discernable. Further plant species above ground biomass and plant nutrient concentration data have not been obtained and analyzed as the experiment is still being run at the University of Maryland greenhouse complex.

The preliminary September 2007 data do not support our research hypothesizes at this time. However, we believe that this is mainly due to the delayed start of experimental treatments to the marsh mesocosms. The delay in flooding and salinity treatments allowed for the establishment of vegetation communities resistant to environmental perturbation. For the experiment to have it's best chance for success the mesocosm plant communities needed to be subjected to salinity and flooding treatments at the time of seedling germination (April/early May). Currently the mesocosms have been under salinity and flooding treatments from July 2007 to June 2008. We are confident that the next round of sampling will detect treatment effects as the germinating plants have been exposed to the salinity/flooding treatments as originally proposed.

Project Status Update and Products

Due to delays in contracting, time required to purchase building materials and plants for the mesocosms, construction time, and troubleshooting the tidal simulation system, mesocosms were not operational until mid-summer 2007. Initially we had planned to complete the greenhouse portion of the study by the end of 2007, but we decided to continue operating the mesocosms until mid-summer of 2008 so that sufficient time would be available to adequately assess treatment effects. Therefore, we requested and were granted a no cost extension until February 28, 2009. Sufficient funds are available for materials and labor to continue mesocosm operation until mid-summer, terminate the experiment, harvest soils and plants from the mesocosms, and process and analyze plant and soil samples.

Because the study is ongoing, no presentations have been given or papers published yet. Once the experimental portion of the study is complete and the data analyzed we plan to present the results at an international conference (e.g., Society of Wetland Scientists, 2009 in Madison, WI) and submit a manuscript on the study to a peer-reviewed journal.



Literature Cited

- Anderson, R. R., R. G. Brown, and R. D. Rappleye. 1968. Water quality and plant distribution along the upper Patuxent River, Maryland. *Chesapeake Science* 9: 145-156.
- Baldwin, A. H., K. L. McKee, and I. A. Mendelssohn. 1996. The influence of vegetation, salinity, and inundation on seed banks of oligohaline coastal marshes. *American Journal of Botany* 83: 470-479.
- Baldwin, A. H., and I. A. Mendelssohn. 1998. Effects of salinity and water level on coastal marshes: An experimental test of disturbance as a catalyst for vegetation change. *Aquatic Botany* 1250: 1-14.
- Baldwin, A. H., and E. F. DeRico. 1999. The seed bank of a restored tidal freshwater marsh in Washington, DC. *Urban Ecosystems* 3: 5-20.
- Baldwin, A. H., M. S. Egnotovich, and E. Clarke. 2001. Hydrologic change and vegetation of tidal freshwater marshes: Field, greenhouse, and seed-bank experiments. *Wetlands* 21: 519-531.
- Baldwin, A. H., and F. N. Pendleton. 2003. Interactive effects of animal disturbance and elevation on vegetation of a tidal freshwater marsh. *Estuaries* 26: 905-915.
- Baldwin, A. H. 2004. Restoring complex vegetation in urban settings: the case of tidal freshwater marshes. *Urban Ecosystems* 7: 137.
- Baumann, R. H., J. W. Day, Jr., and C. A. Miller. 1984. Mississippi deltaic wetland survival: Sedimentation versus coastal submergence. *Science* 224: 1095.
- Berggren, T. J., and J. T. Lieberman. 1977. Relative contributions of Hudson, Chesapeake, and Roanoke striped bass, *Morone saxatilis*, to the Atlantic coast fishery. *Fisheries Bulletin* 76: 335-345.
- Boesch, D. F., M. N. Josselyn, A. J. Mehta, J. T. Morris, W. K. Nuttle, C. A. Simenstad, and D. J. P. Swift. 1994. Scientific assessment of coastal wetland loss, restoration and management in Louisiana. *Journal of Coastal Research* SI20: 1-103.
- Broome, S. W., I. A. Mendelssohn, and K. L. McKee. 1995. Relative growth of *Spartina patens* (Ait.) Muhl. and *Scirpus olneyi* Gray occurring in a mixed stand as affected by salinity and flooding depth. *Wetlands* 15: 20-30.
- Cowardin L.M., Carter V., Golet F.C. & LaRoe E.T. Classification of wetlands and deepwater habitats of the United States. FWS/OBS-79/31. 1979. Washington, D.C., U.S. Fish and Wildlife Service.
Ref Type: Report
- Crain, C. M., B. R. Silliman, S. L. Bertness, and M. D. Bertness. 2004. Physical and biotic drivers of plant distribution across estuarine salinity gradients. *Ecology* 85: 2539-2549.



- Darke, A. K., and J. P. Megonigal. 2003. Control of sediment deposition rates in two mid-Atlantic Coast tidal freshwater wetlands. *Estuarine Coastal and Shelf Science* 57: 255-268.
- Day, J. W., J. Rybczyk, F. Scarton, A. Rismondo, D. Are, and G. Cecconi. 1999. Soil accretionary dynamics, sea-level rise and the survival of wetlands in Venice Lagoon: A field and modelling approach. *Estuarine Coastal and Shelf Science* 49: 607-628.
- Donnelly, J. P., and M. D. Bertness. 2001. Rapid shoreward encroachment of salt marsh cordgrass in response to accelerated sea-level rise. *Proceeding of the National Academy of Sciences* 98: 14218-14223.
- Faulkner, S. P., W. H. Patrick, Jr., and R. P. Gambrell. 1989. Field techniques for measuring wetland soil parameters. *Soil Science Society of America Journal* 53: 883-890.
- Flynn, K. M., K. L. McKee, and I. A. Mendelssohn. 1995. Recovery of freshwater marsh vegetation after a saltwater intrusion event. *Oecologia* 103: 63-72.
- Ford, M. A., D. R. Cahoon, and J. C. Lynch. 1999. Restoring marsh elevation in a rapidly-subsiding salt marsh by thin-layer deposition of dredge material. *Ecological Engineering* 12: 189-205.
- Gough, L., and J. B. Grace. 1998. Effects of flooding, salinity and herbivory on coastal plant communities, Louisiana, United States. *Oecologia* 117: 527-535.
- Hotes, S., E. B. Adema, A. P. Grootjans, T. Inoue, and P. Poschlod. 2005. Reed die-back related to increased sulfide concentration in a coastal mire in eastern Hokkaido, Japan. *Wetlands Ecology and Management* 13: 83-91.
- IPCC. Climate Change 2001: The Scientific Basis. Contribution of Working Group I to the Third Assessment Report of the Intergovernmental Panel on Climate Change. United Kingdom and New York, Cambridge University Press.
- Kearney, M. S., R. E. Grace, and J. C. Stevenson. 1988. Marsh loss in Nanticoke Estuary, Chesapeake Bay. *Geographical Review* 78: 206-220.
- Kearney, M. S., J. C. Stevenson, and L. G. Ward. 1994. Spatial and temporal changes in marsh vertical accretion rates at Monie Bay: implications for sea-level rise. *Journal of Coastal Research* 10: 1010-1020.
- Kozlowski, T. T. 1997. Responses of woody plants to flooding and salinity. *Tree Physiology Monograph* No. 1: 1-29.
- Lyles S.D., Hickman L.E. & Debaugh H.A. Sea level variations for the United States 1855-1986. 1988. Rockville, Maryland, National Oceanic and Atmospheric Administration, National Ocean Service.
Ref Type: Report
- McKee, K. L., and I. A. Mendelssohn. 1989. Response of a freshwater marsh plant community to increased salinity and increased water level. *Aquatic Botany* 34: 301-316.



- Meade, R. H. 1972. Transport and deposition of sediments in estuaries. *Geological Society of America Memoir* 133: 91-120.
- Mendelssohn, I. A., K. L. McKee, and W. H. Patrick. 1981. Oxygen deficiency in *Spartina alterniflora* roots: metabolic adaptation to anoxia. *Science* 214: 439-441.
- Mendelssohn, I. A., and D. P. Batzer. 2006. Abiotic constraints for wetland plants and animals. Pages 82-114 in D. P. Batzer, and R. R. Sharitz editors. *Ecology of freshwater and estuarine wetlands*. University of California Press, Berkeley and Los Angeles, California.
- Mitsch W. J., and J. G. Gosselink. 2000. *Wetlands*, Third edition., Third edition. John Wiley and Sons, New York.
- Morris, J. T., P. V. Sundareshwar, C. T. Nietch, B. Kjerfve, and D. R. Cahoon. 2002. Responses of coastal wetlands to rising sea level. *Ecology* 83: 2869-2877.
- Naidoo, G., K. L. McKee, and I. A. Mendelssohn. 1992. Anatomical and metabolic responses to waterlogging and salinity in *Spartina alterniflora* and *S. patens* (Poaceae). *American Journal of Botany* 79: 765-770.
- Neff, K. P., and A. H. Baldwin. 2004. Seed dispersal into wetlands: techniques and results for a restored tidal freshwater marsh. *Wetlands* 25: 392-404.
- Odum W.E., Smith III T.J., Hoover J.K. & McIvor C.C. The ecology of tidal freshwater marshes of the United States east coast: A community profile. FWS/OBS-83/17, 1-177. 1984. Washington, D.C., U.S. Fish and Wildlife Service.
Ref Type: Report
- Odum, W. E. 1988. Comparative ecology of tidal freshwater and salt marshes. *Annual Review of Ecology and Systematics* 19: 147-176.
- Officer, C. B. 1981. Physical dynamics of estuarine suspended sediments. *Marine Geology* 40: 1-14.
- Patrick, W. H., R. P. Gambrell, and S. P. Faulkner. 1996. Redox measurements of soils. Pages 1255-1273 in A. Klute editor. *Methods of soil analysis, Part 3. Chemical Methods*. Soil Science Society of America and American Society of Agronomy, Madison, Wisconsin.
- Peet, R. K. 1974. The measurement of species diversity. *Annual Review of Ecology and Systematics* 5: 285-307.
- Peet, R. K., T. R. Wentworth, and P. S. White. 1998. A flexible, multipurpose method for recording vegetation composition and structure. *Castanea* 63: 262-274.
- Perry, J. E., and C. H. Hershner. 1999. Temporal changes in the vegetation pattern in a tidal freshwater marsh. *Wetlands* 19: 90-99.
- Peterson, J. E., and A. H. Baldwin. 2004. Seedling emergence from seed banks of tidal freshwater wetlands: Response to inundation and sedimentation. *Aquatic Botany* 78: 243-254.



- Peterson, J. E., and A. H. Baldwin. 2004. Variation in wetland seed banks across a tidal freshwater landscape. *American Journal of Botany* 91: 1251-1259.
- Pezeshki, S. R., and R. D. DeLaune. 1993. Effects of soil hypoxia and salinity on gas exchange and growth of *Spartina patens*. *Marine Ecology-Progress Series* 96: 75-81.
- Reed, D. J. 1995. The Response of Coastal Marshes to Sea-Level Rise - Survival Or Submergence. *Earth Surface Processes and Landforms* 20: 39-48.
- Roman, C. T., J. A. Peck, J. R. Allen, J. W. King, and P. G. Appleby. 1997. Accretion of a New England (USA) salt marsh in response to inlet migration, storms, and sea-level rise. *Estuarine Coastal and Shelf Science* 45: 717-727.
- Stevenson, J. C., M. S. Kearney, and E. C. Pendleton. 1985. Sedimentation and erosion in a Chesapeake Bay brackish marsh system. *Marine Geology* 67: 213-235.
- Stevenson, J. C., L. G. Ward, and M. S. Kearney. 1986. Vertical accretion rates in marshes with varying rates of sea-level rise. Pages 241-259 in D. A. Wolfe editor. *Estuarine variability*. Academic Press, New York, New York.
- Stevenson, J. C., and M. S. Kearney. 1996. Shoreline dynamics on the windward and leeward shores of a large temperate estuary. Pages 233-259 in K.F.Nordstrom, and C.T.Roman editors. *Estuarine Shores: Evolution, Environments and Human Alterations*. John Wiley and Sons, Ltd..
- Taylor, J. A., A. P. Murdock, and N. I. Pontee. 2004. A macroscale analysis of coastal steepening around the coast of England and Wales. *Geographical Journal* 170: 179-188.
- Tiner R. W. 1993. Field guide to coastal wetland plants of the southeastern United States. The University of Massachusetts Press, Amherst, Massachusetts.
- Tiner R.W. & Burke D.G. Wetlands of Maryland. 1-193. 1995. U.S. Fish and Wildlife Service, Ecological Services, Region 5, Hadley, Massachusetts and Maryland Department of Natural Resources, Annapolis, Maryland.
Ref Type: Report
- Turner, R. E., E. M. Swenson, C. S. Milan, J. M. Lee, and T. A. Oswald. 2004. Below-ground biomass in healthy and impaired salt marshes. *Ecological Research* 19: 29-35.
- Valery, L., V. Bouchard, and J. Lefeuvre. 2004. Impact of the invasive native species *Elymus athericus* on carbon pools in a salt marsh. *Wetlands* 24: 268-276.
- Webb, E. C., I. A. Mendelssohn, and B. J. Wilsey. 1995. Causes for vegetation dieback in a Louisiana salt marsh: a bioassay approach. *Aquatic Botany* 51: 281-289.
- Webb, E. C., and I. A. Mendelssohn. 1996. Factors Affecting Vegetation Dieback of an Oligohaline Marsh in Coastal Louisiana: Field Manipulation of Salinity and Submergence. *American Journal of Botany* 83: 1429-1434.



APPENDIX A

EXPERIMENT PHOTOGRAPHS



Photograph showing a 19 liter bucket filled with collected marsh topsoil



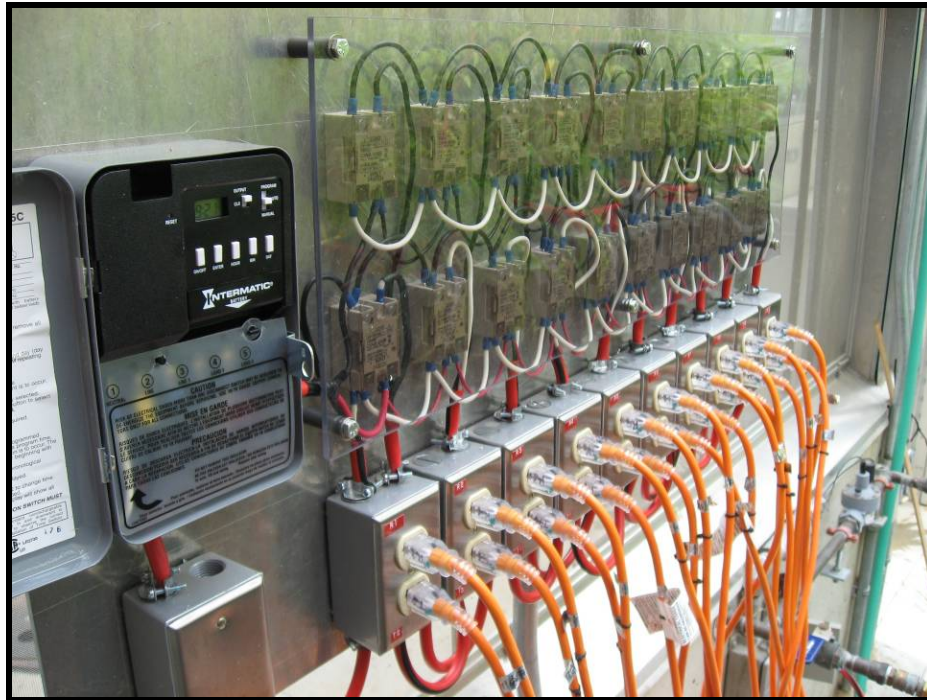
Marsh mesocosms in May 2007 prior to experimental treatments



Randomly planting supplemental plant species not recruited from the seedbank May 31, 2007



Marsh mesocosms in July 2007 just before the start of treatments



Timing box and relay switchboard for controlling the flow of water into and out of the mesocosm troughs



View of the marsh mesocosms in July 2007.

Assessing the role of road salt run-off on the critical ecological interactions that regulate carbon processing in small, headwater streams in the Chesapeake Bay watershed

Basic Information

Title:	Assessing the role of road salt run-off on the critical ecological interactions that regulate carbon processing in small, headwater streams in the Chesapeake Bay watershed
Project Number:	2007MD148B
Start Date:	3/1/2007
End Date:	2/29/2008
Funding Source:	104B
Congressional District:	MD 7th
Research Category:	Water Quality
Focus Category:	Non Point Pollution, Ecology, Nutrients
Descriptors:	
Principal Investigators:	Christopher Swan

Publication

Assessing the role of road salt run-off on the critical ecological interactions that regulate carbon processing in small, headwater streams in the Chesapeake Bay watershed.

MWRRC Project #2007MD148B

*Christopher M. Swan
Department of Geography & Environmental Systems
University of Maryland, Baltimore County
Baltimore, Maryland 21250*

Interim Project Report

Rationale for Project Extension

Due to a severe drought during summer 2007, I was unable to complete the extensive field component of the study proposed. A final report will be forthcoming in October 2008. However, after multiple attempts at the field work, I opted to design and carry out a complementary laboratory study to address, in part, the tasks proposed. Following is a summary of those studies.

Published Abstracts

P. Bogush, S.S. Kaushal & C.M. Swan. The interaction of road salt de-icer and dissolved organic carbon on microbial respiration in stream sediments. Ecological Society of America, San Jose, California, 2007

Student Support

Two graduate students (Peter Bogush, Carrie dePalma; both MS students enrolled in the Marine, Estuarine, and Environmental Science program) were supported in summer 2007 to work on the field project and to carry out the laboratory study summarized below. That study will comprise a significant portion of Peter Bogush's Master's thesis. He is scheduled to defend by the end of the Fall 2008 semester. I have another graduate student, Robin Van Meter (Ph.D., also enrolled in MEES) working on an associated project looking at the effects of road-salt contamination in ponds and associated effects on food webs. Robin aided with the project tasks. Rebecca Reeves, and undergraduate enrolled at UMBC in the Department of Geography & Environmental Systems, was supported by an NSF REU to the Baltimore Ecosystem Study LTER and also worked on the project.

Statement of Water Quality Problem

The ecological condition of streams and rivers reflect the myriad of disturbances humans make in a watershed. Elevated nutrient inputs via agricultural practices, drastically exaggerated flow regimes due to increases in impervious surface cover, and the resulting disruption of the balance between sedimentation and erosional forces typify the degraded stream ecosystem. The consequence for humans is the wholesale degradation of water

quality (Herlihy et al., 1998) as habitat is modified, reducing the capacity of the biota to properly mediate natural rates of nutrient cycling (e.g., carbon mineralization, denitrification; Groffman & Mayer, 2005). Researchers have recently discovered that streams draining human-dominated landscapes can experience enhanced loading of road salt deicer (Environment Canada, 2001; Kaushal et al., 2005). Elevated levels of chloride are reported to increase with road density and impervious surface cover, reaching levels known to impair freshwater life ($>250 \text{ mg l}^{-1}$; Hart et al., 1991; Kaushal et al., 2005). The potential for anthropogenic salinization to alter critical ecosystem processes performed by streams, specifically carbon processing, is largely unknown. Given the energetic reliance of forested stream food webs on riparian-derived, carbon-rich detritus (e.g., senesced leaf litter, wood), carbon processing in small, headwater streams is an important ecosystem function potentially at risk from elevated salt loading occurring in the region. The overall goals of this project are:

- (1) to identify microbial-invertebrate ecological features critical to decomposition that are impaired by salinization,
- (2) to determine the magnitude by which salinization alters decomposition rates, and
- (3) by working in a pristine environment, provide a solid benchmark by which future decisions can be made regarding road salt management.

Project Objectives

While many pollutants are federally regulated, no such regulations exist for road salt. Empirical tests of the effects of road salt on stream macroinvertebrates do exist (e.g., Blasius & Merritt, 2002), and even studies of leaf decomposition in streams receiving road salt have been done (e.g., Niyogi et al., 2001), but no work to date has explicitly manipulated road salt runoff and ascertained the consequences for various ecosystem processes *in situ*. While performing studies in streams receiving various levels of salt is a valuable endeavor, there can be many co-varying factors (e.g., land use practice, nutrient inputs) that can also lead to degradation of carbon processing. Therefore, large-scale manipulations under natural conditions are needed to provide natural resource managers and decision-makers with solid information on the role salt plays in streams. The specific tasks to be undertaken are:

Task I. Manipulate salt at the reach-scale in a small, forested stream to learn how whole-reach metabolism and local community structure will react to salt stress,

Task II. Perform reciprocal transplants of leaf litter between the salt addition reach and the un-manipulated upstream control reach to learn how microbial colonization under the salt-regime changes decay in the impacted vs. un-impacted shredder communities, and

Task III. Perform feeding studies in the lab with the dominant shredder taxa found under each salt condition on salt vs. non-salt conditioned litter to determine potential changes in shredder feeding efficiencies.

Project Results to Date

Rationale

Given the drought, a stream mesocosm study was carried out to address **Tasks II and III**. Small recirculating streams were maintained indoors and the interactive effect of salt loading and invertebrate feeding activity on carbon mineralization estimated. Specifically, I asked (1) does salt loading alter microbial mineralization of carbon on leaf litter, and (2) does invertebrate feeding activity alter the magnitude of the salt effect on C mineralization rates?

Methods

Recirculating stream mesocosms were created using round 26.6 l containers. Mesocosms were designed to maintain a water level of 10 cm over 1.5 cm of natural stream sediments collected from a local headwater stream (Patapsco State Park). A small submersible pump returned water from the internal center container to the outer channel, creating a flow-through environment designed to mimic the stream at baseflow. Flow in the mesocosms averaged 8.6 cm s^{-1} .

Sensenced leaf litter from American Beech was placed in litter bags (7 x 11 mm mesh) into a first-order, spring fed stream on August 13, 2008 and allowed to incubate and colonize with bacteria and fungi for 10 d. Litter was returned to the lab and ~2g wet mass of litter added to 10 separate mesocosms. All ten mesocosms received 30 individual *Gammarus* sp. (Amphipoda) and a single *Tipula* sp. (Diptera) as the shredders. These taxa are common to the streams studied at Patapsco State Park. Salt concentrations in five randomly chosen mesocosms was raised to 5 g Cl l^{-1} . To isolate the effect of shredder feeding activity on microbial degradative ability, six 2.5 cm leaf discs were placed in 300 mm mesh cages inside each mesocosm, inhibiting access by the shredding invertebrates. The invertebrates were allowed to feed for 7 d prior to the salt addition.

After 24 h of salt exposure, microbial respiration on the leaf surfaces was measured using a standard dark bottle incubation. Water from each mesocosm was placed into two 55 ml centrifuge tubes, six leaf discs from each shredder treatment (inside and outside the cages) placed separately in each tube. Dissolved oxygen was measured in each tube, then allowed to incubate in the dark at ambient temperatures under gentle agitation for ~24 h. Dissolved oxygen was then taken, leaf litter removed, dried to a constant mass at $70 \text{ }^{\circ}\text{C}$, then combusted for 45 min at $550 \text{ }^{\circ}\text{C}$ to determined ash-free dry mass (Benfield, 2006). Oxygen uptake rates ($\text{mg O}_2 \text{ h}^{-1} \text{ g}^{-1} \text{ AFDM}$) was then calculated for each salt x shredder combination.

Data was analyzed using a nested ANOVA, with shredder treatment nested within salt treatment, and post-hoc comparisons made between treatments. Significance was determined for pairwise comparisons after adjusting p-values using the Tukey HSD method. Analyses were carried out in SAS (version 9.2). Assumptions of normality of residuals were met (Shapiro-Wilkes test), however I did observe unequal variances between the shredder treatments. To address this, I grouped the residual variances by treatment using the GROUP option in PROC MIXED using the method of Littell et al., 1996.

Results & Discussion

This study revealed that in the short term (24 h), as may be typical of a natural discharge event, salt loading interacts strongly with shredder presence to alter rates of carbon mineralization on leaf litter. Salt significantly depressed microbial respiration rates by more than 38% (242.8 vs. 149.8 mg O₂ h⁻¹ g⁻¹ AFDM, $P < 0.0001$) within 24 hours of the addition regardless of shredder treatment. However, there was a significant amelioration of this effect when invertebrates had access to the leaf litter (Table 1; Fig. 1). In the absence of salt, shredders had no effect on oxygen uptake rates (Fig. 1.), but in the presence of salt, shredder access to leaf litter reduced the negative impact of salt by 41.9 mg O₂ h⁻¹ g⁻¹ AFDM ($P < 0.01$).

These results suggest that in the short term, salt heavy salt loading (e.g., 5 g Cl l⁻¹ in this study) has the potential to strongly reduce rates of carbon mineralization. However, if invertebrate detritivores can endure such pulses, then their presence seems to reduce the magnitude of the salt disturbance. Recent work suggests that many invertebrate taxa in Maryland streams can endure elevated chloride levels (Morgan et al 2007). Therefore, maintaining habitat conditions such that shredder taxa can survive might be an important consideration when managing the predicted negative impacts of salt loading to streams in the mid-Atlantic region.

Table 1. Nested ANOVA results. “Salt” indicates the salt treatment (+,-), and “Shredder(Salt)” is the shredder treatment (+,-) nested within salt treatment.

SOV	DF	F	P
Salt	1,16	37.7	<0.001
Shredder (Salt)	2,16	4.6	0.0260

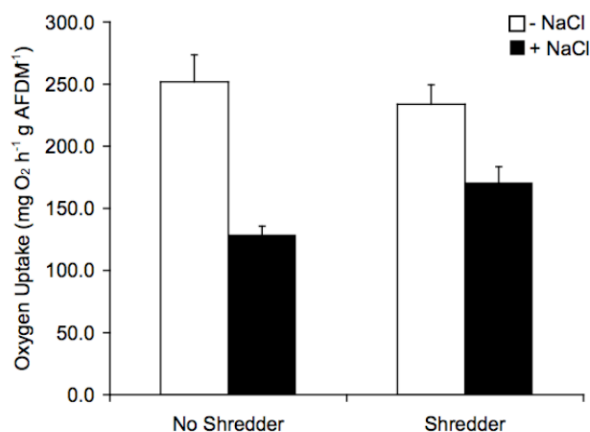


Figure 1. Results from laboratory manipulation of the presence/absence of salt stress at levels reported in freshwater in the Chesapeake Bay region (5 g Cl l⁻¹; Kaushal et al., 2005), and the presence/absence of invertebrate consumers (shredders) on microbial carbon mineralization (i.e., oxygen uptake) on leaf litter. These results were after 24 h of salt exposure. The presence of road salt resulted in ~50% reduction in carbon mineralization rate, but the effect was ameliorated by the presence of invertebrate consumers. Bars are means + 1 standard error, n=5 per treatment combination.

Conclusions

No federal regulations currently exist for road salt, emphasizing the importance of the observation that chloride concentrations are rising in receiving streams and rivers as impervious surface cover on the landscape increases (Kaushal et al., 2005). This, in

conjunction with the predicted disproportionate increase in population growth in the mid-Atlantic region (US Census Bureau, 2005), underscores the need to understand the water quality implications of salt loading to streams and rivers. Small, headwater streams are energetically supported by organic matter inputs as leaf litter from streamside forests, and decay of the material is a complex interaction between invertebrate consumers, microbial communities and litter quality (e.g., nutrient content; Fisher & Likens, 1973; Webster & Benfield, 1986; Wallace et al., 1997; Hall et al., 2001). Mineralization of this organic matter is an important ecosystem process since it describes the rate at which nutrient input (carbon) is removed and passed either up the food web to higher trophic levels or respired (Wallace et al., 1997). I show here that the microbial community responsible for carbon mineralization is negatively impacted by salt at levels currently occurring in the environment (Fig. 1). I interpret these results (Fig. 1) to suggest that road salt stress, which is predicted to continue to increase as impervious surface cover increases on the landscape, disrupts the capability of stream food webs to mediate organic matter dynamics. Interestingly, the presence of invertebrate consumers, which are known to suffer substantially from other sources of anthropogenic disturbance, including very high levels of salt (e.g., higher than we manipulated), seem to ameliorate this negative effect.

I plan to take this work to the field this summer-fall to explore the reach scale effects on patterns in whole-stream metabolism, and any subsequent effects on invertebrate dynamics (address **Task I**, support evidence gathered to address **Tasks II & III**). The results presented here, while intriguing, did not allow for invertebrate emigration, and were at fairly high levels of chloride (but within the range reported for freshwater ecosystems in the region; Kaushal et al 2005). By experimentally introducing salt to a local stream, I can both assess whole stream metabolism and invertebrate dispersal patterns. The predicted results should complement the laboratory findings.

References

- Blasius, B.J. & R.W. Merritt. 2002. Field and laboratory investigations on the effects of road salt (NaCl) on stream macroinvertebrate communities. *Environmental Pollution* 120: 219-231.
- Benfield, E.F. 2006. Decomposition of leaf material. Chapter 30 In F.R. Hauer and G.A. Lamberti (eds.) *Methods in Stream Ecology*. Academic Press, San Diego.
- Environment Canada. 2001. *Assessment Report – Road Salts*.
- Fisher, S.G. & G.E. Likens. 1973. Energy flow in Bear Brook, NH: an integrative approach to stream ecosystem metabolism. *Ecological Monographs* 43:412-439.
- Groffman, P.M., A.M. Dorsey & P.M. Mayer. 2005. Nitrogen processing within geomorphic features in urban streams. *Journal of the North American Benthological Society* 24:613-625.
- Hall, R.O., Likens, G.E. & Malcom H.M. 2001. Trophic Basis of Invertebrate Production in 2 Streams at the Hubbard Brook Experimental Forest. *Journal of the North American Benthological Society* 20:432-447.

- Hart, B.T, P. Bailey, R. Edwards, K. Hortle, K. James, A. McMahon, C. Meredith, & K Swadling. 1991. A review of the salt sensitivity of the Australian freshwater biota. *Hydrobiologia* 210:105-144.
- Herlihy, A.T., J.L. Stoddard & C.B. Johnson. 1998. The relationship between stream chemistry and watershed land cover data in the Mid-Atlantic Region, U.S. *Water, Air, and Soil Pollution* 105:377-386.
- Kaushal, S.S., P.M. Groffman, G.E. Likens, K.T. Belt, W.P. Stack, V.R. Kelly, L.E. Band & G.T. Fisher. 2005. Increased salinization of fresh water in the northeastern U.S. *Proceedings of the National Academy of Sciences* 102:13517-13520.
- Littell, R. C., G. A. Milliken, W. W. Stroup, and R. D. Wolfinger. 1996. Heterogeneous variance models. Chapter 8 in *SAS System for Linear Models*. SAS Institute Incorporated, Cary, North Carolina.
- Morgan, R.P., III, K.M. Kline and S.F. Cushman. 2007. Relationships among nutrients, chloride and biological indices in urban Maryland streams. *Urban Ecosystems* 10:153-166.
- Niyogi, D.K., W.M. Lewis & D. M. McKnight. 2001. Litter breakdown in mountain streams affected by mine drainage: biotic mediation of abiotic controls. *Ecology* 11:506-516
- Wallace, J.B., S.B. Eggert, J.L. Meyer, & J.R. Webster. 1997. Multiple trophic levels of a forest stream linked to terrestrial litter inputs. *Science* 277:102-104.
- Webster, J.R. & E.F. Benfield. 1986. Vascular plant breakdown in freshwater ecosystems. *Annual Review of Ecology and Systematics* 17:567-594.

Sublethal Reproductive and Developmental Responses in the Fathead Minnow (*Pimephales promelas*) Exposed to Endocrine Disruptors in Poultry Litter

Basic Information

Title:	Sublethal Reproductive and Developmental Responses in the Fathead Minnow (<i>Pimephales promelas</i>) Exposed to Endocrine Disruptors in Poultry Litter
Project Number:	2007MD149B
Start Date:	5/1/2007
End Date:	10/1/2007
Funding Source:	104B
Congressional District:	MD-5
Research Category:	Water Quality
Focus Category:	Toxic Substances, Ecology, Agriculture
Descriptors:	
Principal Investigators:	Allen Davis, Allen Davis

Publication

Sublethal Reproductive and Developmental Responses in the Fathead Minnow (*Pimephales promelas*) Exposed to Endocrine Disruptors in Poultry Litter

Sara J. Pollack
Marine-Estuarine-Environmental Science
April 25th, 2008

The Eastern Shore of the Chesapeake Bay is one of the largest poultry production regions in the United States. As such, approximately 1.6 billion lbs. of manure or litter are generated annually (USDA 2002). The most cost effective use of this litter is as an organic fertilizer for agricultural fields. However, poultry litter contains a multitude of compounds including pesticides, feed additives for controlling disease, and natural steroid hormones excreted by poultry into their feces, all of which may target the endocrine system in all vertebrates (Yonkos 2005; Chesapeake Bay Foundation 2004; Hanselman et al. 2003). The natural stability and insolubility of these compounds may pose significant, long-term risk to the endocrine system of aquatic organisms, particularly fish dwelling in surface waters that receive run-off from poultry litter-treated agricultural fields (Yonkos 2005; Herman and Mills 2003). Here, I tested the response of fathead minnows (*Pimephales promelas*) to exposure to poultry litter leachate.

Adult minnows (P₁ Generation) were first exposed to two different concentrations of a poultry litter leachate (High and Low; PLL) for 21 days. Reproductive endpoints assessed included fecundity per breeding group and secondary sex characteristics in male fish. Additionally, offspring generated from the P₁ adult fish were exposed from egg to 21 days to poultry litter treatments for the F₁ or offspring generation.

The P₁ adult fish exhibited a significant decline in fecundity in poultry litter exposed groups compared to controls. P₁ male fish had a significant reduction in the expression of their secondary sex characteristics in all treated groups compared to controls. These morphological traits are crucial to the successful breeding for males in the population. Males in the E2 and High PLL treatments had fewer breeding tubercles than other treated males or controls and males in all treatments had smaller dorsal epithelial pad dimensions on average over time compared to controls. Interestingly, tubercle number and dorsal epithelial pad measures declined after only two weeks of exposure and the most noted differences were observed at day 21. Vitellogenin production (an egg yolk pre-cursor protein used as a biomarker to determine estrogenic exposure in male fish) was significant and increased in a dose dependent manner with respect to the Low PLL, High PLL and E2 treated male fish.

In the F₁ Generation, overall health and survival did not differ significantly among treatments. However, the High PLL exposed F₁ Generation fish from the High PLL P₁ Generation groups had a significantly skewed gender ratio toward female, leaving far fewer males in the population compared to the other treated groups.

The overuse of poultry litter as a fertilizer has become a topic of regional concern. Agricultural run-off carrying unknown contaminant mixtures enter lotic and lentic systems that feed into the Chesapeake Bay. My results demonstrate that exposure of fish to poultry litter may induce endocrine disrupting responses with respect to reproductive capacity. A decrease in the number of male breeding tubercles, and diminished dorsal epithelial pad in adult exposed fish also suggest a feminization of males from these exposures. Animals within a population that exhibit a reduced or compromised ability to reproduce may not contribute their genes to subsequent generations which in turn may have significant consequences on population dynamics over time. More generally, the response of this model fish species in environmental studies suggests that other organisms, especially other species of fish, may have their endocrine systems adversely affected by poultry litter inputs to aquatic systems.

Developing Permeable Sorptive Barriers for Petroleum Contaminant Removal from Groundwater Using High Carbon Content Fly Ash

Basic Information

Title:	Developing Permeable Sorptive Barriers for Petroleum Contaminant Removal from Groundwater Using High Carbon Content Fly Ash
Project Number:	2007MD150B
Start Date:	5/1/2007
End Date:	10/1/2007
Funding Source:	104B
Congressional District:	MD-5
Research Category:	Water Quality
Focus Category:	Toxic Substances, Hydrology, Groundwater
Descriptors:	
Principal Investigators:	Allen Davis, Allen Davis

Publication

Developing Permeable Sorptive Barriers for Petroleum Contaminant Removal from Groundwater Using High Carbon Content Fly Ash

Summary Report

Submitted to:

**Maryland Water Resources Center
for the Summer Graduate Fellowship**

Date: April 28, 2008

Mehmet M. Demirkan

**Department of Civil and Environmental Engineering
Geotechnical Engineering Program
University of Maryland-College Park**

Remediation of groundwater contaminated with petroleum-based products has been an important task for engineers and scientists in recent years. As a result, the difficulty of reducing subsurface contamination levels has resulted in the research and development of several innovative in-situ treatment technologies. One of the passive remediation technologies gaining wide acceptance is permeable reactive barrier (PRB). In this technique, the pollutants are immobilized permanently or their levels are reduced to the Maximum Contamination Limits (MCL) while the plume is passing through an underground barrier system. PRBs provide versatile containment option because they are a passive means of stripping contaminants from groundwater and they can be applied to different sites and contaminants by choosing an appropriate reactive medium. Reactive media constitutes the major cost for the PRB application. Due to high cost of manufactured filling materials such as zero valent iron and activated carbon, current research is underway to investigate the effectiveness of alternative reactive materials.

Legislations have been promulgated in many states to incorporate recycled materials into engineering applications. One alternative material that is abundant in Maryland as well as in various parts of the United States is the high carbon content (HCC) Class F fly ash. According to American Coal Ash Association (ACAA), the total ash production of 858 power electrical plants in the United States is approximately 108 millions tons per year and only 30% of this ash is being beneficially reused and the remaining has to be landfilled. Furthermore, the beneficial reuse percentage of fly ash in the concrete industry has been in a decline due to an increase in the amount of unburned carbon in the fly ash by introducing the low NO_x burners to the coal combustion system of power plants.

In this research, it was hypothesized that the unburned carbon contained in the fly ash can be used as a sorptive medium for petroleum hydrocarbons in the subsurface. The overall goal of this study was to evaluate the effectiveness of high carbon content fly ash as a sorptive agent for subsurface remediation of petroleum-contaminated groundwater. To accomplish this goal, experimental and numerical analyses were conducted. Naphthalene and *o*-xylene were employed as model subsurface contaminants.

The performance of high carbon content as a reactive medium in a permeable reactive barrier was investigated through column sorption-desorption experiments, column biodegradation experiments, and numerical design of reactive barriers. Column sorption-desorption tests were conducted on fly ash-sand mixtures (40% fly ash and 60% sand by weight) in sterile conditions. After completion of the experiments, the data was modeled using VMOD-MT3DMS. For the column biodegradation experiments, an isolated culture was used for inoculation and to simulate the biodegradation process in sand and fly ash-sand mixture columns. The results of the biodegradation experiments were also

numerically modeled in order to assess effectiveness of the biokinetic parameters estimated from experiments. Following the column experiments, a numerical model of typical PRB was constructed in order to investigate the barrier life expectancies. The model output for different fly ash types and groundwater velocities were used to develop design charts for practical applications.

The findings of the column sorption desorption tests on the mixtures of sand with three fly ashes, DP, PS, and MT, with LOI content of 20.5%, 10.7%, and 3.1%, respectively, and PAC have shown that high carbon content fly ashes are strong sorbents with sorption properties comparable to a commercially powder activated carbon with retardation capacity of 48 to 78% for naphthalene and 15 to 48% for *o*-xylene. These ranges were very comparable to the range observed for retardation within PAC. Retarded naphthalene and *o*-xylene amounts increased with increasing LOI content (MT, PS, DP fly ashes and PAC, respectively) in the column tests. For example, the DP fly ash exhibited sorption properties comparable to a commercially powder activated carbon

The measured hydraulic conductivities of fly ash-sand mixtures in the column sorption-desorption tests were comparable with the typical field hydraulic conductivities reported for PRBs. The bromide tracer test data indicated that dispersivity values range between 0.09 and 0.76 cm, and 0.04-0.96 cm for fly ash-sand and PAC-sand mixtures, respectively. These values fall in a typical range of values reported for sorptive media with relatively high fines content.

pH readings during column experiments showed that pH initially remained constant for several pore volumes of flow, then decreased at the later stages, and eventually dropped to a level comparable to the pH of artificial groundwater solution (i.e., pH =6.9). The buffering capacities of the Maryland fly ashes tested in this study were diminished and the pH in the system was governed by the PIPES buffer.

Numerical simulations conducted on the column sorption desorption data revealed that the breakthrough curves determined using the batch parameters shifted rightward implying that the naphthalene sorption is overpredicted by using batch adsorption test derived parameters. It is possible that a combination of factors such as solid-to-liquid ratio, sorption nonlinearity, and nonequilibrium (rate-limited) sorption caused the observed discrepancy between the batch and column-derived parameters.

Freundlich isotherm coefficients calculated from the column data were 27.3 to 47.3% lower than the batch-determined ones. Column sorption-desorption data was successfully described using a Freundlich isotherm. The areas under the contaminant breakthrough curves were used to calculate the retarded contaminant mass during the experiment. The calculations revealed that the retarded naphthalene amount increased with increasing LOI values (MT, PS,

DP fly ashes and PAC, respectively). The retarded mass per gram sorptive medium calculated from Port C is consistently higher than the one calculated at port B, which indicated that the retarded mass increased along the height of the column.

Similar to the naphthalene tests, *o*-xylene breakthrough curves have sharp adsorption fronts during the sorption phase of the experiments. A tailing of desorption front was observed in all tests. It was speculated that the effects of equilibrium sorption-desorption was most evident from the self-sharpened adsorption fronts of the breakthrough curve without any tailing. Thus, the sharp front adsorption curves suggested that the sorption equilibrium was achieved during the *o*-xylene adsorption onto all media. *O*-xylene breakthrough curves also exhibited tailing at the desorption front.

The results of the biodegradation test revealed high levels of biodegradation occurred when fly ash was employed as the reactive medium. These high levels of biodegradation were a result of increased residence time associated with retardation of the contaminant due to sorption onto fly ash. This finding implies that sorption was a key factor in the biodegradation dynamics of the substrates during the biodegradation process. Therefore, even though there may be concerns about the reduction of the local bioavailability of the substrate due to sorption, the residence time associated with biodegradation was enhanced for systems undergoing a sorptive transport. Attached biomass and DO measurements conducted during the experiments supported that the increase in the biodegradation was due to sorption-derived long retention times.

Life expectancies of the bioreactive barriers were calculated for different barrier dimensions and aquifer conditions using a numerical model. Fly ashes with higher sorption potential (i.e., higher LOI) performed better as greater amounts of contaminant were captured by the barrier. The groundwater velocity had a significant effect on the overall fate of the contaminant treated in the barrier, and higher groundwater flows resulted in shorter barrier lives. Barriers exposed to slower groundwater velocities had a better performance when microbial decay is occurring in the barrier.

This study represents an important step towards implementation of a currently landfilled waste material in a environmental cleanup process. The performance and the environmental impact of the material was tested with respect to various applications. These broad assessment on “waste material” showed that high carbon content fly ash has a great potential as remediation medium for soil and groundwater mitigation against petroleum contamination.

There is an increasing need in using sustainable technologies in environmental remediation and as a result, recycled materials are increasingly being more incorporated into design. This study also enhances the understanding of the role of standard testing procedures on recycled materials.

Approaches like this one will enhance the incorporation of recycled materials into remediation applications, and will provide information to facilitate more sustainable engineering applications.

Hydraulic Consequences of Riparian Vegetation on Bank Roughness in Urban Stream Corridors

Basic Information

Title:	Hydraulic Consequences of Riparian Vegetation on Bank Roughness in Urban Stream Corridors
Project Number:	2007MD154B
Start Date:	5/1/2007
End Date:	10/1/2007
Funding Source:	104B
Congressional District:	MD-5
Research Category:	Climate and Hydrologic Processes
Focus Category:	Hydrology, Floods, Conservation
Descriptors:	
Principal Investigators:	Allen Davis, Allen Davis

Publication

Summer 2007 Project Progress Report
Erik Hankin
Advisor: Dr. Karen Prestegaard
Department of Geology

The lower portions of the northwest and northeast branches of the Anacostia River are within a channel designed to carry flood flows downstream. The channel banks are either concrete (smooth) or lined with boulder rip-rap. Both types of materials are designed to protect the channel bank from erosion. Neither of these materials provides shade, organic matter, or cover for biota that use river margins as their habitats. A proposal was made to plant native grasses along these floodways to provide habitat.

However, there is a question as to what effect will the plantings of these native grasses and herbs have on the capacity of the channel to convey flood discharges. Will the grasses increase or decrease the flood-carrying capacity of the channels during high flows. There is a concern that any vegetation will cause roughness and decrease the conveyance capacity of floods. A portion of this project aims to determine what effect native grasses have on the capacity of the channel to convey flood discharges.

The purpose of the Anacostia River portion of this project is to determine what effect native grasses have on the capacity of the channel to convey flood discharges using the hypothesis that native grass and herb plantings will decrease flow resistance and increase the flood-carrying capacity of the channels at high flows. The study shall provide a detailed assessment of whether the plantings of native grasses and herbs on the banks of a rip-rap protected channel affects flow resistance and the carrying capacity of the channel and detailed guidance on how to determine the changes in flow resistance of the channel banks due to re-vegetation. This data will then be coupled with flow resistance data from other banks along Paint Branch and Little Paint Branch in an attempt to understand the causes of erosion along straight reaches.

Three sites along the banks of the treatment site were used; one site consists of native vegetation, one is a mixture of native and introduced, and the third is a "kill site" with little to no vegetation due to herbicidal treatment. Each site is 6 x 6 meters and is composed of five transects lined parallel to the stream channel, all 1.5 meters apart. The transects are fairly homogeneous with large (up to 1 meter in length) rip-rap boulders placed along the bank.

This summer, a research team, consisting of Erik Hankin, Zach Blanchet, and Dr. Karen Prestegaard, went about the task of measuring rock and plant roughness heights for each site. Along each transect, bank and vegetation roughness heights were measured every 5 centimeters for the entire 6 meter length. In addition to roughness height measurements, plants were also identified. This ecological information will later be used when determining the relationship between plant shape and flow resistance.

The preliminary data show that rock roughness heights are all similar for the three sites with averages around 24 cm. This comes as no surprise as the banks are lined with

imported rip-rap. The “kill site” has the smallest average plant roughness height (22 cm), followed by the native plant site (38 cm). The site with a mixture of native and invasive plants has the highest average roughness height at 47 cm.

Unfortunately, due to the extreme lack of rain this summer, it was not possible to measure the effects of the vegetation on the flow regime during high flows. As a result, more time was spent studying possible sites for the rest of the project regarding stream bank erosion on straight reaches. Straight reaches along Paint Branch and Little Paint Branch will be gauged and measured for cross section, grain size distribution, and bank roughness heights. The sites include Cherry Hill Road Community Park and the Paint Branch Golf Club for Paint Branch and Fairland Recreational Park for Little Paint Branch. These sites all have straight reaches but differ in dimension and bank vegetation species and distribution.

Many thanks are due to the Maryland Water Resources Research Center for their generous funding of this project over the summer of 2007.

Grant No. 07HQGR0098 Development of Detailed Lock Model – Phase 1 through Phase 3

Basic Information

Title:	Grant No. 07HQGR0098 Development of Detailed Lock Model – Phase 1 through Phase 3
Project Number:	2007MD189S
Start Date:	4/13/2007
End Date:	2/29/2008
Funding Source:	Supplemental
Congressional District:	Md-5
Research Category:	Engineering
Focus Category:	Management and Planning, Water Use, Surface Water
Descriptors:	
Principal Investigators:	Allen Davis, Paul Schonfeld

Publication

Draft Report on Detailed Lock Model Phase 3

By Shiaaulir Wang, Ning Yang and Paul Schonfeld

*Department of Civil and Environmental Engineering
University of Maryland, College Park*

June, 2008

Table of Contents

Table of Contents	2
List of Tables	3
List of Figures	4
Introduction.....	5
Lock Control Policy	5
SPF (Shortest Processing Time First)	5
FSPF (Fairer Shortest Processing Time First)	7
Multi-Recreation Lockage	8
Multi-Recreation Craft during Regular Lockage	9
Multi-Rec during Chamber Turn Back	10
Navigable Pass	10
Operation Logic	11
Open Pass.....	14
Multi-cut Lockage Efficiency Enhancements.....	15
Using Efficiency Enhancement Equipments	15
Help Equipment	15
Schemes of Handling Extracted Cut	16
Serving Rec. Vessels during Chamber Turnback	17
DLM Shipment List	17
Shipment Data.....	17
Read DLM Traffic	19
Vessel Type.....	19
Cut Information.....	22

List of Tables

Table 1 Lock Information	11
Table 2 Information of Navigable Pass	11
Table 3 Processing Time Distributions for Navigable Pass.....	11
Table 4 Chamber Specification for Vessel Assistance	16
Table 5 Processing Time Distributions for Chamber with Vessel Assistance.....	16
Table 6 Policies for Recreational Vessels.....	17
Table 7 DLM Data for Vessel Traffic.....	17

List of Figures

Figure 1 Operation Logic for SPF Control	6
Figure 2 Operation Logic of FSPF Control	8
Figure 3 "Start of Lockage" Event for Recreational Vessels.....	9
Figure 4 "Start of Chamber Turnback" Event.....	10
Figure 5 Arrive Lock for Navigable Pass	12
Figure 6 End of Entry for Navigable Pass	13
Figure 7 End of Chambering for Navigable Pass	13
Figure 8 End of Fly Exit / Rec. EOL for Navigable Pass	14
Figure 9 DLM Shipment List.....	19
Figure 10 DLM Shipment List.....	21

Introduction

In continuing the work from Phases 1 and 2 of this project, the DLM development focuses on the following tasks in the Phase 3:

- modeling more control policies
- enhancing the efficiency of multi-cut lockages
- locking recreational vessels in groups
- modeling multi-vessel lockages
- considering mixed vessel lockages
- modeling interference for multi-chamber locks
- including random minor closures
- considering open pass and navigation pass

Lock Control Policy

In this phase, two more control policies are modeled. SPF (Shortest Processing Time First) has already been discussed in the simulation text book. It provides a way of re-sequencing the queue. Due to the re-sequencing, we should reconsider whether FCFS is the fairest way to provide the service. Some studies (Ting and Schonfeld, Wang and Schonfeld) have been conducted to evaluate the performance between FCFS and SPF at single waterway lock or in waterway network. A fairer SPF (FSPF) has also been proposed to consider the fairness constraint (Ting and Schonfeld, Wang and Schonfeld).

SPF (Shortest Processing Time First)

From definition, Shortest Processing Time First operation might select the tow based on the “average service time tow”. The tow with the lowest service time (usually the smallest tow) has the first priority to be processed. However, with different tow sizes, measuring the service or delay times per barge should be better than per tow due to the size variations. Thus, the SPF in current model is designed to assign the tow with minimum service time per barge (i.e. usually the largest tow) rather than the minimum service time per tow (i.e. the smallest tow). The SPF operation logic is shown in Figure 1. The SPF factor is calculated based on the average service time per barge.

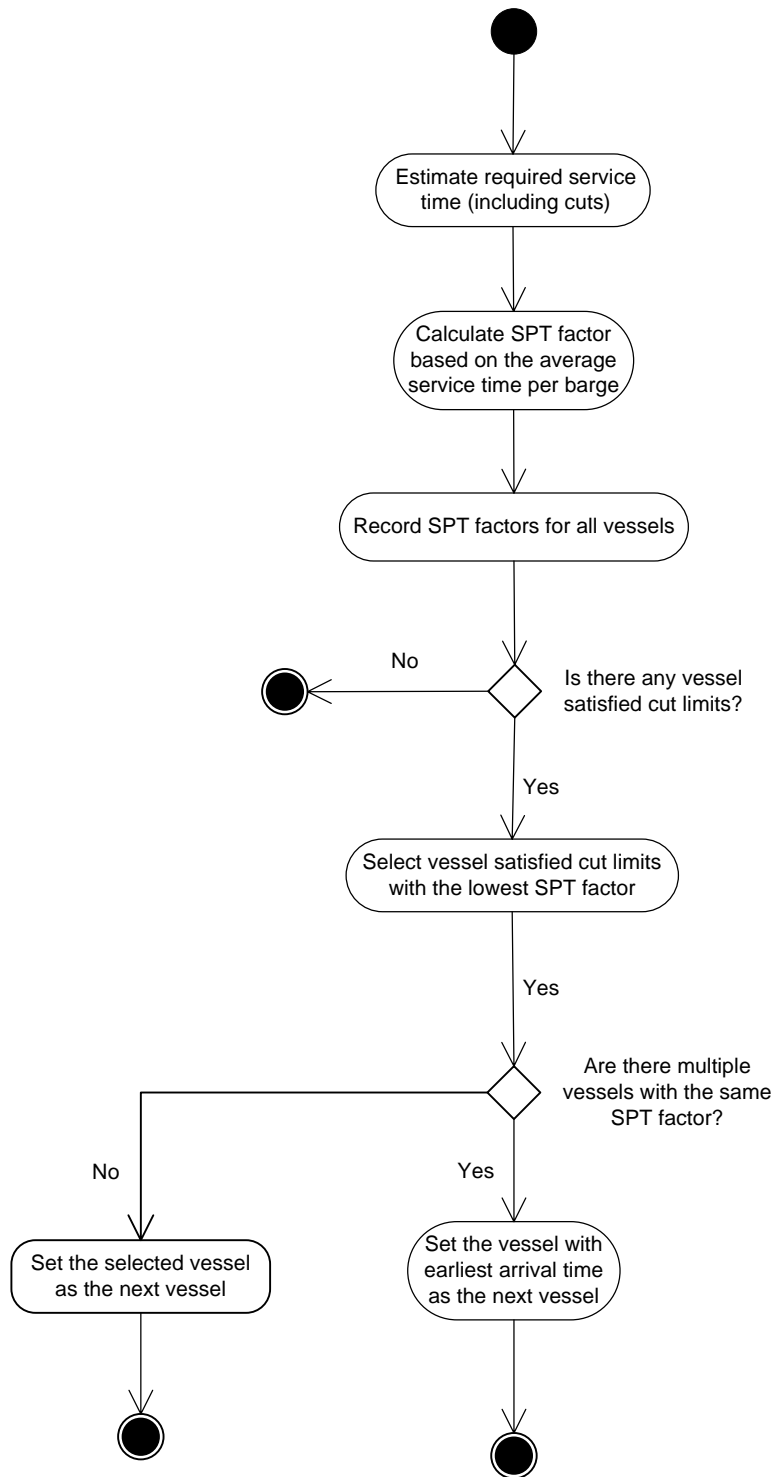


Figure 1 Operation Logic for SPF Control

There are some assumptions of SPF:

1. Shortest processing time records the 'shortest service time per barge' and assigns the available chamber to this tow; however, all exclusive rules should be

- considered.
2. For the same number of cuts, the tow with more barges has higher priority than one with fewer barges.
 3. For different number of cuts, we need to estimate the total incremental chamber turnback time for tows with more cuts; furthermore, we can calculate the average service time per barge for each tow and determine which tow is the next vessel.
 4. If there are multiple vessels with the same SP time, then we select the next vessel based on the FIFO operation rule.

In the current DLM, the processing time is determined by the number of cuts. Therefore, the tow with the fewest cuts has the highest priority with SPF policy.

FSPF (Fairer Shortest Processing Time First)

From the system point of view, SPF can save more system total delays through the pre-specified dispatching priority. However, small tows may experience more delays with SPF than FCFS. In order to balance the system efficiency and fairness among individual tows, FSPF is proposed to be intermediate between SPF and FCFS. FSPF is the control policy to take care the tows waiting for a certain number of lockages (F^*) based on the SPF rules. F^* is the fairness value pre-defined in the input table. Different fairness values will influence the system performance. In general, if F^* decreases, FSPF will be quite similar to FCFS. But if F^* increases, FSPF will be close to SPF.

Furthermore, the average number of tows in the queue is a significant indicator for evaluating the system. FSPF with lower fairness value gives smaller tows more chances to leave the waiting queues while they keep being over passed by larger tows. Also, in the contrast, the system will be more efficient with lower barge delays and shorter barge queues based on the higher F^* . All other assumptions of FSPF are similar to those of SPF. The FSPF operation logic is shown in Figure 2.

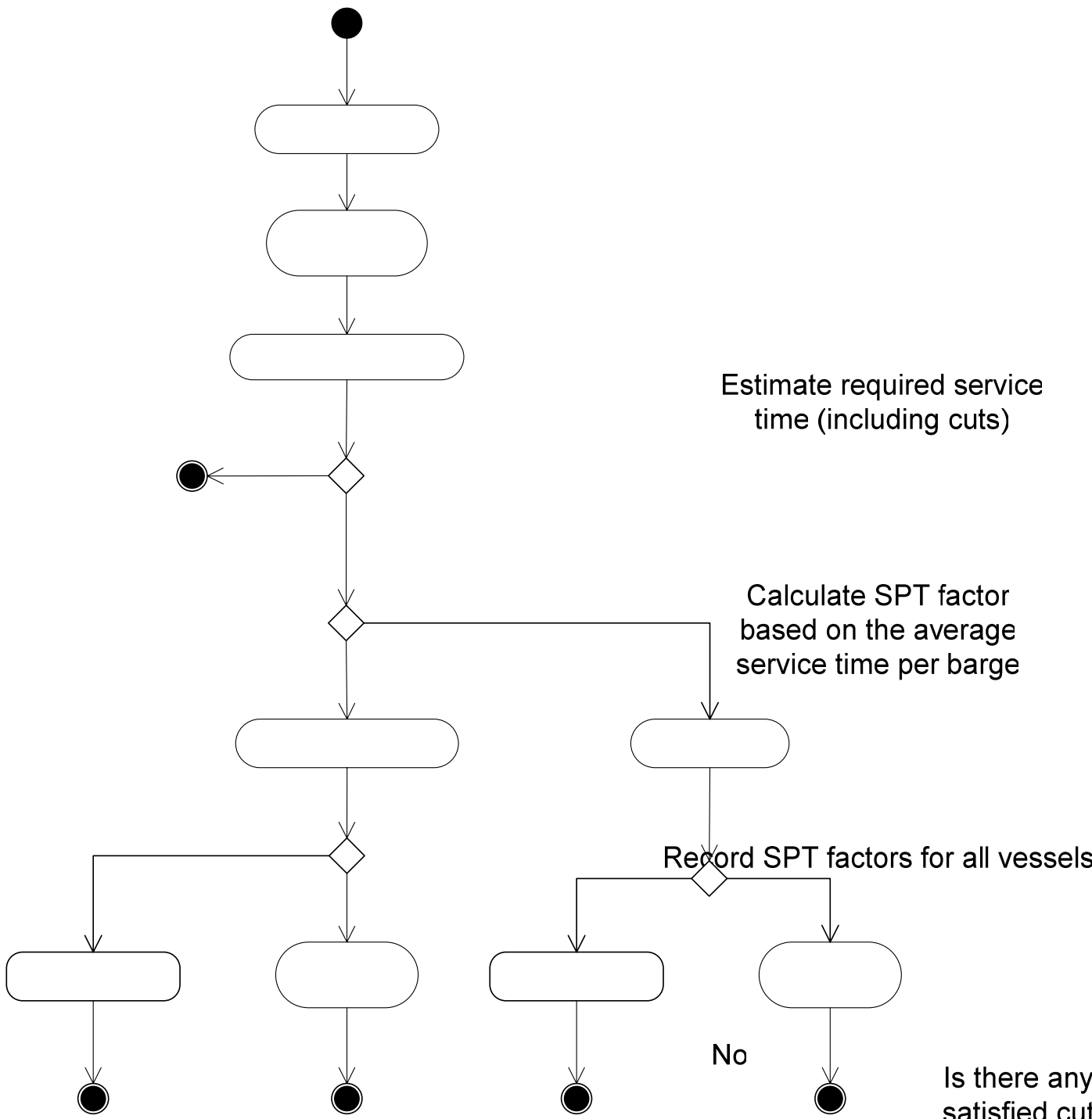


Figure 2 Operation Logic of FSPF Control

Multi-Recreation Lockage

As discussed in phase 2, there are special policies for recreational vessel, such as waiting for commercial lockages and exclusive serving periods. In addition to those rules

Is there any vessel waiting
8 for more than F^* lockages?

Yes

No

applicable only for recreational vessels, recreational vessels are usually locked together as a group as long as the chamber is able to accommodate them. Therefore, there is an option of locking recreational vessels individually or as group. User can indicate the option in the table for policies applicable to recreational vessels (as shown in Table 6, column of “MultiRecVesselLockage”).

Multi-Recreation Craft during Regular Lockage

The lockage process of recreational vessel is recorded at the times of SOL (start of lockage) and EOL (end of lockage). There is additional time for each additional recreational boat being added into lockage process. As shown in Figure 3, the total lock processing time for a group of recreational vessels will be estimated as the original lock processing time plus the additional time for each additional vessel. For example, if 10 recreation vessels are locked as group and 2 minutes extra time per boat, the total processing time is the processing time for the first recreation vessel (from processing time distribution for recreational craft) plus the additional time of 18 minutes (i.e. 2×9 for additional 9 boats).

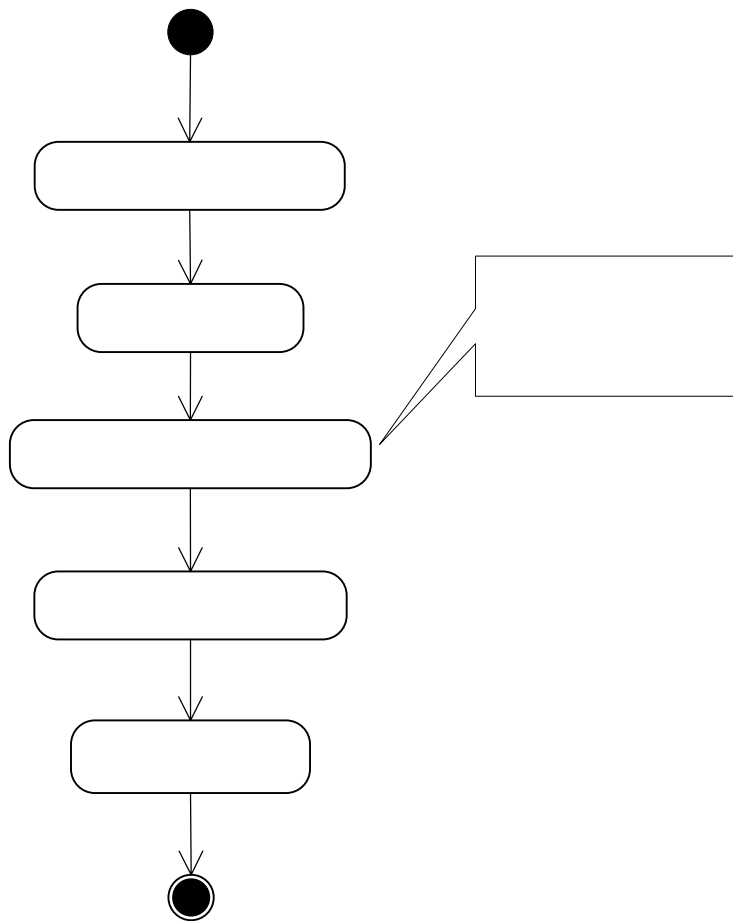


Figure 3 "Start of Lockage" Event for Recreational Vessels

Multi-Rec during Chamber Turn Back

As discussed in the previous section, recreation vessels can be locked through between cuts if that is allowed. If there are multiple recreation vessels, the processing time will be the turnback time plus the additional time for each recreation vessel (as shown in Figure 4). For example, if 5 recreation vessels can be locked through during the chamber turnback and 2 minutes extra time per boat, the total processing time for this recreational lockage is the chamber turnback time (from chamber turnback time distribution) plus the additional time of 10 minutes (i.e. 2×5 for additional 5 boats).

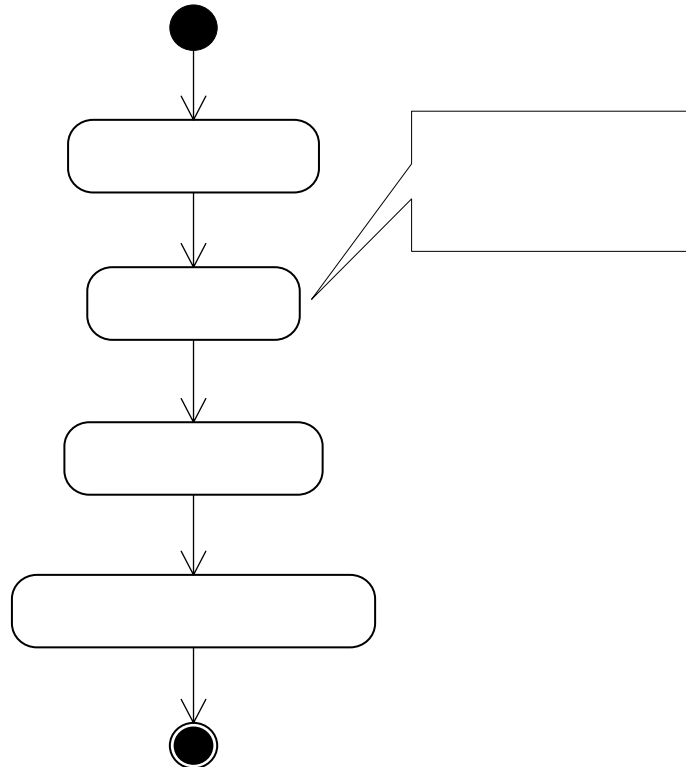


Figure 4 "Start of Chamber Turnback" Event Record Start Chamber Turnback Time

Navigable Pass

A navigable pass occurs at some locks based on the water levels and seasonal factors if locks are able to provide those types of lockages. Some locks, such as L&D 52 and L&D 53 on the lower Ohio River have movable wickets dams; others have relatively low fixed crest dams. These dam types afford vessels the opportunity to move past a lock site without actually locking through the lock chambers. They pass by the lock by navigating over the dam, hence the term navigable pass. Whether a vessel can pass a lock using navigable pass or must lock through the chambers depends upon water levels. The lock may be in navigable pass for weeks on end, or it may alternate between locking and navigable pass several times in one week. Historic LPMS/OMNI data can provide statistics which describe which times of the year navigable pass is likely to occur, and how long is it likely to last.

Estimate Chamber Turnback Time

Schedule the End of Chamber Turnback

In DLM, the feature of navigable pass is indicated in the table of lock information (as shown in Table 1). If a navigable pass is allowed at the specific lock, the user can further indicate the period during which a navigable pass is likely to occur. Table 2 shows there are 2 periods of navigable pass during a test operation, from Jan 2nd, last 12 hours, and Jan 3rd, last 12 hours. When simulation runs to the start time of navigable pass, the navigable pass mode at this lock is on and all the vessels in queue will use navigable pass over the dam. If there is vessel in the middle of regular lockage (of approach, entry, chambering or exit), the lockage process will be completed regardless the navigable pass period. DLM allows vessels in queue start navigable pass only after the regular lockage process for the previous vessel is completed. Thus, although the navigable pass mode is on, vessels in queue should start their navigable pass only right after the previous vessel's end of exit.

Table 1 Lock Information

tblLock : Table								
LockID	LockName	ReachID	NumberOfChambers	LevelOfDetail	LockPolicyID	NavigablePass	NumberOfPeriod	
54	Marnet	212	2	10	1	<input checked="" type="checkbox"/>	2	
(AutoNumber)		0	0	0	0	<input type="checkbox"/>	0	

Table 2 Information of Navigable Pass

tblNavigablePassTimeWindow : Table							
NavigablePassTimeID	LockID	Period	NavigablePassStartTime	StartMonth	StartDay	Duration	
1	54	1	1/2/2004	1	2	12	
2	54	2	1/3/2004	1	3	12	
0	0	0		0	0	0	

When a lock is in navigable pass mode, processing time distributions are needed for upbound and a downbound vessels. Those distributions are provided in tblChamberOpsLevel11 with lockage type "N". With a navigable pass, vessels pass over the dam without any assigned chamber. There is no extra cut for any vessel. Therefore, though the processing time distributions provided in tblChamerOpsLevel11 are chamber-based, they are the same for both chambers (as shown in Table 3). If vessels are in queue, they will be removed from queue based on either a FIFO or N-Up M-Down policy.

Table 3 Processing Time Distributions for Navigable Pass

tblChamberOpsLevel11 : Table						
ChamberID	VesselType	LkgType	AdditionalVesselIndicator	TotalCutsRequired	Cut	
83	T	N	<input type="checkbox"/>	1	F	
84	T	K	<input type="checkbox"/>	1	F	
83	H	N	<input type="checkbox"/>	1	F	
84	T	N	<input type="checkbox"/>	1	F	
83	R	N	<input type="checkbox"/>	1	F	
84	R	N	<input type="checkbox"/>	1	F	
83	T	N	<input type="checkbox"/>	1	F	
84	L	N	<input type="checkbox"/>	1	F	
83	L	N	<input type="checkbox"/>	1	F	
84	H	N	<input type="checkbox"/>	1	F	

Operation Logic

In DLM, the navigable pass mode is switched on and off at the timing points input by user. Start and end events for navigable pass are pushed onto simulation event list.

When a navigable pass starts, vessels “assigned to available chambers” will be released back to lock queue with other “unassigned” vessels in queue. It is noticed that during a navigable pass, there is no service priority among vessels. That is, government vessels, recreational craft or commercial tows are considered together in lock queue and served based on their arrival orders.

Figure 5 first shows how the navigable pass is considered in DLM when a vessel arrives at lock. Since only “Start of Lockage” and “End of Lockage” are recorded for navigable pass, there are no more events in between SOL and EOL for any navigable pass vessel.

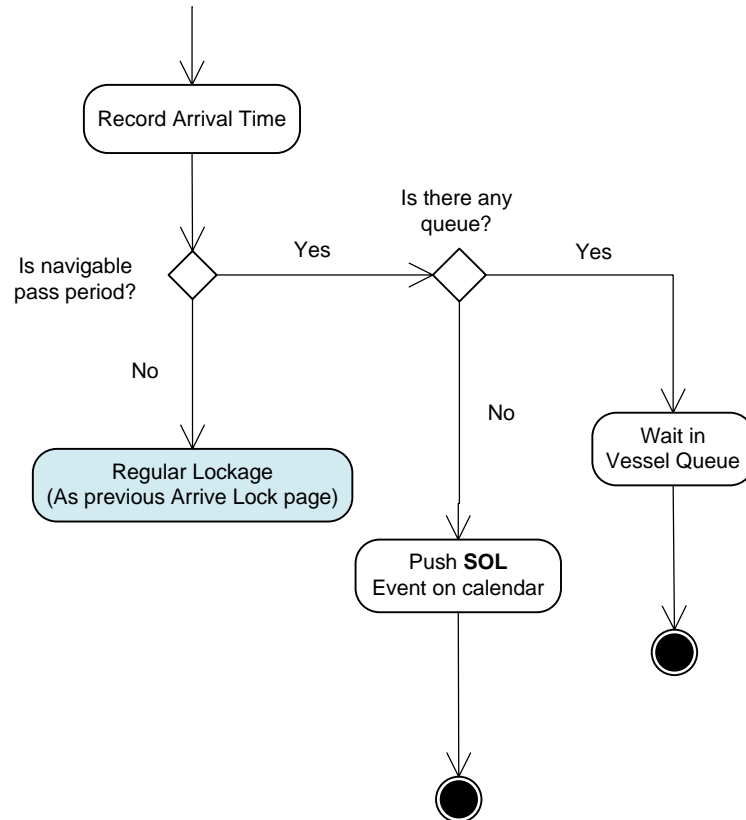


Figure 5 Arrive Lock for Navigable Pass

In DLM, there are no more lockage components for navigable pass, the process of “look for next vessel” will be omitted in the events of end of entry and end of chambering (as shown in Figure 6 and Figure 7).

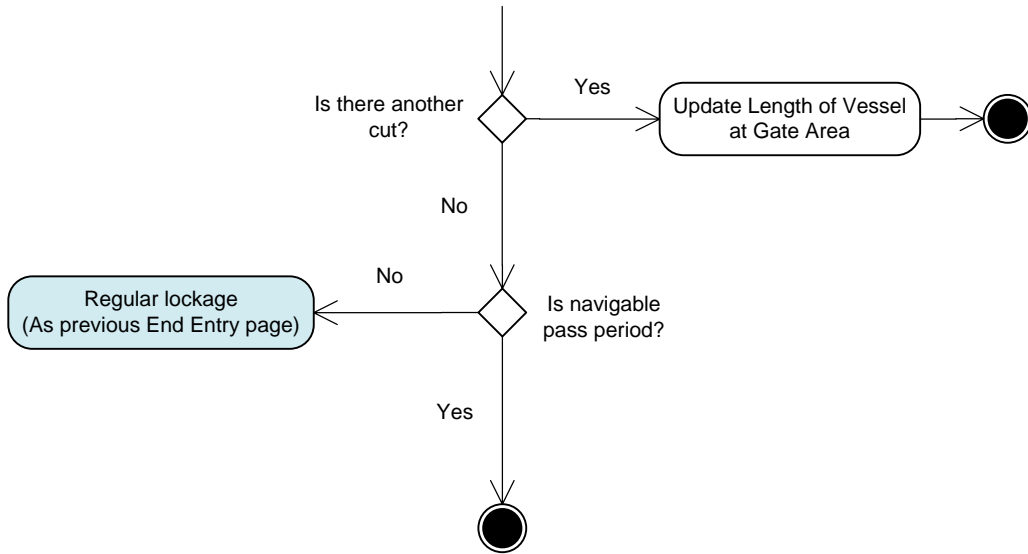


Figure 6 End of Entry for Navigable Pass

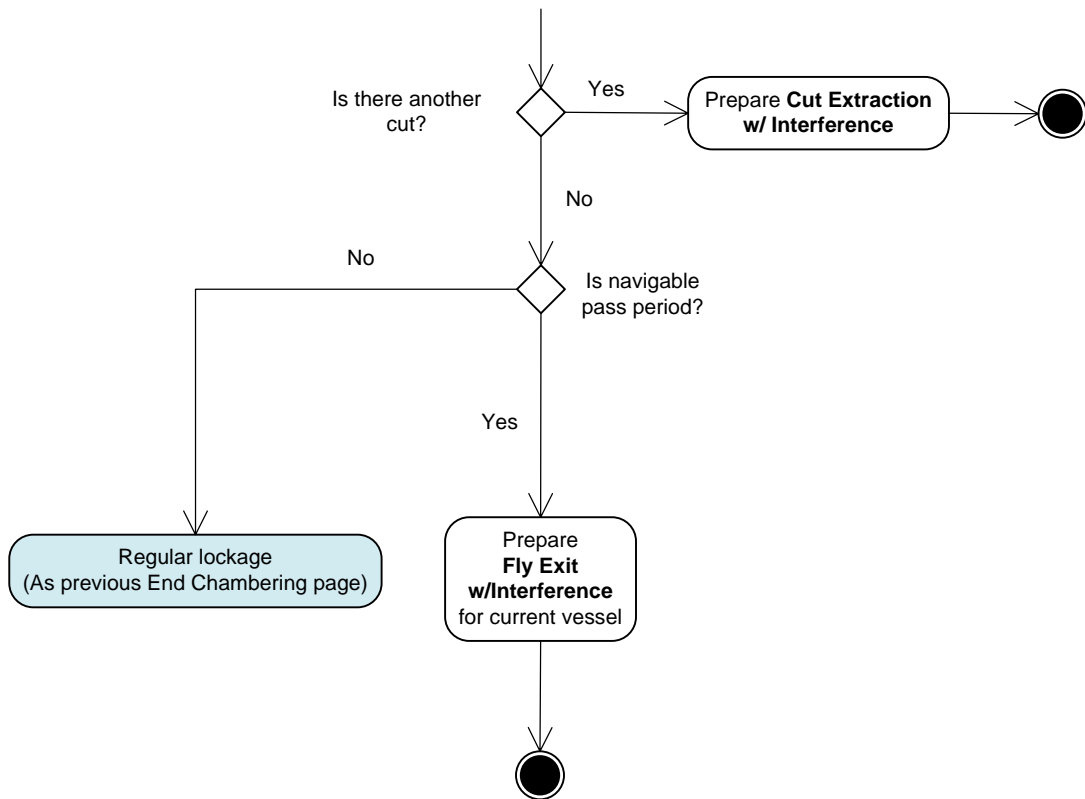


Figure 7 End of Chambering for Navigable Pass

Since navigable pass mode could possibly be on when there is still vessel using regular lockage process, “straight lockage”. Therefore, it is necessary to check exit type of the “last vessel” using regular lockage. If the next vessel in queue travels in the

opposite direction of the “last vessel”, DLM resets the exit type of the last vessel with a fly exit (rather than exchange exit) since the next vessel is going to use the navigable pass. If the next vessel in queue moves in the same direction, the last vessel is in its turnback exit and the next vessel starts its pre-approach. In this case, DLM will complete one more lockage for the next vessel, which has started its pre-approach and will complete its lockage with fly exit, before starting navigable pass.

Figure 8 shows how the navigable pass is considered when a vessel is making the fly exit (or a recreational craft reaches its end of lockage).

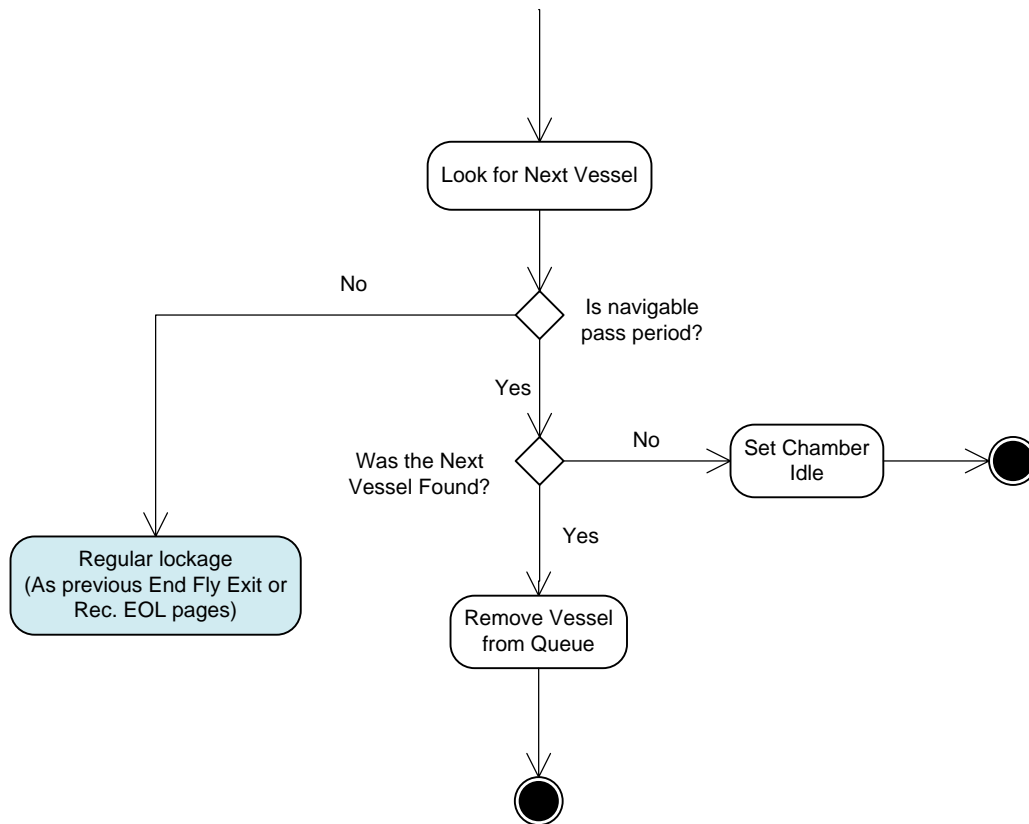


Figure 8 End of Fly Exit / Rec. EOL for Navigable Pass

Open Pass

Another specialty type of lockage involves open pass lockage. During this lockage type, water levels are such that the upper pool and lower pool are essentially the same elevation. In this case, the upper and lower gates of a lock chamber are kept in the open position, and a vessel travels through the chamber without a “chambering” event. These events are usually quite rare, but they may be more frequent at tidal locks. The DAPP must be able to determine statistics that describe open pass events, and the detailed lock model must be able to switch from locking mode to open pass mode. When in open pass mode, the chamber will use normal approach, entry and exit times, but the

chambering time will be equal to zero. Since the processing time distributions for open pass lockage (approach, entry and exit only) may not be currently available, DLM does not exactly perform open pass lockages.

Multi-cut Lockage Efficiency Enhancements

Using Efficiency Enhancement Equipments

Since the locks on the waterway can hold only eight jumbo (35 ft. × 195 ft.) barges plus a towboat, when a tow with a larger number of barges reaches a lock, the towboat must split the tow into units or "cuts" that fit the lock. The towboat must lock through with the first cut, push it out of the lock, and then lock back through to get the second cut of barges.

Help Equipment

(1) Tow Haulage

Tow haulage is a procedure for drawing barges through a lock by using equipment on the lock itself to minimize the maneuvering of a towboat when a tow exceeds the length of the lock. Tow haulage equipment on a lock can pull the first cut through by itself, so that the towboat can stay in its original pushing position and lock through with the second cut.

Lock operation for oversize tows is more efficient with tow haulage equipment. Towboats are used more expeditiously, and shippers can take advantage of the economy of large tows. Larger tows represent a potential for significant cost reduction for both shippers and their customers. Tow haulage equipment has been installed at twelve locks on the McClellan-Kerr in Arkansas.
(<http://www.swl.usace.army.mil/navigation/mckarns.html#haulage>)

(2) Helper Boats

Self-help is referred to as "industry self-help". Self-help means that industry will help itself. They do this by having a volunteer boat come up on the exiting end of the lockage and serve as a boat that pulls cuts. This is faster than tow haulage and they can get the cut further away from the gate.

Sometimes, the lock provides helper boats. The helper boat, usually a low-power, typically 800 horsepower towboats (push boat) used to assist tows approach to a lock chamber, pull the unpowered cut to the end of the guidewall during a multi-cut lockage, remove ice and debris from the lock approach and chamber, and provide emergency assistance.

The time saving gained from a helper boat varies based on location, flow conditions, weather and other factors. Under normal flow conditions at most Upper Mississippi River sites, initial study analysis indicates a saving of approximately 5-to-15 minutes per lockage; in contrast, the Illinois Waterway locks typically report limited or no time savings. However, on both rives, a greater time savings is gained

during high water flows. An additional time savings can be gained by also using helper boats to pull the first cut to the end of the guidewall so that a 1,200-foot tow can be reattached outside of the chamber.

(UMR-IWW System Navigation Study Newsletter, January 1997, Vol.4 No.1)

(<http://www2.mvr.usace.army.mil/UMRS/NESP/Documents/1997%20Jan%20Nav%20Study%20Newsletter.pdf>.)

If self-help is used, interference would occur. Therefore, if both chambers are operable, the self-help might not be used. The boat providing the help would either cause gate interference while waiting for the next cut or it would cause both gate and approach area interference if it takes the cut somewhere “away” from the lock.

Schemes of Handling Extracted Cut

In order to consider the availability of assistance for cut extraction, a column of “HelpEquipment” should be provided in the table “tblChamber” as one of the chamber specifications. If it is checked, the help equipment at current chamber is available. In order to simplify the model, DLM first assumes that if a lock has help equipment, it will fully utilize the equipment and does not let it sit idle. That is, an option of with or without equipment is considered.

Table 4 Chamber Specification for Vessel Assistance

tblChamber : Table										
ChamberID	LockID	ChamberDesc	Main	Length	Width	CutLimit	ControlPolicyID	DynamicControl	HelpEquipment	
83	54	Marmet	<input checked="" type="checkbox"/>	360	56	5	1	<input checked="" type="checkbox"/>	<input checked="" type="checkbox"/>	
84	54	Marmet	<input type="checkbox"/>	360	56	1	8	<input type="checkbox"/>	<input type="checkbox"/>	
0	0		<input type="checkbox"/>	0	0	0	0	<input type="checkbox"/>	<input type="checkbox"/>	

Help equipment affects the processing time distributions. In the DLM model, the cut approach time is generated from the distribution of turn back approach time and the cut extraction time is generated from the distribution of turn back exit time. Since using help equipments can save processing times for multi-cut lockage, the processing time distribution for the intermediate cuts and the last cut with and without help equipments would be different. Therefore, an additional column of “AssistLevel” is added in the table “tblChamberOpsLevel12”. Under the simplest case, with or without help equipment, if there is no available help equipment, “0” is indicated as “AssistLevel”. If there is help equipment, value of “1” is given to “AssistLevel”. In addition, it is noted that the help equipment is only used for multi-cut tows under regular lockage (straight lockage), but not other lockage or vessel types.

Table 5 Processing Time Distributions for Chamber with Vessel Assistance

tblChamberOpsLevel12 : Table							
AssistLevel	ChamberID	VesselType	LkgType	AdditionalVesselIndicator	TotalCutsRequired	Cut	
1	83	T	S	<input type="checkbox"/>	3	I	
1	83	T	S	<input type="checkbox"/>	1	F	
1	83	T	S	<input type="checkbox"/>	2	F	
1	83	T	S	<input type="checkbox"/>	3	F	
1	83	T	S	<input type="checkbox"/>	2	L	
1	83	T	S	<input type="checkbox"/>	3	L	

	0	83	T	S	<input type="checkbox"/>	3	I
	0	83	T	S	<input type="checkbox"/>	3	L
	0	83	T	S	<input type="checkbox"/>	2	L
	0	83	T	S	<input type="checkbox"/>	3	F
	0	83	T	S	<input type="checkbox"/>	2	F
	0	83	T	S	<input type="checkbox"/>	1	F

Serving Rec. Vessels during Chamber Turnback

Another way to increase the efficiency is locking through the recreation vessels during the chamber turnback between cuts of multi-cut lockage. That is, if a 2-cut tow is going downbound, lock operator will allow upbound recreation craft to be served during the chamber turnback between the 1st and 2nd cuts. As can be seen in Table 6, the policy is defined as “AllowedInTB”. If it is check marked, recreation vessel is allowed to be locked through during the chamber turnback.

Table 6 Policies for Recreational Vessels

tblRecPolicy : Table								
	RecPolicyID	LockID	ChamberID	WaitLockage	MultiRecVesselLockage	AllowedInTB	NumOfPeriods	
▶	1	54	83	0	<input checked="" type="checkbox"/>	<input checked="" type="checkbox"/>	0	
	2	54	84	3	<input checked="" type="checkbox"/>	<input checked="" type="checkbox"/>	3	
*	0	0	0	0	<input type="checkbox"/>	<input type="checkbox"/>	0	

The processing time of locking recreational vessel will be chamber turnback time plus additional time for each recreation vessel served during the turnback.

DLM Shipment List

In addition to being a lock module within NaSS, DLM is also designed to be driven independently to provide detailed analysis at any single lock. When DLM is operated as an independent model, vessel traffic should be either prepared in advance as a shipment list or generated within the model based on arrival rates and distributions. For test and validation purposes, a shipment list is used for vessel inputs. However, for planning purposes, it is preferable to generate vessel traffic while running the simulation in order to take into account the future traffic changes.

As in running NaSS, the shipment list for DLM should include the trip information such as arrival times, origin/destination, vessel types, barge sizes and other details. The number of required cuts could then be determined by the barge sizes and chamber size. Unlike the shipment list used in NaSS, there are no “other visits” (i.e. stops for loading/unloading) between origin and destination nodes for each single trip since it is already the shortest trip by passing only one lock. Though there might not have loading/unloading, docking/undocking activities during the trips, vessel configurations or chamber packing/unpacking maneuvers could have been done while locking the vessels.

Shipment Data

Currently, the detailed shipment list (DSL) for a single lock is generated by DAPP. The information for each individual trip is covered by 7 tables (as shown in Table 7).

Table 7 DLM Data for Vessel Traffic

Shipment List

<i>tblPowerTrips</i>
<i>tblVisit</i>
<i>tblPowerTransaction</i>
<i>tblBargeTransaction</i>
<i>tblPowerVessel</i>
<i>tblVesselClass</i>
<i>tblVesselType</i>

For a single lock, origin and destination nodes are two ends of lock reach. First of all, *tblPowerTrips* provide the information of trip date and its O/D and *tblVisit* shows the visits for each single trip. In DLM, there are only two “visits” of origin and destination. At the “origin” visit, each trip starts with its power vessel shown in *tblPowerTransaction*, as well as barges (with or without commodity), shown in *tblBargeTransaction*. Power vessels (i.e., towboat) are always added at the origin visit only. Barges are added as sets based on the barge type (i.e., VesselClassID) and carried commodity (i.e., CommodityID). A tow trip could have several barge sets which have varied barge type and loaded commodities.

(a)

tblPowerTrips : Table					
	PowerTripID	TripDate	OriginNodeID	DestinationNodeID	TripTrackingFlag
	1	8/9/2006 1:05:00 PM	214	213	
	2	4/23/2006 7:30:00 AM	213	214	
	3	4/23/2006 3:30:00 PM	214	213	
	4	6/19/2006 2:45:00 PM	213	214	
	5	6/20/2006 11:10:00 AM	214	213	
	6	8/13/2006 10:55:00 AM	213	214	
	7	8/13/2006 6:35:00 PM	214	213	
	8	11/11/2006 9:20:00 AM	213	214	
	9	11/11/2006 4:45:00 PM	214	213	
	10	5/26/2006 4:05:00 PM	214	213	

(b)

tblVisit : Table				
	VisitID	PowerTripID	ActionNodeID	VisitOrder
▶	1	1	214	1
	2	1	213	2
	3	2	213	1
	4	2	214	2
	5	3	214	1
	6	3	213	2
	7	4	213	1
	8	4	214	2
	9	5	214	1
	10	5	213	2

(c)

tblPowerTransaction : Table				
	PowerTransactionID	VisitID	PowerVesselID	AddOrRemove
	1	1	0021552	<input checked="" type="checkbox"/>
	2	3	0065505	<input checked="" type="checkbox"/>
	3	5	0065505	<input checked="" type="checkbox"/>
	4	7	0065505	<input checked="" type="checkbox"/>
	5	9	0065505	<input checked="" type="checkbox"/>
	6	11	0065505	<input checked="" type="checkbox"/>
	7	13	0065505	<input checked="" type="checkbox"/>
	8	15	0065505	<input checked="" type="checkbox"/>
	9	17	0065505	<input checked="" type="checkbox"/>
	10	19	0224533	<input checked="" type="checkbox"/>

(d)

tblBargeTransaction : Table							
	BargeTransactionID	VisitID	VesselClassID	AddOrRemove	Quantity	CommodityID	QtyTons
		3	23	<input checked="" type="checkbox"/>	1	2	0
	2	4	23	<input type="checkbox"/>	1	2	0
	3	5	23	<input checked="" type="checkbox"/>	1	2	0
	4	6	23	<input type="checkbox"/>	1	2	0
	5	7	94	<input checked="" type="checkbox"/>	1	2	0
	6	8	94	<input type="checkbox"/>	1	2	0
	7	9	94	<input checked="" type="checkbox"/>	1	2	0
	8	10	94	<input type="checkbox"/>	1	2	0
	9	11	23	<input checked="" type="checkbox"/>	1	2	0
	10	12	23	<input type="checkbox"/>	1	2	0

Figure 9 DLM Shipment List

Although a tow speed is specified for each single reach, including a lock reach, currently tow speed is not applied while running DLM since a lock reach is defined between two approach points and all the lockage times are determined from various processing time distributions.

Read DLM Traffic

While driving DLM as a stand-alone model, all the shipment data are loaded at the beginning. The relevant cut information is also calculated based on the packing algorithm used by the network model, BasinSym. In addition to the arrival time and detailed barge/commodity information, DLM also need vessel type information and dimensional information for each cut. Vessel type information is used to model the concerns of chamber preference, chamber exclusion, lockage priority, as well as various lock control policies. The dimensional information for each cut is necessary for considering interference and multi-vessel lockage.

Vessel Type

- If there are barges (non-powered) with a power vessel, that is considered a commercial tow trip. If there are no barges with power vessel, it could be trips of towboats, government, passenger, recreation, etc. That information

is provided in *tblPowerVessel*, in which the vessel class is indicated for each individual power vessel. Based on the vessel class, vessel type is then given in *tblVesselClass*. All the vessel types are defined in *tblVesselType*.

(a)

tblPowerVessel : Table					
	PowerVesselID	VesselClassID	HP	LDA	Beam
▶	0000220	20	900		
	0003314	6	3600	115.5	23.4
	0003955	1	575	85	21
	0003968	1	1000	69.3	17.5
	0011867	17	1200		
	0015933	17	850	45	
	0021552	1	600	82	24
	0027144	20	2900	104.7	31.7

(b)

tblVesselTypes : Table			
	VesselTypeID	VesselTypeCode	VesselTypeDesc
		14 B	Barge
		1 C	Dry Cargo Vessel
		2 E	Liquid Cargo Vessel
		3 F	Fishing Vessel
		4 G	Federal Govt. Vessel
		5 J	Dredge Vessel
		6 K	Crewboat Vessel
		7 M	Non-Cargo Vessel
		8 N	Government-NonFederal
		9 P	Passenger Boat or Ferry
		10 R	Recreational Vessel
		11 T	Tow or Tug Boat
		12 U	Federal Govt. Contractor Vessel
		13 Z	Other

(c)

Among those vessel types, DLM re-categorizes them as follows in order to apply some locking algorithm:

- B is non-powered barge.
- T, C, E, F, J, K, M and Z are all counted as power vessels without barges, similar to light boats.
- G, N, P and U have high priority in lockage.
- R is recreational vessel.
- Commercial tow is composed of T and B.

Cut Information

The dimensions of the chamber and tow are needed in order to determine the required number of cuts. According to BasinSym, “chamber signature” and “tow signature” are used to define this dimensional information. Chamber signature is a string used to identify chambers of equivalent dimension and assistance availability. The components for the chamber signature are length, width, and assistance. Chamber size can be read from Length and width in *tblChamber*. If assistance is available, the power vessel is locked through with only one cut. If assistance is not available, the power vessel is required to accompany each and every cut. An example of chamber signature for a chamber which is 360 feet long and 56 feet wide with assistance would be 360×56×ASSIST.

Tow signature consist of a dimensional signature of the power vessel and 0 or more barge set signatures where the barge sets have been decomposed to barges of similar dimensions. The power vessel signature is the length and the width in integer feet of the vessel. It can be read from LOA and Beam in *tblPowerVessel*. The barge set signatures consists of length, width and number of barges. The length and width can be read from LOADefault and BeamDefault in *tblVesselClass* based on the VesselClassID in *tblBargeTransaction*. The quantity for each barge set is also shown in *tblBargeTransaction*. If a towboat labeled “0003314” pushes two barge sets of six 60”×27” liquid cargo barges (VesselClassID 27) and nine 61”×31” open hopper barges (VesselClassID 29), the tow signature is expressed as [115×23](60×27×6)(61×31×9).

With tow and chamber signature, cut information for each cut could be calculated. There are three types of cut information:

1. Number of cut,
2. Dimension of each cut, especially length of cut
3. Remaining chamber length after fitting in each cut, especially for single-cut tow

DLM locks different cuts through the lockage process steps, including cut approach, entry, chambering and cut extraction. The length of each cut sitting at the gate area, either waiting for the chambering or waiting for the exit, affects the gate area interference in DLM. With the remaining chamber length left after a small vessel has fitted into the chamber, another small vessel could be locked in a single lockage cycle, thus save the lockage time for two different lockage cycles.

Information Transfer Program Introduction

MWRRC Water Conference: Maryland Water Issues in 2030

Basic Information

Title:	MWRRC Water Conference: Maryland Water Issues in 2030
Project Number:	2007MD190B
Start Date:	3/1/2007
End Date:	2/29/2008
Funding Source:	104B
Congressional District:	MD 5
Research Category:	Water Quality
Focus Category:	Water Supply, None, None
Descriptors:	Water availability, distribution, quality
Principal Investigators:	Allen Davis

Publication

Water Issues in 2030

Maryland Water Resources Research Center

The Center held a one day Conference on Wednesday, October 31st, 2007, in the Benjamin Banneker Room, Stamp Student Union, University of Maryland, College Park, MD. The Maryland Sea Grant College co-sponsored our Conference. Over one hundred attendees participated and were represented by State, Federal and University personnel.

Some of the water issues we will face are Global climate change, swelling populations, and increasing technological advances all continue to affect water availability, distribution, and quality. The future will bring many new challenges and may exacerbate existing challenges that have not been met. As we look back over the past 25 years, our water knowledge and water management technologies are much more advanced. Our problems, however, are not solved. Within this one-day symposium, our challenge is to look to the future to anticipate upcoming water resources challenges globally, and with a specific focus to Maryland.

"Oceans, Climate, and Human Health: The Cholera Paradigm", Rita Colwell, Distinguished Professor, University of Maryland, College Park, and Johns Hopkins University Bloomberg School of Public Health, Senior Advisor and Chairman, Canon US Life Sciences, Inc.

"Maryland Commission on Climate Change: Assessing the Impacts of Climate Change on Maryland", Donald Boesch, President, University of Maryland Center for Environmental Sciences and Professor of Marine Science, Cambridge, MD.

"Water Supply Reliability in 2030 for the Washington Metropolitan Area ", Erik Hagen, Director of Operations for the Section for Cooperative Water Supply Operations (CO-OP) at the Interstate Commission on the Potomac River Basin (ICPRB), Rockville, MD.

"Emerging Contaminants", Yvette M. Selby-Mohamadu, Office of Groundwater and Drinking Water, U.S. Environmental Protection Agency, Washington, DC.

"Planning, Regulatory, Management and Financing Programs to Protect Public Health, Restore and Protect Air and Water Quality, Clean Up Contaminated Land and Ensure Proper Management of Hazardous and Solid Wastes", Robert Summers, Deputy Secretary, Maryland Department of the Environment, Baltimore, MD.

"The Impact of Sprawl on Water Quality in the Chesapeake Bay Watershed", Steven Prince, Professor of Geography, University of Maryland, College Park and Director of the Regional Earth Sciences Application Center.

"The Status of Bay Restoration Efforts in 2010 and Predictions for 2030", Frank Dawson, Director Aquatic Resources, Maryland Department of Natural Resources, Annapolis, MD.

Contact persons:

Dr. Phil Kearney
Associate Director, MWRRRC
kearneyp@umd.edu
301-405-6829

Dr. Allen P. Davis
Director, MWRRRC
apdavis@umd.edu
301-405-1958

Student Support

Student Support					
Category	Section 104 Base Grant	Section 104 NCGP Award	NIWR-USGS Internship	Supplemental Awards	Total
Undergraduate	2	0	0	0	2
Masters	6	0	0	0	6
Ph.D.	4	0	0	2	6
Post-Doc.	0	0	0	1	1
Total	12	0	0	3	15

Notable Awards and Achievements